To the Graduate Council:

I am submitting herewith a dissertation written by Shannon Stewart Eaker entitled "Analysis of Events Governing the Meiotic Division in Mouse Spermatocytes." I have examined the final copy of this dissertation for form and content and recommend that it be accepted in partial fulfillment of the requirements for the degree of Doctor of Philosophy, with a major in Biochemistry and Cellular and Molecular Biology.

Dr. Mary Ann Handel
Major Professor

We have read this dissertation
and recommend its acceptance:

Dr. Jeffery Becker

Dr. Dabney Johnson

Dr. John Koontz

Dr. Bruce McKee

Dr. Cynthia Peterson

Acceptance for the Council:

Dr. Anne Mayhew
Vice Provost and
Dean of the Graduate School

(Original signatures are on file in the Graduate Student Services Office)

ANALYSIS OF EVENTS GOVERNING THE MEIOTIC DIVISION IN MOUSE SPERMATOCYTES

A Dissertation

Presented for the

Doctor of Philosophy

Degree

The University of Tennessee, Knoxville

Shannon Stewart Eaker

August 2001

DEDICATION

In Memory of Virginia Stewart Eaker

ACKNOWLEDGEMENTS

My time spent studying at The University of Tennessee has been both challenging and rewarding. First, I would like to thank my parents David and Becky, my sister Shelby, and the rest of my family for their support throughout my academic career.

I am forever in debt to my mentor Mary Ann Handel, and the past and present members of the Handel laboratory. Mary Ann has been the most helpful and instructive teacher I have ever encountered, always willing to help anyone that is willing to learn. I also would place John Cobb, a past graduate student in the lab, in the same category. His technical knowledge and problem solving skills are second to none. I would like to thank April Pyle, a current graduate student in the lab, for sharing the countless hours of our graduate school stresses, and for her constant support. I would also like to thank past and present members of the Handel lab: Amy Inselman, Trisha Smith, Lori Kellam, Brent Bowker, Cynthia Park, Debby Andreadis, and Laura Richardson. Without them, I never would have made it.

Outside of the lab, I would like to thank all of the teachers I have had at UT. Thanks to all of my committee members (Drs. John Koontz, Bruce McKee, Cynthia Peterson, Jeff Becker, and Dabney Johnson) for their support, criticisms, and for actually making committee meetings enjoyable. Thanks to Charlie Barnett and Harry Crissman for always believing in me.

I would like to thank all of my friends for their support and retainment of sanity. Thank you Jamie Lewis, Jason Karnes, Jon Boggs, Erin Seago, Chad Royston

and Mark Clark for the hours of entertainment, and Shawni and Brody for always being there.

ABSTRACT

The meiotic division is essential for successful gametogenesis. However, many events occurring during male and female meiotic development remain poorly understood. While it is known that chromosomes must pair, recombine, and segregate to form gametes, critical questions remain. How and when do these events occur with respect to each other? What mechanisms monitor their developmental success? Insight into these questions is provided in this dissertation, using the mouse spermatocyte as a model. The purpose of this work is to aid in the overall understanding of mammalian meiosis.

After an introduction into mammalian meiosis in Part I, a temporal order of events occurring during meiosis in the mouse spermatocyte is provided in Part II. The development of events such as chromosome pairing, spindle formation, and localization of cell cycle proteins was monitored using immunofluorescence. This work established a framework for which developmental progress can be monitored in normal and abnormal environments.

In Part III, the MLH1-deficient mouse was used to study an abnormal G2/M transition. Spermatocytes lacking the DNA mismatch repair protein MLH1 are characterized by univalent chromosomes at metaphase I, and do not progress into the first anaphase. Apoptosis, or programmed cell death, was seen in *Mlh1*$^{-/-}$ metaphase spermatocytes.

In Part IV, spermatocytes heterozygous for Robertsonian-chromosome translocations were also used to study abnormalities in the G2/M transition. Many of these spermatocytes failed to properly pair homologous chromosomes during MI.

Many metaphase spermatocytes also contained unaligned/lagging chromosomes. Apoptosis was seen in a large portion of the spermatocytes containing unaligned chromosomes, possibly in response to the activation of a spindle checkpoint mechanism. Although functional sperm are produced in these mice, many were found to be aneuploid for chromosomes involved in Robertsonian translocations.

The findings of this dissertation aid in the overall understanding of meiotic development and regulation, which is discussed in the closing Part V. By the establishment of a meiotic timeline, genetic abnormalities can be and were studied in the context of normal meiotic progression. Situations in which meiotic abnormalities arise are provided in Parts IV and V. These findings provide insight into the consequences of chromosomal abnormalities and failure in the DNA repair mechanism during meiosis, possibly reflecting the creation of errors in our own species.

TABLE OF CONTENTS

CHAPTER PAGE

PART I: INTRODUCTION

I MEIOTIC CELL CYCLE PROGRESSION IN THE MOUSE……. 2

LIST OF REFERENCES…… 17

PART II: TEMPORAL ORDERING OF EVENTS DURING THE MEIOTIC G2/M TRANSITION IN THE MALE MOUSE

ABSTRACT……. 21

I INTRODUCTION…… 22

II MATERIALS AND METHODS……. 26

III RESULTS AND DISCUSSION……..…… 30

LIST OF REFERENCES……. 63

PART III: MEIOTIC ABNORMALITIES AND APOPTOSIS DURING METAPHASE IN MLH1-DEFICIENT MOUSE SPERMATOCYTES

ABSTRACT……. 69

I INTRODUCTION…… 71

II MATERIALS AND METHODS……. 74

III RESULTS…… 78

CHAPTER PAGE

IV DISCUSSION…….. 98

LIST OF REFERENCES…….103

PART IV: EVIDENCE FOR MEITOIC SPINDLE CHECKPOINT FROM ANALYSIS OF SPERMATOCYTES FROM ROBERTSONIAN-CHROMOSOME-HETEROZYGOUS MICE

SUMMARY ……106

I INTRODUCTION……108

II MATERIALS AND METHODS…… 115

III RESULTS…… 121

IV DISCUSSION……. 153

LIST OF REFERENCES…… 165

PART V: CONCLUSION

I SUMMARY …….. 171

LIST OF REFERENCES …….. 184

VITA ……. 185

LIST OF TABLES

TABLE PAGE

PART III: MEIOTIC ABNORMALITIES AND APOPTOSIS DURING METAPHASE IN MLH1-DEFICIENT MOUSE SPERMATOCYTES

1 Analysis of FISH signal domains in MI spermatocytes from *Mlh1*$^{-/-}$ males ……..…… 81

PART IV: EVIDENCE FOR MEITOIC SPINDLE CHECKPOINT FROM ANALYSIS OF SPERMATOCYTES FROM ROBERTSONIAN-CHROMOSOME-HETEROZYGOUS MICE

1 Sperm FISH analysis of frequencies of aneuploid sperm from B6 and Rb-heterozygous mice……..…. 124

2 Frequencies of unpaired chromosomes in MI spermatocytes of Rb-heterozygous mice …… 129

3 Frequencies of apoptosis and chromosome misalignment in metaphase spermatocytes……. 145

LIST OF FIGURES

FIGURE PAGE

PART I: INTRODUCTION

1 Immunofluorescent staining of mouse spermatocytes through meiosis using developmental marker antibodies ……..…… 4

2 Timeline representation of protein localization throughout meiosis in mouse spermatocytes ……. 8

3 Diagram of the spindle assembly checkpoint mechanism by kinetochore/microtubule attachment in meiosis ……. 11

PART II: TEMPORAL ORDERING OF EVENTS DURING THE MEIOTIC G2/M TRANSITION IN THE MALE MOUSE USING IMMUNOFLUORESCENCE

1 Immunofluorescent images from surface-spread chromatin preparations …..……..……. 31

2 Immunofluorescent images from fibrin clot embedded spermatocytes …….……..…….. 34

3 Localization of the acetylated form of histone H3 throughout spermatogenesis ……... 39

4 Rad51 localization during early meiotic prophase ……..… 43

5 MPM-2 localization throughout meiotic prophase and the division phase ……..……. 46

6 Western blot analysis of PLK1 ……...… 48

7 PLK1 localization in late prophase and metaphase I spermatocytes ……. 50

8 Developmental immunofluorescent localization of CENP-E and CENP-F in cytological preparations ……. 53

9 Western blot analysis of CENP-E and CENP-F ...……. 55

FIGURE PAGE

10 Developmental immunofluorescent localization of XMAD2 in cytological preparations ……..… 58

11 Western blot analysis of XMAD2 …….. 60

PART III: MEIOTIC ABNORMALITIES AND APOPTOSIS DURING METAPHASE IN MLH1-DEFICIENT MOUSE SPERMATOCYTES

1 FISH analysis of MI chromosomes in *Mlh1*$^{-/-}$ and *Mlh1*$^{+/+}$ spermatocytes, either treated with okadaic acid (OA) or untreated ……..……..... 79

2 Pachytene spermatocytes from *Mlh1*$^{-/-}$ mice are competent to condense chromosomes in response to OA treatment ……..…….. 84

3 Immunofluorescence staining of pachytene (A and C) and metaphase (B and D) spermatocytes using antibodies against the synaptonemal complex protein SYCP3 (red) and the phosphorylated form of histone H3-Ser 10 (green) …….. 87

4 Abnormalities during chromosome alignment and segregation in *Mlh1*$^{-/-}$ spermatocytes seen by microscopy ……..…… 90

5 The frequency of tubules with apoptotic cells in *Mlh1*$^{-/-}$ mice increases dramatically at 22 days of age …… 93

6 Apoptosis in *Mlh1*$^{-/-}$ spermatocytes …… 95

PART IV: EVIDENCE FOR MEITOIC SPINDLE CHECKPOINT FROM ANALYSIS OF SPERMATOCYTES FROM ROBERTSONIAN-CHROMOSOME-HETEROZYGOUS MICE

FIGURE PAGE

1 Diagrammatic representation of a Rb chromosome meiotic pairing configuration involving chromosomes 2 (green) and 8 (yellow) ……..…….. 111

2 Illustrations of sperm stained by the three-color FISH method ……..……..…….. 122

3 Air-dried meiotic metaphase I (MI) chromosome spreads labeled with chromosome paint probes (2: green, 8: red) ……..……..……. 127

4 Pairing abnormalities in surface-spread spermatocytes from Rb/+ mice ……..…… 132

5 Confocal imaging of MI chromosomes and spindles from B6 and Rb/+ spermatocytes …… 134

6 The frequencies of spermatogenic cell stages from B6 (white bars) and Rb/+ (black bars) adult mice …… 137

7 Frequencies of seminiferous tubules at indicated stages and of apoptotic tubules (red bar) in B6 (white bars) and Rb/+ (black bars) adult mice ……140

8 Apoptotic cells in stage-XII tubule sections of B6 (A) and Rb/+ (B) 23-day old mice …… 142

9 CENP-E staining in prometaphase and metaphase spermatocytes from B6 and Rb/+ mice …….. 148

10 CENP-F staining in prometaphase and metaphase spermatocytes from B6 and Rb/+ mice …….. 150

PART V: CONCLUSION

1 Immunofluorescent staining of *Mei1*$^{+/+}$ and *Mei1*$^{-/-}$ mouse spermatocytes ……. 173

FIGURE PAGE

2 Localization of PLK1 in C57 and Rb/+ metapahse spermatocytes ……..…… 176

3 γ-H2AX (green) and SYCP3 (red) staining in a Rb/+ spermatocyte …...…… 181

PART I

INTRODUCTION*

*Part I is adapted and expanded from Handel MA, Cobb J, Eaker S (1999): What are the spermatocyte's requirements for successful meiotic division? J Exp Zool 285:243-250.

CHAPTER I

Meiotic Cell Cycle Progression in the Mouse

For successful reproduction, the proper completion of meiosis must unfold. Each gamete must receive one copy of each chromosome from the parental provider. Gametocytes must pair chromosomes, and initiate recombination. Not only is recombination an essential step in order to establish heterogeneity in offspring, but these recombination sites are also required for holding homologous chromosomes together for alignment during the first metaphase. Chromosomal condensation, spindle formation, and chromosomal alignment must occur properly and in a timely fashion. Events unfolding during this process occur temporally in succession or in concert. Failure in these events can lead to costly abnormalities and aneuploidy, as Klinefelter and Down syndromes (reviewed in Hassold and Hunt, 2001). Therefore, it is essential to understand both how and when specific cellular events take place during the mammalian meiotic division, as well as how these same events occur in an abnormal environment.

Gametogenesis in the male mouse occurs in three successive stages. The first stage is mitotic proliferation of spermatogonia. After a number of divisions, these spermatogonia differentiate into the first meiotic cell, the leptotene spermatocyte (Figure 1), defined by the initial appearance of lateral elements that will eventually form the synaptonemal complex. Leptonema is followed by zygonema, during which regions of homologous chromosome pairing are first detected. Proper pairing is mediated by the synaptonemal complex, as visualized by antibodies against the

SYCP3 protein in Figure 1. Zygotene spermatocytes enter the next stage, pachynema, when homologous chromosome pairing is complete. Pachynema ends with desynapsis and disassembly of the synaptonemal complex, a hallmark of the diplotene stage. The first evidence of chromosomal condensation is detected at diplotene by the phosphorylation of serine10 on histone H3 (Cobb et al., 1999b). Nuclear envelope breakdown, spindle formation, and chromosomal alignment onto the metaphase plate take place during prometaphase I and into metaphase I. After these events occur, anaphase I is initiated, separating homologous chromosomes to their respective poles, and forming two secondary spermatocytes. Within each of these spermatocytes, spindles reform and become bipolar. Chromosomes once again align during the initiation of the second meiotic division, MII. This division is more mitotic-like than the first division, separating sister homologs held together by cohesion proteins instead of recombination chiasmata. After chromosome alignment, anaphase II begins, separating each pair of sister chromatids. The products of a single primary spermatocyte are four round spermatids. Each round spermatid will enter spermiogenesis, and will develop into a functional spermatozoon.

Development and Regulation During Extended Prophase of Mouse Spermatogenesis

Meiotic development is essential to the production of functional gametes. Transitions in the cell cycle machinery are involved in activating/inhibiting this process. During both male and female meiosis, the mechanisms controlling development of two kinds: extrinsic and intrinsic (reviewed in Albertini and

Figure 1. Immunofluorescent staining of mouse spermatocytes through meiosis using developmental marker antibodies. SYCP3-red (A, B and C); β-tubulin-red (D, E and F); phosphoH3-green.

A. Leptonema/Zygonema	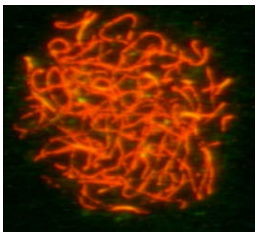	Synapsis begins in Zygonema DMC1 required
B. Pachynema	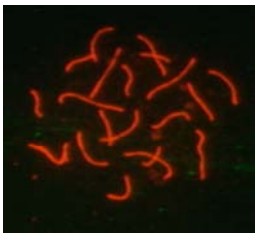	Chromosome synapsis H1t appears CDC25C appears Meiotic competence acquired
C. Diplonema	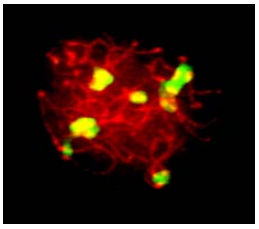	Desynapsis Nuclear envelope breakdown Histone H3 phosphorylation begins
D. Prometaphase	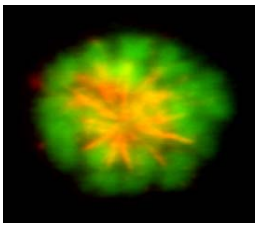	Monopolar spindle formation Complete chromosomal condensation
E. Metaphase I	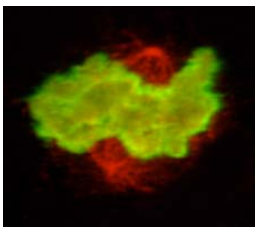	Chromosomes aligned/joined only by chiasmata TOPO II required Spindle formation
F. Anaphase I	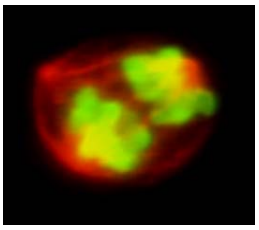	Homologs separate

Carabatsos, 1998). Extrinsic mechanisms involve hormonal influences from surrounding cells, Sertoli cells during spermatogenesis and follicular cells during oogenesis. These extrinsic factors are thought to be involved in the wave-like progression of stages in the seminiferous tubule. These stages, numbered I through XII in the mouse, are defined by specific sets of cell associations (Oakberg, 1956; Oakberg, 1957). Intrinsic mechanisms regulating spermatogenetic progress and meiosis involve the cell cycle machinery, with the probable major player being maturating-promoting factor (MPF). This kinase phosphorylates many substrates involved in cell cycle progression, and also plays a role in cyclin degradation.

Another requirement for meiotic progression is recombination. This process requires proteins involved in producing DNA double-strand breaks as well as mismatch and homologous DNA repair in order to form meiotic cross-overs, or chiasmata. The SPO11 protein has been shown to generate the double-strand breaks required for recombination in both male and female mice, and mice lacking the *Spo11* gene undergo apoptosis prior to the pachytene stage, the possible result of a pachytene checkpoint mechanism (Baudat et al., 2000; Romanienko and Camerini-Otero, 2000). In the mouse, the protein RAD51 is thought to correspond with "early recombination" or "meiotic nodules" (Moens et al., 1997; Plug et al., 1998). Foci of the DNA repair protein MLH1 may indicate sites of the "late recombination" nodules in the synaptonemal complex. MLH1 foci have been postulated to correspond to sites of reciprocal cross-over events (Baker et al., 1996; Plug et al., 1998). It is assumed that competence to enter meiotic metaphase arises soon after these recombination steps take place, concurrent with the appearance of the testis-specific histone H1t and

CDC25C phosphatase (Cobb et al., 1999a). The first appearance of H1t is concurrent with the disappearance of RAD51 foci (Moens et al., 1997). Understanding the temporal order of events and mechanisms of meiosis (Figure 2) can aid understanding the origin of meiotic abnormalities.

Requirements for Entry Into and Exit From the Meiotic Division Phase

After spermatocytes exit the extended prophase, they enter the meiotic division phase, the end result of which is separation of homologous chromosomes and sister chromatids. Within the testis, division-phase spermatocytes are present in stage XII of the seminiferous epithelium (Oakberg, 1956). Few in number, these cells are difficult to isolate or maintain in culture. These technical problems were overcome by tubule microdissection methods, taking advantage of stereomicroscopic transillumination to identify specific stages in the seminiferous tubule based on stage-specific light absorption patterns (Parvinen et al., 1993). This allows immunolocalization of proteins in specific stages of division, from which a developmental timeline of protein localization can be formed.

During entry into the first metaphase (MI), numerous chromosomal and structural changes occur in the mouse spermatocyte. Chromosomal condensation, initiated in the heterochromatic regions, can be detected in mouse spermatocytes with antibodies against the phosphorylated form of histone H3 on serine10 (pH3)(Cobb et al., 1999b). The pH3 antibody can be used to identify chromosomes during all stages of division, since this phosphorylation remains until after the second anaphase. Phosphorylation of histone H3 occurs before complete disassembly of the

Figure 2. Timeline representation of protein localization throughout meiosis in mouse spermatocytes. L/Z = leptotene/zygotene; Acetyl-H3 = acetylation of lysine 9 and lysine 14 on histone H3; Phospho-H3 = phosphorylation of serine10 on histone H3. Red-dotted arrow = increase in protein levels; Blue-dotted arrows = kinetochore localization.

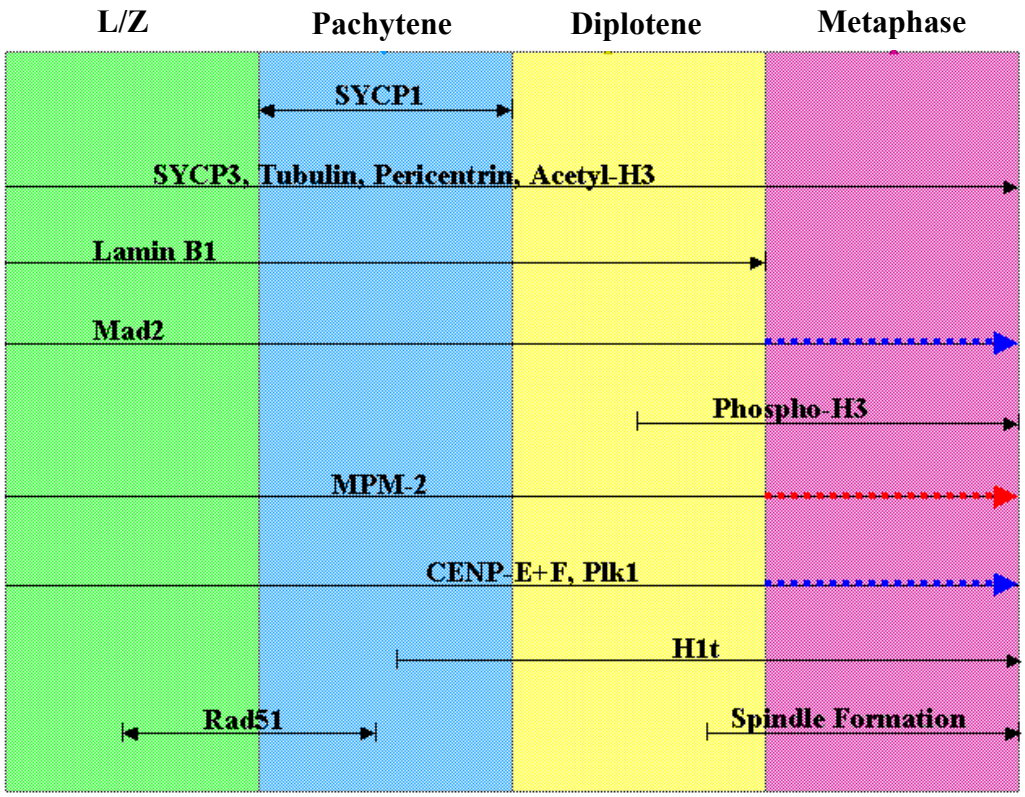
L/Z
Pachytene
Diplotene
Metaphase
SYCP1
SYCP3, Tubulin, Pericentrin, Acetyl-H3
Lamin B1
Mad2
Phospho-H3
MPM-2
CENP-E+F, Plk1
H1t
Rad51
Spindle Formation

synaptonemal complex, and is thus one of the earliest events signaling the onset of the meiotic division.

Nuclear envelope breakdown, detected by antibodies against lamin B1 and β–tubulin, occurs prior to spindle formation and chromosome alignment onto the metaphase plate (Kallio et al., 1998; Moss et al., 1993). Spindle formation is initiated by two adjacent centrosomes located next to the nucleus that undergo migration and separation to the poles during prometaphase (Kallio et al., 1998). During migration and microtubule elongation, kinetochores of the homologous chromosomes attach to the microtubules radiating from the spindle poles. The attachment of homologous pairs of chromosomes and their bipolar orientation on the spindle apparatus constitutes successful metaphase, and is probably the signal for the onset of anaphase and chromosome segregation.

Since accurate meiotic chromosome segregation is essential for the formation of euploid gametes, it is likely that the process of attachment to and alignment onto the meiotic spindle is monitored by a mechanism similar or analogous to that present during mitosis (Figure 3). Such a checkpoint might be the determinant of spermatocyte competence to execute anaphase segregation of homologous chromosomes. Insect spermatocytes monitor chromosome-spindle tension to signal the onset of anaphase (Nicklas, 1997). Most of our evidence about spindle checkpoint mechanisms during mammalian meiosis derives from studies in oocytes (Hunt and LeMaire-Adkins, 1998). Surprisingly, oocytes with univalent sex chromosomes exhibit abnormalities in chromosome attachment and orientation on the spindle, but do not show any delay in the metaphase to anaphase transition (LeMaire-

Figure 3. Diagram of the spindle assembly checkpoint mechanism by kinetochore/microtubule attachment in mitosis. Microtubule and CENP-E attachment eventually lead to the activation of the anaphase-promoting complex (APC).

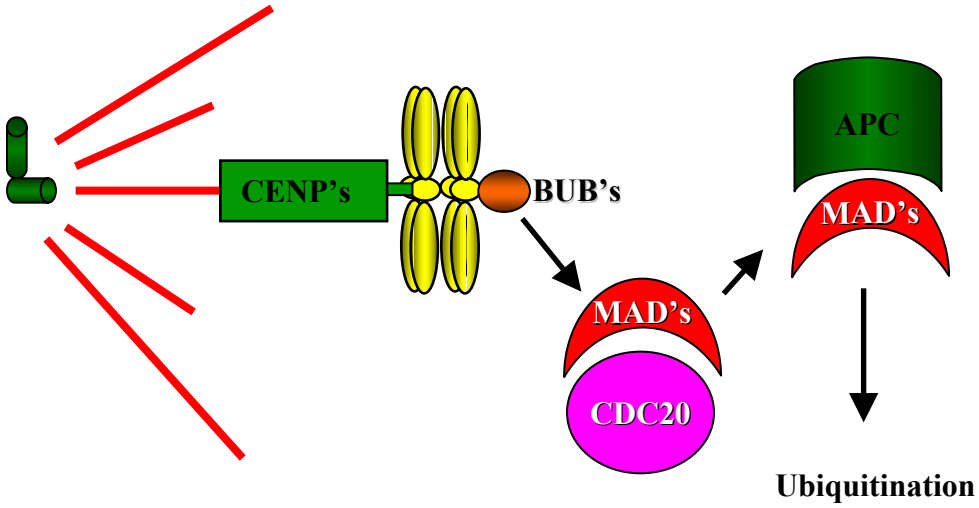
CENP's
BUB's
MAD's
CDC20
APC
MAD's
Ubiquitination

Adkins et al., 1997). However, spermatocytes containing unpaired sex chromosomes show a metaphase arrest (Burgoyne et al., 1992; Kot and Handel, 1990; Sutcliffe and Burgoyne, 1989). Evidence for a possible spindle checkpoint mechanism detecting chromosomal abnormalities during mammalian meiosis is scarce.

Gaps in Our Knowledge of Meiotic Development

Many of the events during the meiotic division are not well understood, and this is especially true for the G2/M transition. Knowledge of how and when various meiotic events take place with respect to each other is also lacking. The roles of checkpoint mechanisms governing accurate progress of these events are well studied in the yeast and mammalian mitotic system, but knowledge is deficient about their role in the mammalian meiotic system. For instance, in the budding yeast, the pachytene checkpoint (monitoring recombination), is well understood (reviewed in Roeder and Bailis, 2000), but remains to be elucidated in the mammalian meiotic system. Knock-out studies and immunofluorescent localization will provide insight into the function of many genes responsible for checkpoint control during meiotic development. For example, it was recently shown that mouse spermatocytes lacking the synaptonemal complex protein SCP3 arrest in early meiotic prophase and undergo apoptosis (Yuan et al., 2000). When placed in a p53-deficient background, the phenotype of SCP3-deficiency was unchanged, showing that apoptosis due to the failure of SC formation is p53-independent (Yuan et al., 2001). It was also shown that a possible "synapsis checkpoint" in X*Sxr*^{a}O mouse spermatocytes, inducing

apoptosis, was also p53-independent (Odorisio et al., 1998). Thus it remains to be determined what mechanism(s) regulate meiotic prophase events such as synapsis.

Most data concerning possible spindle assembly checkpoint mechanisms in mammalian meiosis are limited to the localization of putative checkpoint proteins identified in other model organisms. The spindle assembly checkpoint has been well defined in the budding yeast, with many protein players involved in the mechanism having been identified (Figure 3). These proteins include the Bub (budding uninhibited by benzimidazole) and Mad (mitotic arrest-deficient) protein families, whose homologs have been identified in the human and mouse (Li and Benezra, 1996; Taylor et al., 1998; Taylor and McKeon, 1997). While little is known about the action of these proteins during mammalian meiosis, proteins such as CENP-E, CENP-F and MAD2 have been localized to the kinetochores of chromosomes from early prophase through anaphase in mouse spermatocytes (Kallio et al., 2000; Kallio et al., 1998)(Part 2 of this Dissertation). CENP-E is a kinesin-like motor protein thought to be involved in the mechanistic process of chromosomal alignment during mitosis (Yen et al., 1992), and is localized to the centriolar region from early prophase up to prometaphase (Part 2, Figure 7). CENP-E then localizes to the kinetochore/microtubule attachment sites during metaphase. CENP-F is localized in the spermatocyte nuclear matrix until prometaphase, then in metaphase it relocates to the spindle microtubule attachment sites (Kallio et al., 1998)(Part 2, Figure 7). Kinetochores of unaligned chromosomes stain intensely for antibodies against CENP-E in HeLa cells (Chan et al., 1998) and mouse spermatocytes (Eaker et al., 2001). This localization suggests that cells can recognize chromosomal abnormalities during

metaphase, and recruit more of the motor protein to the unaligned kinetochore. These localizations imply function for spindle checkpoint elements during the spermatocyte meiotic division, but more functional studies must take place in order to determine the exact mechanism.

Conclusion

Insight into how and when events occur during normal meiotic division, as well as to the consequences when these events unfold in an abnormal environment is provided in this Dissertation. These topics will be presented by the following specific aims:

Specific Aim of Part II: To elucidate the temporal order of events occurring during the mouse meiotic division using immunofluorescence.

This work tested the hypothesis that events occurring during the meiotic division are sequential and can be studied by a variety of techniques, primarily immunofluorescence, using staged spermatocytes. These data serve to set the framework for future studies.

Specific Aim of Part III: To study the meiotic abnormalities during the metaphase transition in MLH1-deficient mouse spermatocytes.

This work tested the hypothesis that when the DNA mismatch repair protein MLH1 is removed from mouse spermatocytes, meiotic division does not occur normally, and cell death occurs in response to univalence and/or a failure of chromosome alignment onto the metaphase plate.

Specific Aim of Part IV: To study the Robertsonian-heterozygous mouse as a model for abnormal meiotic development.

This work tested the hypothesis that Robertsonian-heterozygous mice, having an increased level of sperm aneuploidy and pairing defects during pachytene, do not properly align homologous chromosomes onto the metaphase plate. This defect, when present during meiotic divisions, leads to an activation of a spindle assembly checkpoint and programmed cell death.

LIST OF REFERENCES

Albertini DF, Carabatsos MJ. 1998. Comparative aspects of meiotic cell cycle control in mammals. J Molecular Med Imm 76:795-799.

Baker SM, Plug AW, Prolla TA, Bronner CE, Harris AC, Yao X, Christie DM, Monell C, Arnheim N, Bradley A, Ashley T, Liskay RM. 1996. Involvement of mouse *Mlh1* in DNA mismatch repair and meiotic crossing over. Nat Genet 13:336-342.

Baudat F, Manova K, Yuen JP, Jasin M, Keeney S. 2000. Chromosome synapsis defects and sexually dimorphic meiotic progression in mice lacking *Spo11*. Mol Cell 6:989-998.

Burgoyne PS, Sutcliffe MJ, Mahadevaiah SK. 1992. The role of unpaired sex chromosomes in spermatogenic failure. Andrologia 24:17-20.

Chan GKT, Schaar BT, Yen TJ. 1998. Characterization of the kinetochore binding domain of CENP-E reveals interactions with the kinetochore proteins CENP-F and hBUBR1. J Cell Biol 143:49-63.

Cobb J, Cargile B, Handel MA. 1999a. Acquisition of competence to condense metaphase I chromosomes during spermatogenesis. Dev Biol 205:49-64.

Cobb J, Miyaike M, Kikuchi A, Handel MA. 1999b. Meiotic events at the centromeric heterochromatin: histone H3 phosphorylation, topoisomerase II alpha localization and chromosome condensation. Chromosoma 108:412-425.

Eaker SS, Pyle AD, Cobb JA, Handel MA. 2001. Evidence for meiotic spindle checkpoint from analysis of spermatocytes from Robertsonian-chromosome-heterozygous mice. J Cell Sci, *In Press.*

Hassold T, Hunt P. 2001. To ERR (meiotically) is human: the genesis of human aneuploidy. Nature Reviews Genetics 2:280-291.

Hunt PA, LeMaire-Adkins R. 1998. Genetic control of mammalian female meiosis. In MA Handel (ed): "Meiosis and Gametogenesis," 37. 525 B Street, Suite 1900, San Diego, CA 92101-4495: Academic Press Inc, pp 359-381.

Kallio M, Eriksson JE, Gorbsky GJ. 2000. Differences in spindle association of the mitotic checkpoint protein Mad2 in mammalian spermatogenesis and oogenesis. Dev Biol 225:112-123.

Kallio M, Mustalahti T, Yen TJ, Lahdetie J. 1998. Immunolocalization of alpha-tubulin, gamma-tubulin, and CENP-E in male rat and male mouse meiotic divisions: Pathway of meiosis I spindle formation in mammalian spermatocytes. Dev Biol 195:29-37.

Kot MC, Handel MA. 1990. Spermatogenesis in XO*Sxr* mice: Role of the Y chromosome. J Exp Zool 256:92-105.

LeMaire-Adkins R, Radke K, Hunt PA. 1997. Lack of checkpoint control at the metaphase/anaphase transition: A mechanism of meiotic nondisjunction in mammalian females. J Cell Biol 139:1611-1619.

Li Y, Benezra R. 1996. Identification of a human mitotic checkpoint gene: hsMAD2. Science 274:246-248.

Moens PB, Chen DJ, Shen ZY, Kolas N, Tarsounas M, Heng HHQ, Spyropoulos B. 1997. Rad51 immunocytology in rat and mouse spermatocytes and oocytes. Chromosoma 106:207-215.

Moss SB, Burnham BL, Bellvé AR. 1993. The differential expression of lamin epitopes during mouse spermatogenesis. Mol Reprod Dev 34:164-174.

Nicklas RB. 1997. How cells get the right chromosomes. Science 275:632-637.

Oakberg EF. 1956. Duration of spermatogenesis in the mouse and timing of stages of the seminiferous epithelium. Am J Anat 99:507-516.

Oakberg EF. 1957. Duration of spermatogenesis in the mouse. Nature 180:

Odorisio T, Rodriguez TA, Evans EP, Clarke AR, Burgoyne PS. 1998. The meiotic checkpoint monitoring synapsis eliminates spermatocytes via p53-independent apoptosis. Nat Genet 18:257-261.

Parvinen M, Toppari J, Lahdetie J. 1993. Transillumination phase contrast microscope techniques for evaluation of male germ cell toxicity and mutagenicity. In RE Chapin and JJ Heindel (ed): "Methods in Toxicology," 3, part A. San Diego: Academic Press, pp 142-165.

Plug AW, Peters AHFM, Keegan KS, Hoekstra MF, de Boer P, Ashley T. 1998. Changes in protein composition of meiotic nodules during mammalian meiosis. J Cell Sci 111:413-423.

Roeder GS, Bailis JM. 2000. The pachytene checkpoint. Trends Genet 16:395-403.

Romanienko PJ, Camerini-Otero RD. 2000. The mouse *Spo11* gene is required for meiotic chromosome synapsis. Mol Cell 6:975-987.

Sutcliffe MJ, Burgoyne PS. 1989. Analysis of the testes of H-Y negative XO*Sxr*^{b} mice suggests that the spermatogenesis gene (*Spy*) acts during the differentiation of the A spermatogonia. Development 107:373-380.

Taylor SS, Ha E, McKeon F. 1998. The human homologue of Bub3 is required for kinetochore localization of Bub1 and a Mad3/Bub1-related protein kinase. J Cell Biol 142:1-11.

Taylor SS, McKeon F. 1997. Kinetochore localization of murine Bub1 is required for normal mitotic timing and checkpoint response to spindle damage. Cell 89:727-735.

Yen TJ, Li G, Schaar BT, Szilak I, Cleveland DW. 1992. CENP-E is a putative kinetochore motor that accumulates just before mitosis. Nature 359:536-539.

Yuan L, Liu JG, Zhao J, Brundell E, Daneholt B, Hoog C. 2000. The murine *SCP3* gene is required for synaptonemal complex assembly, chromosome synapsis, and male fertility. Mol Cell 5:73-83.

Yuan L, Liu J-G, Hoja M-R, Lightfoot DA, Hoog C. 2001. The checkpoint monitoring chromosomal pairing in male meiotic cells in p53-independent. Cell Death Diff 8:316-317.

PART II

TEMPORAL ORDERING OF EVENTS DURING THE MEIOTIC G2/M TRANSITION IN SPERMATOGENESIS*

*The work for this part was accomplished by efforts of Shannon Eaker and Amy Inselman.

ABSTRACT

Understanding the order of events is an essential aspect of developmental biology. During cell division, specific events must occur to enable the initiation of later events. This is equally true for the meiotic processes leading to formation of mammalian gametes. Synaptonemal complex formation and disassembly, chromosome condensation, nuclear envelope breakdown and spindle formation during the G2/M transition of meiosis have all been studied, but the exact timing of these events in relationship to one another is not well understood. The approach taken to address this problem was to develop a stage-specific "timeline" documenting the localization of structural and enzymatic proteins in meiotic mouse spermatocytes. Experiments were conducted to localize chromosomal proteins (histone H1t, phosphorylated histone H2AX, acytelated histone H3, phosphorylated histone H3, recombination-mediating protein RAD51), structural proteins (synaptonemal complex protein SYCP3, tubulin, pericentrin), and cell cycle proteins (CENP-E, CENP-F, MAD2, MPM-2, PLK1). Surface-spread chromatin preparations, fibrin clot-embedded spermatocytes and isolated stage XII tubule segments were used in conjunction with immunofluorescence and western blot analysis to develop a stage-specific temporal order of the events that accompany the dramatic changes occurring during the meiotic G2/M transition. This framework creates a reference point for future experiments, and will be useful for the characterization of meiotic mutations. In addition, this “baseline” can be used to infer regulatory relationships among proteins during the meiotic G2/M transition.

CHAPTER I

INTRODUCTION

Establishing the timing and order of how and when cellular events unfold is a critical aspect of developmental biology, especially since many biological processes are initiated by the ending of a preceding process. For example, during cell division, spindle formation and chromosome condensation must precede cytokinesis in order for an accurate division to unfold. Cell division is not, however, error free. Failure in processes such as chromosome alignment or spindle formation during meiosis can lead to the production of aneuploid gametes, potentially resulting in lethality. In order to understand both normal mechanisms and the etiology of error, it is important to document and establish a timeline of the developmental events leading to meiotic divisions.

Spermatogenesis is a complex series of precisely timed events. Although the testis is formed in the fetus, it is not until after birth that a series of spermatogonial mitotic divisions leads to the production of meiotic prophase spermatocytes. After the extended meiotic prophase and two divisions, spermiogenesis leads to the formation of mature spermatozoa. This work has focused on ordering the events that occur during meiosis, with an emphasis on extended prophase and the transition into metaphase of the first division.

During the first stage of meiotic prophase, leptotene, the axial elements of the synaptonemal complex (SC) begin to form, and meiotic recombination is initiated. It is during leptotene that the chromosomes begin a homology search (Scherthan et al.,

1998). Initiation of chromosome pairing is characteristic of zygonema, the stage following leptonema. Recombination is one of the most important events during meiosis (reviewed in Hassold et al., 2000). Firstly, it is largely responsible for the genotypic variation observed within a population. Secondly, the chiasmata produced during recombination are required for maintaining the pairing of the homologous chromosomes up to the first meiotic division. Without proper pairing, chromosomes will fail to align correctly during metaphase, leading to aneuploidy or possibly cell death. During pachynema, the longest phase of meiotic prophase, the chromosomes are fully synapsed and recombination events go to completion or near completion. The large increase in cell size occurring in this stage may reflect the need to prepare for the meiotic divisions and/or spermiogenesis. Competence to enter the first meiotic division is established during mid-pachytene (reviewed in Handel et al., 1999), coinciding with the appearance of the testis-specific histone H1t and the accumulation of CDC25C (Cobb et al., 1999a). Other requirements for the division include synapsis and an increase in MPF and topoisomerase II activity. The phase following pachynema, diplonema, is characterized by the initiation of chromosome desynapsis and chromosome condensation, commencing in the heterochromatic regions.

After the extended prophase of meiosis I, the spermatocytes undergo dynamic structural rearrangements, such as nuclear envelope breakdown, chromosome condensation and spindle formation. The first meiotic division is the reductional segregation of homologous chromosomes, from a 2N to 1N chromosomal constitution, or 4C to 2C DNA content. The second division is more like mitosis, in

that sister chromatids are separated equationally, reducing the DNA content from 2C to 1C.

Existing evidence suggests the presence of checkpoints at various stages of meiotic prophase and the division phases, ensuring the correct chromosomal constitution of the gametes. Many proteins involved in meiotic checkpoints and repair mechanisms in other model organisms have been localized to the synaptonemal complex in mouse spermatocytes (reviewed in Tarsounas and Moens, 2001). The pachytene checkpoint, monitoring the completion of recombination and proper chromosome synapsis, has been well documented in the budding yeast (Roeder and Bailis, 2000). The power of yeast genetics allows the characterization of many checkpoint proteins, while most mammalian meiotic genes are discovered through sequence homology and are difficult to study in vivo. A similar scenario is seen with respect to the mitotic spindle assembly checkpoint, monitoring spindle damage and proper alignment of chromosomes onto the metaphase plate (reviewed in Amon, 1999). Many kinetochore-associated and soluble proteins, such as the BUB and MAD family members, are thought to relay signals from damaged spindles or unaligned chromosomes to the cell cycle machinery. These signals initiate an "anaphase-wait" signal, inhibiting the ubiquitination activity of the anaphase-promoting complex (APC). Although this mechanism has been well studied in the yeast and mitotic systems, knowledge of this mechanism and the players involved is lacking for mammalian meiosis.

Documentation of the temporal order of meiotic events in mouse spermatocytes can yield information about the roles of the potential players in these

checkpoints and overall developmental processes. This work has focused on using immunolocalization to develop such a timeline. This not only provides a framework for which a "baseline" developmental timetable can be produced, but can also be a valuable tool in determining how and when specific proteins function. This knowledge can also be used to determine gene function in mutants retrieved from phenotype-driven mutagenesis screens.

CHAPTER II

MATERIALS AND METHODS

Germ Cell Isolation

C57BL/6J mice (The Jackson Laboratory, Bar Harbor, ME) were housed under 14 hour light /10 hour dark photo-periods at constant temperature (21° C), with free access to standard laboratory chow and water. Mice were sacrificed by cervical dislocation, the testes were removed, detunicated and digested in 0.5mg/ml collagenase (Sigma) in Krebs-Ringer bicarbonate (KRB) buffer at 32° C for 20 minutes, followed by digestion in 0.5mg/ml trypsin (Sigma) in KRB at 32° C for 13 minutes to obtain isolated germ cells. After digestion, the germ cells were filtered through an 80μM mesh filter and washed three times in KRB. Spermatocytes were processed as described below for fibrin clot embedding or surface-spread chromatin preparations.

Fibrin Clot Embedding

Spermatocytes isolated from germ cell preparations were embedded in fibrin clots as previously described (Eaker et al., 2001). Briefly, isolated spermatocytes were brought to a concentration of 25 X 10^{6} cells/ml. On a Gold Seal Rite-On Fluorescent Antibody slide (Fisher Scientific), 1.5 μl of the cell suspension was added to 3 μl of fibrinogen (Calbiochem, 10mg/ml) prepared fresh. To the cell/fibrinogen mix, 2.5 μl of thrombin (Sigma, 250 units) was added with mixing and clots were allowed to form. Slides with clots were fixed in 4% paraformaldehyde.

Before processing for immunolocalization, the fibrin clots were washed in 0.2% Triton X-100 (Sigma) followed by blocking in PBS/10% goat serum (Gibco BRL) for 30 minutes.

Surface-Spread Chromatin Preparations

Surface-spread chromatin preparations for visualization of the synaptonemal complex were performed as previously described (Cobb et al., 1999a). Briefly, germ cells were fixed in 2% paraformaldehyde/0.03% SDS before being spread onto Shandon slides (Shandon Lippshaw, Pittsburgh, PA). The slides were allowed to air dry and then blocked in wash buffer (0.3% BSA, 1.0% goat serum in PBS) before being processed for immunolocalization.

Isolation of Meiotically Dividing Spermatocytes

To obtain cytological preparations enriched in meiotically dividing spermatocytes (stage XII of the mouse seminiferous epithelium), a variation of the transillumination procedure (Parvinen et al., 1993) was used (Eaker et al., 2001). Testes from adult mice were detunicated and digested with 0.5mg/ml collagenase in KRB for 8 minutes at 32 ^{o}C to obtain isolated seminferous tubules. Transillumination patterns were observed with a dissecting microscope, and used to identify stage XII segments of the seminferous tubules. The desired stage XII segments were excised and transferred onto a microscope slide in KRB. The tubules were attached to the slide by placing a coverslip over the segment followed by submersion of the entire slide in liquid N_2 for 30 seconds. The coverslip was

removed and the slide was fixed in 3:1 ethanol/acetic acid. Prior to incubation with antibody, the slides were washed in PBS/0.2% Triton X-100 for 5 minutes followed by blocking in PBS/10% goat serum for 30 minutes.

Immunoblot Analysis

Cell isolation and preparation of lysates were performed as previously described (Cobb et al., 1999b). Proteins were separated by SDS-PAGE, 150V for 45 min. Proteins were then transferred to a nitrocellulose membrane, blocked in PBS containing 2% BSA, 0.1% Tween-20, 100nM NaCl, 10mM Tris pH 7.5, then incubated with the primary antibody for 1 hour. After three washes in PBS/0.1% Tween-20, the secondary peroxidase-conjugated antibody was added for 2 hours. The membranes was washed again, then developed by enhanced chemiluminescence detection (ECL; Amersham Corp.).

Immunolocalization

Primary antibodies used included those that recognized the proteins SYCP3 (Eaker et al., 2001), tubulin (Amersham), phospho-histone H3 (Upstate Biotech.), acetylated-histone H3 (Upstate Biotech.), phospho-histone H2AX (Upstate Biotech.), the MPM-2 epitope (Upstate Biotech), CENP-E (Schaar et al., 1997), CENP-F (Liao et al., 1995), *Xenopus* MAD2 (Chen et al., 1996), pericentrin (Covance Inc.), PLK1 (Upstate Biotech), RAD51 (Oncogene), and histone H1t (see below)**.** Following overnight incubation with primary antibody, the slides were incubated with rhodamine- or flourescein-conjugated secondary antibodies (Pierce). Coverslips were

mounted using Prolong Antifade (Molecular Probes) containing DAPI (Molecular Probes) to visualize the DNA. Control slides were incubated with either pre-immune sera or with secondary antibodies only in order to determine antibody specificity. Immunolocalization was observed with an Olympus epifluorescence microscope. All images were captured to Adobe PhotoShop using a Hamamatsu color 3CCD camera.

H1t Antibody Production

The polyclonal antibody recognizing histone H1t was prepared by Covance Research Products (Richmond, CA) against recombinant his-tagged protein expressed in E. coli. The H1t cDNA was synthesized by RT-PCR from testicular RNA and cloned into the pPROExHta expression vector (GibcoBRL, Rockville, MD) and the sequence was verified by direct sequencing. Two guinea pigs were injected intramuscularly with 0.5mg of purified H1t protein in 6M urea followed by booster injections of 0.25mg protein at three-week intervals. Serum was collected at three-week intervals beginning one month after the initial injection. Serum from one of the guinea pigs contained specific antibodies that recognized the H1t protein. The specificity of the antiserum was determined by immunoblotting using extracts from pachytene spermatocytes know to contain the H1t protein. Extracts of germ cells from 9-day old mice were used as a negative control. Serum collected after antigen injection from the positive guinea pig recognized only protein of the appropriate molecular weight on western blots and stained only spermatocytes known to contain the H1t protein (mid-pachytene and later stage spermatocytes). Pre-immune serum did not recognize proteins from spermatocytes on western blots.

CHAPTER III

RESULTS AND DISCUSSION

Synaptonemal Complex Formation and Disassembly

The antibodies used in the development of the timeline were chosen for their usefulness in documenting the numerous changes that occur during the meiotic G2/M transition. Some of the antibodies used were selected for their ability to aid in staging the different cell types during spermatogenesis. The majority of this work has been previously reported and published by other labs. We have repeated many of the localization patterns in order to confirm the staining on our own preparations, to set the framework for staging with a known pattern, and to validate our anti-SYCP3 antibody. Antibodies recognizing the SYCP3 protein, found in the lateral elements of the synaptonemal complex (SC), are commonly used to stage mouse spermatocytes (Figure 1)(Dobson et al., 1994). Previous studies have demonstrated the formation of the SC to be an important event during meiotic prophase, as the male *Sycp3* knockout mouse is sterile, although the central SC protein SCP1 is present but not assembled into SC (Yuan et al., 2000). Immunolocalization, as well as western blot analysis, has demonstrated the presence of the SYCP3 protein in leptotene spermatocytes, coincident with the initial formation of the lateral elements of the SC. As the spermatocyte nears zygonema, the immunological pattern of the SYCP3 protein changes and no longer appears as patches, but is detected along each homologous chromosome as it continues its homology search. Synapsis of homologous

Figure 1. Immunofluorescent images from surface-spread chromatin preparations. Images presented in each column represent antibody localization during a specific meiotic developmental stage; Pach = pachynema, MI = metaphase I, and RS/ES = round spermatids/elongated spermatids. The images presented in rows represent specific antibody localization or DNA staining: anti-SYCP3 (red), DAPI (blue), anti-γ-H2AX, anti-H1t and anti-phospho-H3 (green).

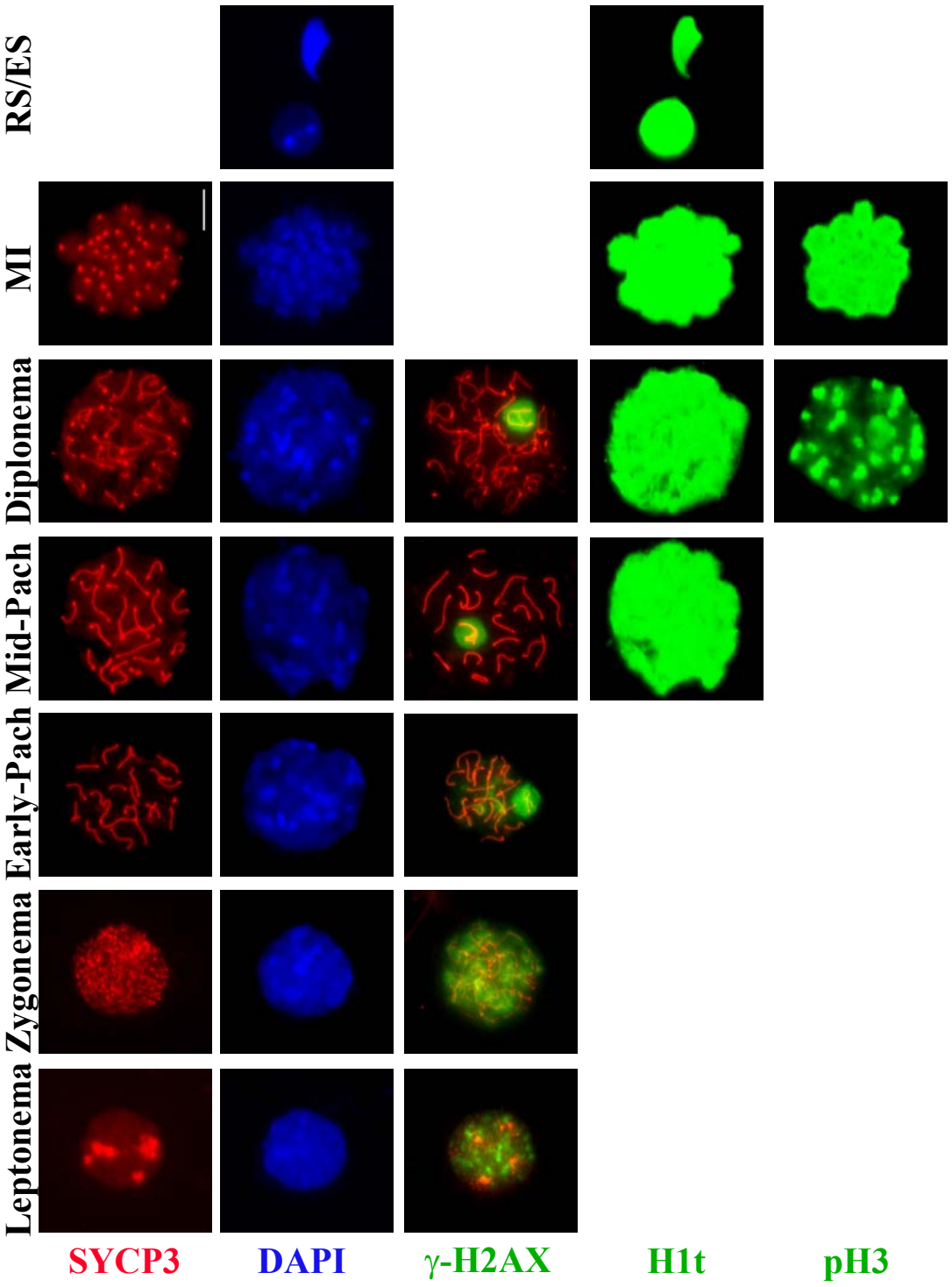
RS/ES
MI
Diplonema
Mid-Pach
Early-Pach
Zygonema
Leptonema
SYCP3
DAPI
γ-H2AX
H1t
pH3

chromosomes is also initiated in zygotene. During pachytene, the central element of the SC, SYCP1/SYN1, is completely formed and is seen connecting each homologous chromosome pair. As the spermatocyte enters diplonema, the SC begins to dissociate in a "zipper-like" fashion, first noticeable at the ends of the chromosomes. Although the SC begins to dissassemble during diplonema, the SYCP3 antibody still localizes to the kinetochores through the first meiotic division (Figure 1) (Moens and Spyropoulos, 1995). However, during the second meiotic division, the SYCP3 protein is lost. The pattern of SYCP3 localization on fibrin clot embedded spermatocytes is similar to the pattern observed on surface-spread chromatin preparations (Figure 2 versus Figure 1). By using antibodies against the SC protein SYCP3, we were able to correctly identify the major stages of spermatocyte development during prophase.

Histones and Histone Modifications in Mouse Spermatocytes

Although the antibody that recognizes the SYCP3 protein is very useful in staging spermatocytes, it cannot be used to discriminate among all spermatocyte stages. For example, early-, mid- and late-pachytene spermatocytes all show similar staining with anti-SYCP3. The antibody that recognizes the histone H1-testis specific variant (H1t), however, can be used to discriminate amoung these cell types, and its localization has been previously validated by other labs as well as our own. H1t replaces the somatic linker histones H1.1 and H1.2 throughout the nucleus (Meistrich et al., 1985). This histone transition is, however, not required for meiosis to proceed, as *H1t*$^{-/-}$ spermatocytes develop normally throughout spermatogenesis (Drabent et al.,

Figure 2. Immunofluorescent images from fibrin clot embedded spermatocytes. The images present in each column represent antibody localization during a specific meiotic developmental stage; Pach = pachynema, and MI = metaphase I. The images presented in each row represent specific antibody localization or DNA stain: anti-SYCP3 (red), DAPI (blue), and anti-phospho-H3, anti-pericentrin and anti-β-tubulin (green). DAPI, SYCP3 and pH3 immunolocalization/staining represent images acquired from the same spermatocyte, while the other images were acquired from different spermatocytes at the same developmental time point.

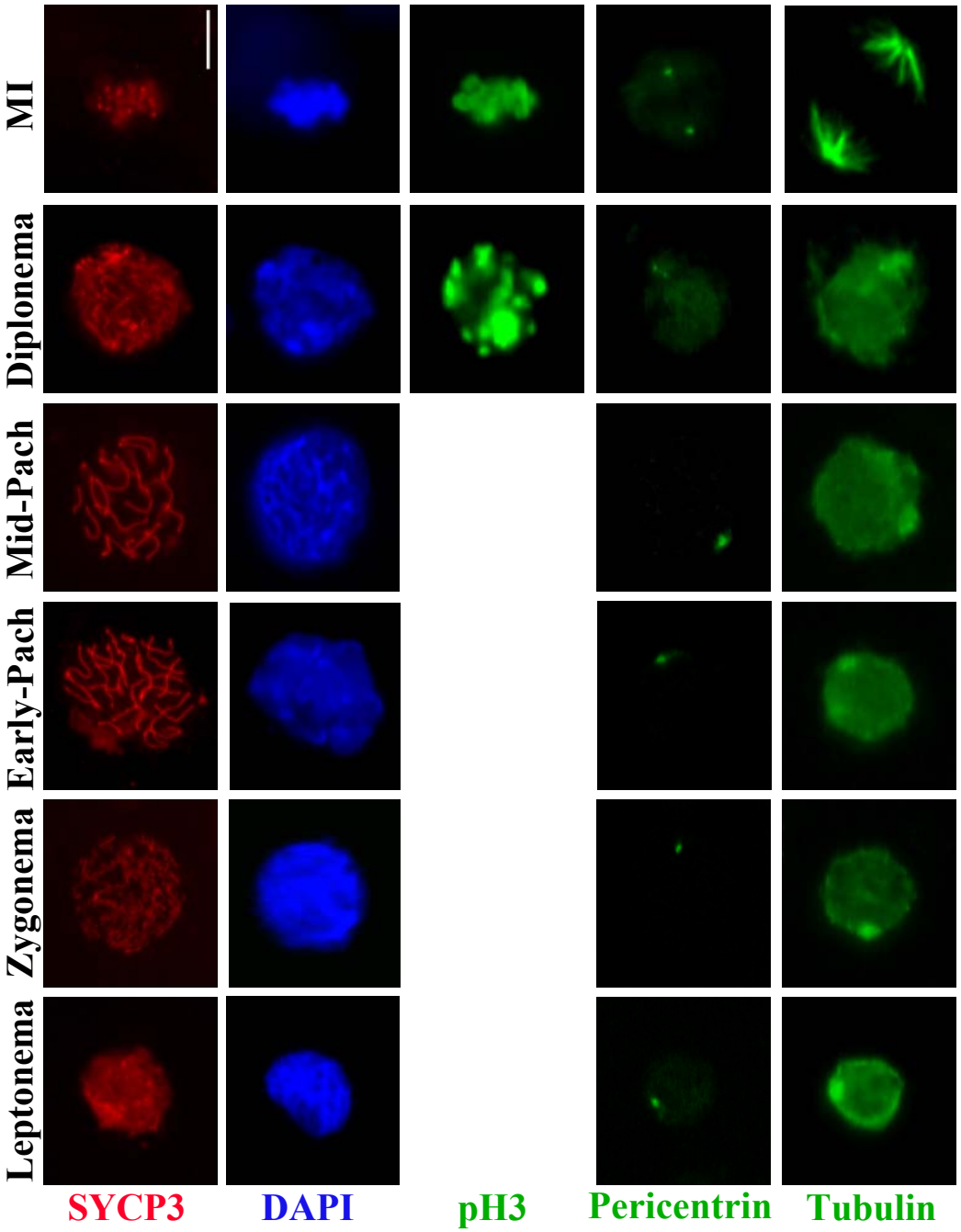
MI
Diplonema
Mid-Pach
Early-Pach
Zygonema
Leptonema
SYCP3
DAPI
pH3
Pericentrin
Tubulin

2000). The histone H1-testis specific variant is first detected in mid-pachytene spermatocytes, remains throughout the division phase, and is still detected in elongating spermatids (Drabent et al., 1996; Moens, 1995; Oko et al., 1996) (Figure 1). Early pachytene spermatocytes do not have the H1t linker histone present. The localization of the H1t protein is seen in both surface-spread chromatin preparations (Figure 1) and in fibrin clot preparations (data not shown). This antibody allows the discrimination of early-pachytene spermatocytes from mid- to late-pachytene spermatocytes. It is also important to note that the initial presence of *H1t* coincides with spermatocyte competence to condense chromatin during pachytene of meiosis (Cobb et al., 1999a).

Recent evidence suggests that recombination-mediated DNA double strand breaks is initiated prior to synapsis (visualized using SC antibodies) in mouse spermatocytes (Mahadevaiah et al., 2001). This was confirmed by the localization pattern of the γ-H2AX antibody, detecting a modified histone associated with chromatin containing double strand breaks. γ-H2AX localization is first seen at leptotene, and is scattered throughout nuclei until pachytene, at which point it becomes concentrated in the sex body, comprised of the condensed sex chromosomes (Figure 1). All γ-H2AX localization is lost during the first metaphase. The transition from zygonema to early pachytene is of key importance, as this marks the loss of the dispersed staining pattern of γ-H2AX, as well as the time point when synapsis is first detected. The temporal relationship between meiotic recombination and synapsis has been a topic of controversy (Santos, 1999). Recombination allows genetic exchange during meiosis, from which DNA double strand breaks are produced and crossover

events occur. Chiasmata are defined as the structural sites where these crossover events take place. Although meiotic recombination precedes synapsis in both mice (Mahadevaiah et al., 2001) and *S. cerevisiae* (Padmore et al., 1991), the opposite is true in *D. melanogaster* (McKim et al., 1998) and *C. elegans* (Dernburg et al., 1998). The mouse *Spo11* gene has been shown to be required for meiotic chromosome synapsis by the production of double strand breaks, and these double strand breaks are required for both DMC1/RAD51 localization and chromosome synapsis (Baudat et al., 2000; Mahadevaiah et al., 2001; Romanienko and Camerini-Otero, 2000). It is crucial to determine how a specific mechanism, such as recombination or synapsis, occurs temporally with respect to other events in order to study the overall mechanism in question. The localization of γ-H2AX may play an important role in establishing the efficiency of DNA repair in meiotic mutants.

Another event during spermatogenesis that can be monitored on both types of preparations (Figures 1 and 2) and is useful for staging spermatocytes is the phosphorylation of the serine 10 residue on histone H3 (Cobb et al., 1999b). The phosphorylation of serine 10 is thought to regulate chromosome condensation (Van Hooser et al., 1998). This phosphorylation might be regulated by members of the aurora kinase B family and interacting phosphatases (Hsu et al., 2000). Phosphorylation of histone H3 originates in the heterochromatic regions of diplotene spermatocytes, and radiates to cover the entire chromatin area at MI (Cobb et al., 1999a). After the second meiotic division, localization of the phospho-H3 antibody is no longer detected, suggesting dephosphorylation of the chromatin at the Ser10

residue and decondensation. This antibody is useful when identifying spermatocytes entering the G2/M transition.

Histone acetylation is known to be involved in transcriptional activity, genomic imprinting, and maintenance of centromere structure (Cheung et al., 2000). To document changes in the acetylation status of the chromatin, the antibody recognizing the acetylation of lysine residues 9 and 14 on histone H3 was used. A decrease in the intensity of the staining was observed with spermatocyte progression through prophase I (Figure 3). The most intense staining was seen in spermatogonia and leptotene spermatocytes. As the cells entered zygonema, a decrease in the intensity of the antibody localization was observed. The lower intensity of antibody localization remained constant until the cells reached the round spermatid stage, when a slight increase in intensity was observed. However, as the cells progress through prophase I, the nuclei increase in size, which may cause the intensity of the staining pattern to decrease without any actual change in acetylation of the chromatin. To clarify the pattern of histone acetylation, a western blot was performed. No change in histone H3 acetylation was observed throughout spermatogenesis (data not shown), supporting the hypothesis that the apparent decrease in acetyl-H3 staining intensity was simply a result of the increase in cell size**.** Interestingly, the transcriptionally inactive heterochromatic areas of the chromosomes, visualized by DAPI staining (data not shown), do not stain with antibody to acetylated H3. This observation supports other evidence suggesting that acetylation positively regulates transcriptional activity.

Figure 3. Localization of the acetylated form of histone H3 throughout spermatogenesis. The images presented in columns represent antibody localization during a specific meiotic developmental stage; SG = spermatogonia, Pach = pachynema, MI = metaphase I, RS/ES = round spermatids/elongated spermatids. Images presented in the bottom row represent an overlay of localization using the acetylated histone H3 antibody (red) and the SYCP3 (green) antibody. Images presented in each column were acquired from the same cell. Inserts in both SG and RS/ES images represent DAPI/DNA staining of the large image.

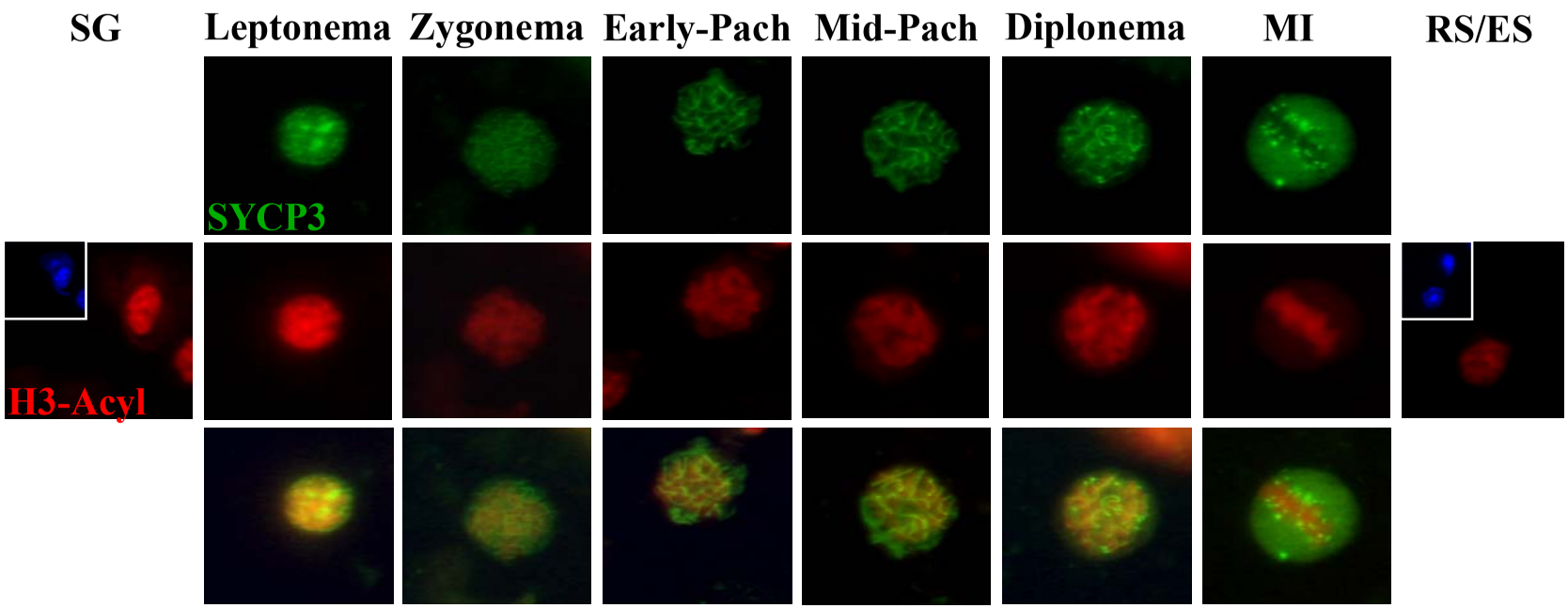
SG
Leptonema
Zygonema
Early-Pach
Mid-Pach
Diplonema
MI
RS/ES
SYCP3
H3-Acyl

Structural Protein Localization in Fibrin-Clot Preparations

Although antibodies such as those that recognize SYCP3, H1t and the phosphorylated form of histone H3 localize on both surface-spread chromatin preparations (Figure 1) and on fibrin clot embedded (Figure 2) spermatocyte preparations, this is not true for all types of antibodies. The surface-spread method of preparation is a rather harsh method which spreads the cells onto a slide, destroying the nuclear envelope. Since the nuclear envelope proteins are washed away, many soluble proteins, as well as the nuclear architecture, are not conserved. The difference between the surface-spread and clot-embedded preparations can be seen when comparing the alignment of the chromosomes onto the metaphase plate, visualized with the phospho-H3 antibody on the fibrin clot preparations (Figure 2). This alignment can be compared to the lack of chromosome alignment observed in the surface-spread chromatin preparation (Figure 1). In order to preserve the three-dimensional structure and the soluble proteins, many antibodies were used on spermatocytes embedded in fibrin clots. Antibodies against structural proteins, such as pericentrin, were used on the fibrin clots to document the numerous structural rearrangements during meiotic prophase and the division phase. Pericentrin, a protein located in the centriolar region of the microtubule organizing center (MTOC), is seen throughout meiosis and becomes bipolar during spindle development (Figure 2). It localizes as punctate spots, co-localizing with another centrosomal protein γ-tubulin. Tubulin localization is also observed throughout meiosis, enveloping the nucleus as a sphere and appearing more prominent near the centriolar region with localization changing at MI to reflect the role of tubulin in spindle formation (Figure 2).

Elongation of the microtubules from the MTOC to the kinetochores is visible during the first metaphase. These antibodies are valuable when studying the G2/M transition in mouse spermatocytes, and possible spindle and chromosomal abnormalities which may arise.

Localization of Cell Cycle Regulating Proteins

Proteins involved in processes such as DNA damage repair, although not necessarily unique to meiosis, serve as useful markers while ordering the timing of events in relation to one another during meiosis. One of these proteins, RAD51, is thought to be involved in repairing double-strand breaks, occurring during recombination (Bishop et al., 1992; Shinohara et al., 1992). The RAD51 antibody co-localizes with antibodies against the SC during early prophase of mouse and rat spermatocytes (Ashley et al., 1995; Haaf et al., 1995; Ikeya et al., 1996; Moens et al., 1997). This localization is seen as a punctate pattern during leptonema, increasing during zygonema, and is visible more intensely on the sex chromosomes during mid- to late-pachytene (Figure 4). RAD51 foci are not seen in spermatocytes which are positive for H1t, also appearing at mid-pachytene. RAD51 antibodies localization is useful when distinguishing early- from late-pachytene spermatocytes. RAD51 antibodies also co-localize with the γ-H2AX antibody (recognizing double-strand breaks, see above), but the RAD51 localization is lost during mid-pachytene while the γ-H2AX localization remains through diplonema. Although this finding suggests that RAD51's role as a recombinase is finished during mid-pachytene, the fact that the γ-H2AX antibody still localizes to the sex body after RAD51 leaves is noteworthy.

Figure 4. RAD51 localization during early meiotic prophase. The images in columns represent antibody localization during a specific meiotic developmental stages; Pach = pachynema. The images in rows represent localization of anti-RAD51 (green) and anti-SYCP3 (red). Images in each column were acquired from the same spermatocytes. The lower row represents an overlay of the RAD51 and SYCP3 immunolocalization.

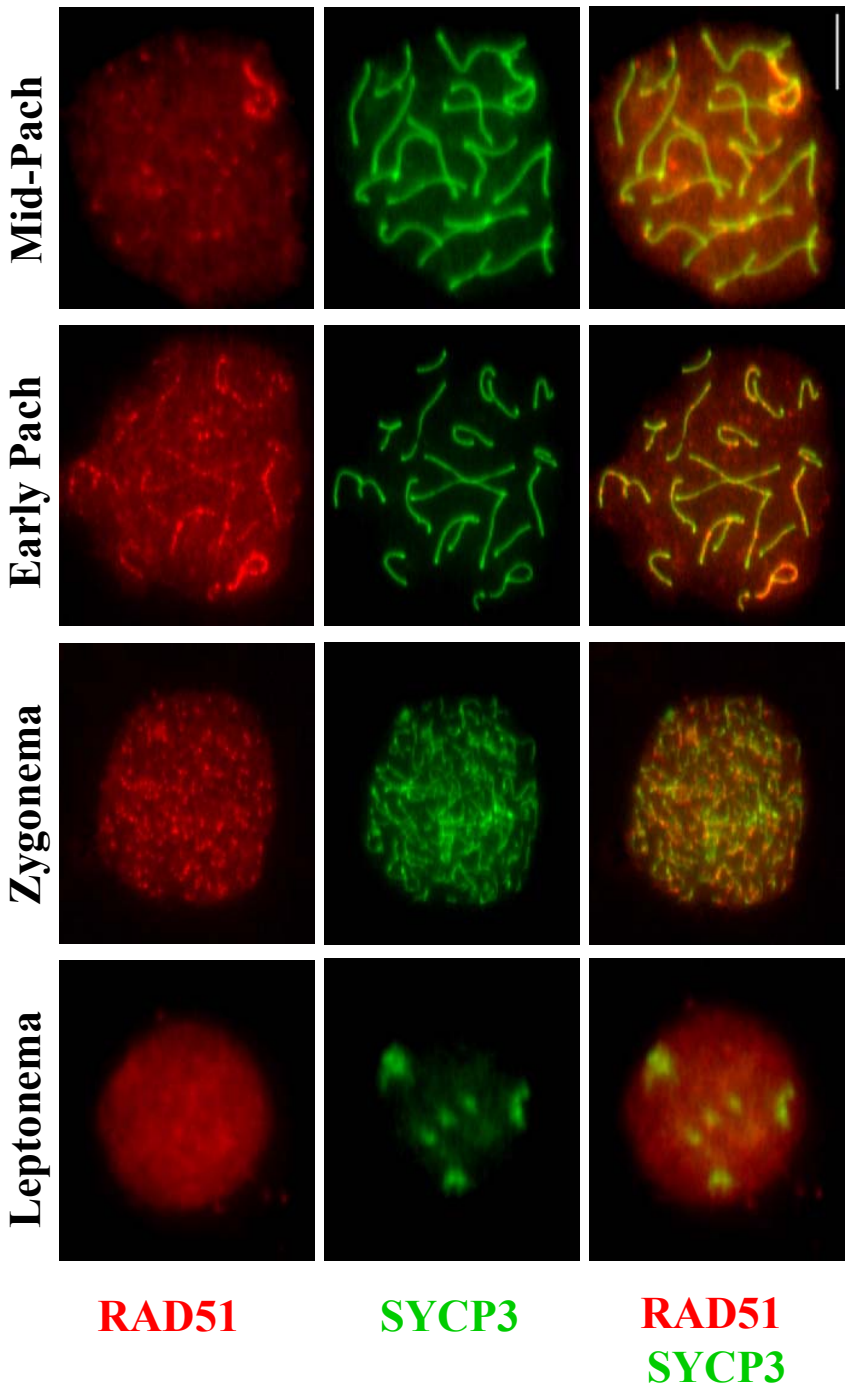
Mid-Pach
Early Pach
Zygonema
Leptonema
RAD51
SYCP3
RAD51
SYCP3

The MPM-2 antibody recognizes phosphorylated epitopes on phosphoproteins during mitosis and meiosis. These proteins become phosphorylated prior to and during cellular division, and are located primarily on the sex chromosomes during meiotic prophase (Figure 5). An increase in MPM-2 localization can be seen during metaphase and anaphase (Figure 5). The increase in MPM-2 intensity suggests the importance of phosphorylation reactions in controlling the meiotic division phase. One kinase which may be necessary in regulating this transition is the Polo-like kinase 1 (PLK). Named after the polo gene of *Drosophila melanogaster*, Polo-like kinases are involved in spindle development (Nigg, 1998) and possibly DNA damage repair (Smits et al., 2000). As seen through western blot analysis, PLK1 is expressed in testicular cells from spermatogonia through round spermatids (Figure 6), and is localized in the centriolar regions by immunofluorescence (Matsubara et al., 1995). However, we have shown that before and during the first meiotic division, PLK1 localizes to the kinetochores of mouse spermatocytes as seen by co-localization with SYCP3 antibodies (Figure 7). This localization has also been seen in mitotic cells (Arnaud et al., 1998) and mouse oocytes (Wianny et al., 1998), suggesting that PLK might play a role in the spindle assembly checkpoint mechanism by monitoring the correct alignment of chromosomes onto the metaphase plate. It was previously shown that kinetochores from unaligned chromosomes of mouse spermatocytes stain more intensely with antibodies against the checkpoint motor proteins CENP-E and CENP-F (Eaker et al., 2001). A difference in intensity was not seen with PLK localization on unaligned versus aligned kinetochores (Part V, Figure 2). The role of PLK in spindle development and/or DNA repair in meiosis remains to be determined.

Figure 5. MPM-2 localization throughout meiotic prophase and the division phase. The images in columns represent antibody localization during specific meiotic developmental stages; MI = metaphase I. The images presented in the top row represent localization of MPM-2 antibody (green), while those in the bottom are representative of an overlay of MPM-2 (green) and anti-SYCP3 (red) localization.

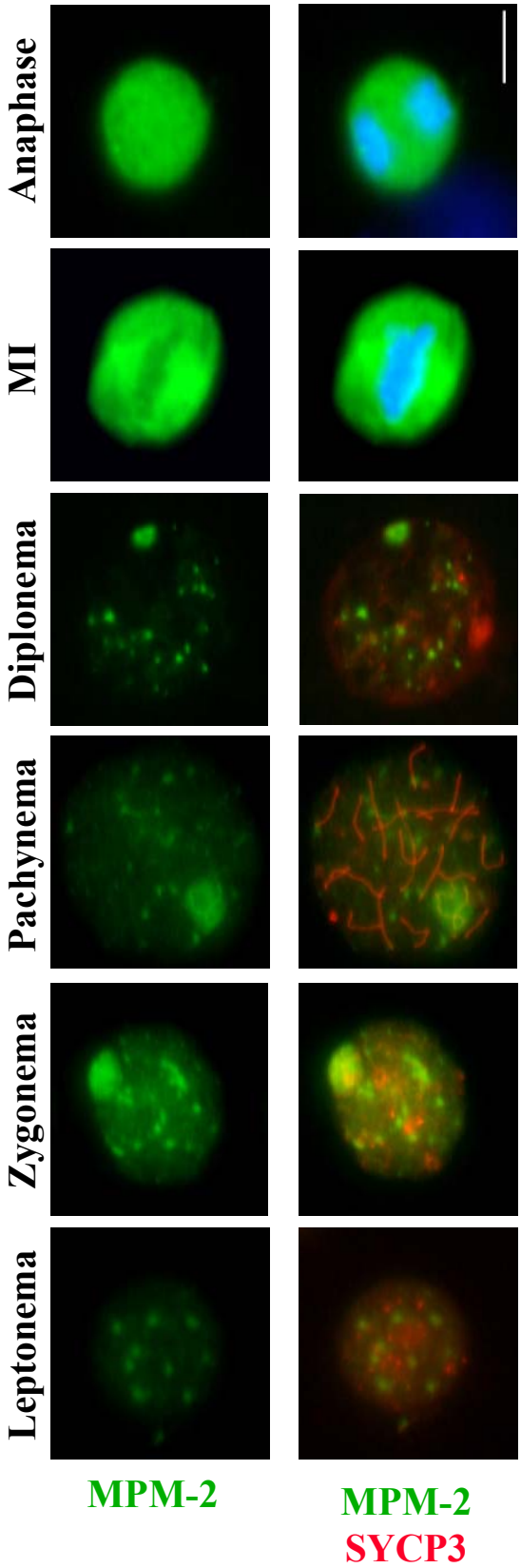
Anaphase
MI
Diplonema
Pachynema
Zygonema
Leptonema
MPM-2
MPM-2
SYCP3

Figure 6. Western blot analysis of PLK1. Columns represent stages; G = spermatogonia, L/Z = leptotene/zygotene, EP = early pachytene, P = pachytene, P+OA = pachytene treated with okadaic acid, XII = stage XII sections, RS = round spermatids, RB = residual bodies, Adult = adult germ cells. Arrow = expected molecular weight of PLK1.

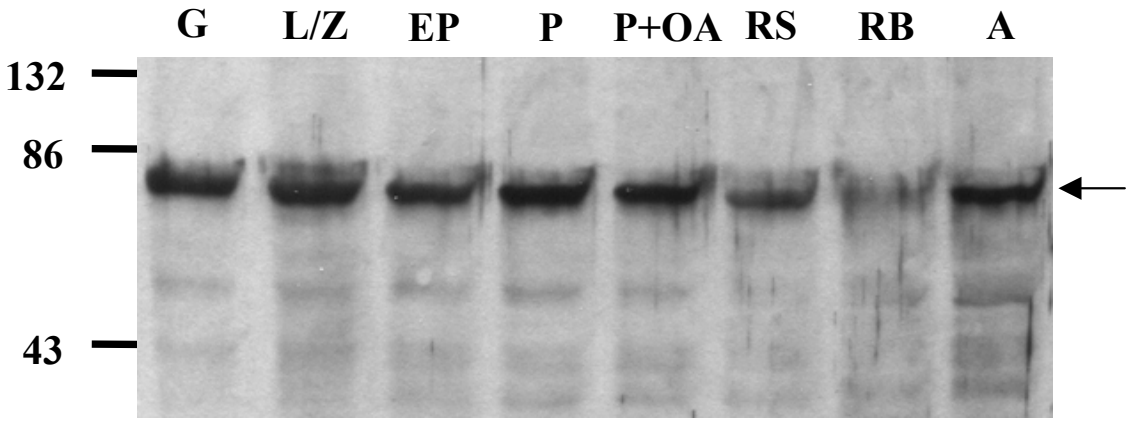
G
L/Z
EP
P
P+OA
RS
RB
A
132
86
43

Figure 7. PLK1 localization in late prophase and metaphase I spermatocytes. The images in columns represent antibody localization during specific meiotic stages. The images presented in rows represent localization of anti-PLK1 (red) and anti-SYCP3 (green) throughout meiosis. Images present in each column were acquired from the same cell. The lower row is representative of an overlay of PLK and SYCP3 immunolocalization, along with DAPI (blue) staining to visualize the DNA.

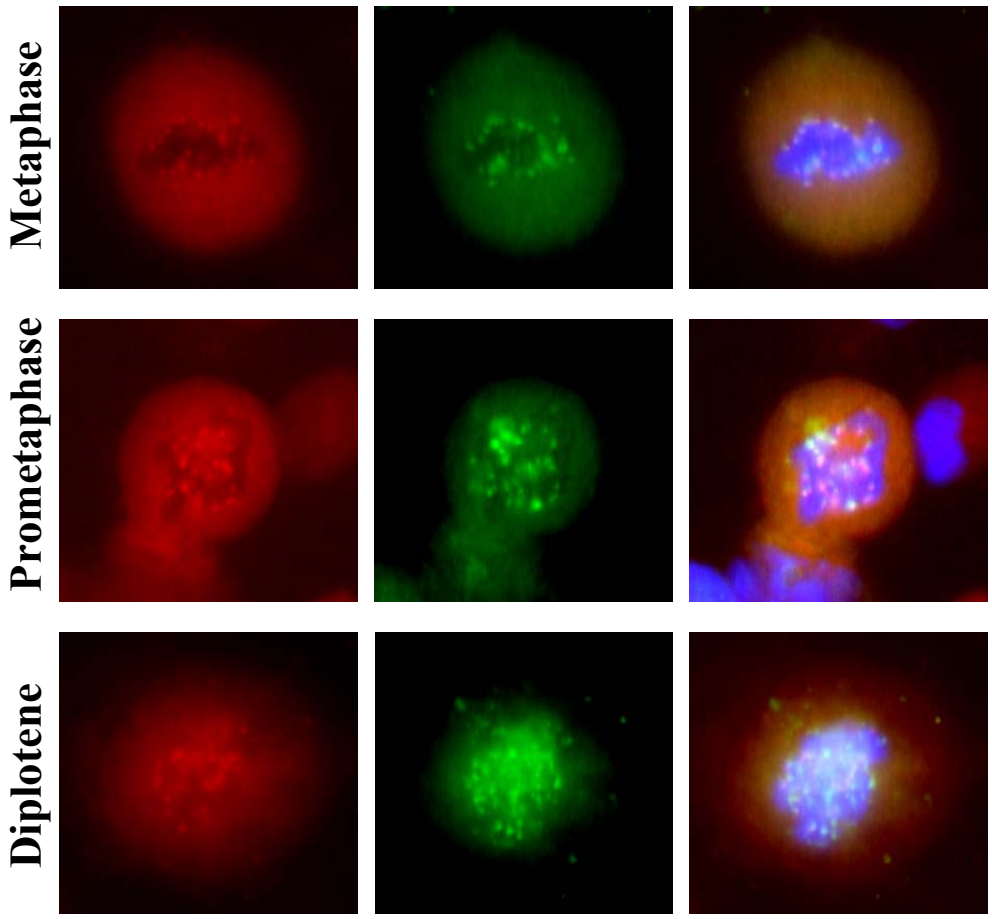
Metaphase
Prometaphase
Diplotene
PLK1
SYCP3
PLK1
SYCP3
DAPI

Localization of Spindle Checkpoint Proteins

The localization of proteins involved in the spindle assembly checkpoint was also investigated in this meiotic timeline. CENP-E, a kinesin-like motor protein, has been localized to the kinetochores of metaphase mouse spermatocytes (Kallio et al., 1998) and pig oocytes (Lee et al., 2000). Figure 8 shows the localization of CENP-E and CENP-F (a related kinesin-like motor protein) throughout meiotic prophase and into metaphase. Both proteins co-localize with the centriolar region during prophase, then relocate to the kinetochore/microtubule attachment sites (visualized with CREST antisera, data not shown) during prometaphase and metaphase. The expression level of CENP-E and CENP-F was also monitored by western blot analysis (Figure 9). Both are present in the mitotically dividing spermatogonia. During leptonema, expression is low, but gradually increases into pachynema and diplonema (Figures 8 and 9). The expression levels from pachytene to metaphase do not drastically change, as monitored by western blot analysis of pachytene spermatocytes and pachytene spermatocytes treated with okadaic acid (OA). OA is a phosphatase inhibitor, which has been shown to initiate the metaphase transition in pachytene spermatocytes (Wiltshire et al., 1995). Although these localizations imply function in monitoring proper metaphase entry, knock-out strategies for both CENP-E and CENP-F will provide vital information as to the role of both proteins during mammalian meiosis.

Another player in the spindle checkpoint mechanism, MAD2, is involved in the "anaphase wait" signal, arresting the cell in metaphase until all chromosomes are

Figure 8. Developmental immunofluorescent localization of CENP-E and CENP-F in cytological preparations. The images in each column represents antibody localization during specific meiotic developmental stages; MI = metaphase I. The images in rows represent specific antibody localization throughout meiotic prophase and division. The first and second rows display anti-CENP-E (green) localization, and anti-CENP-E (green) and either anti-SYCP3 or anti-tubulin (red) co-localization, respectively. The third and fourth rows display CENP-F (green) localization, and CENP-F (green) and either SYCP3 or tubulin (red) co-localization, respectively. For images of CENP-E and CENP-F localization during prometaphase and MI, the antibody against tubulin was used to visualize the microtubules (red). In all other images, the antibody against SYCP3 was used (red).

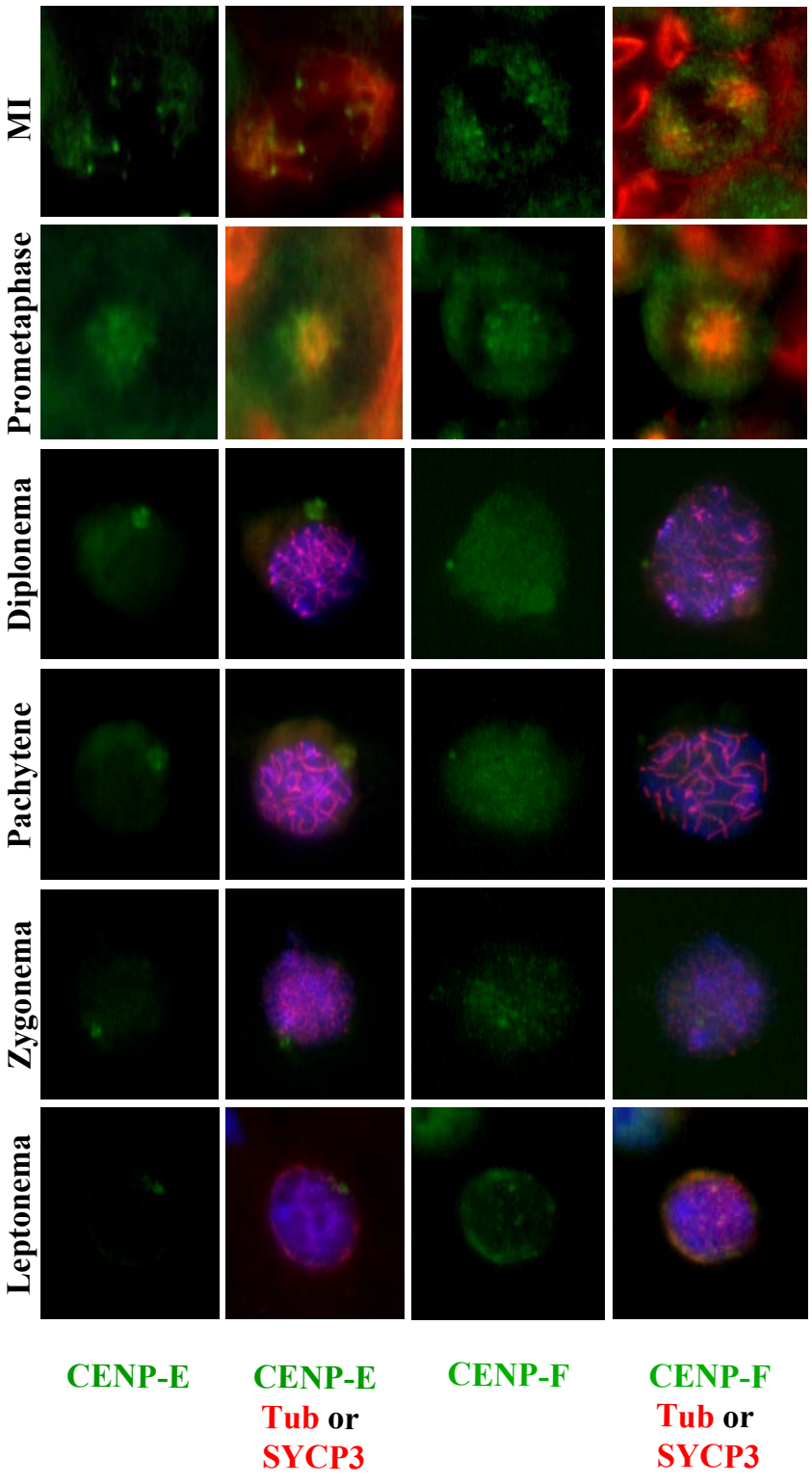
MI
Prometaphase
Diplonema
Pachytene
Zygonema
Leptonema
CENP-E
CENP-E
Tub or
SYCP3
CENP-F
CENP-F
Tub or
SYCP3

Figure 9. Western blot analysis of CENP-E and CENP-F. Columns represent stages; Gonia = spermatogonia, L/Z = leptotene/zygotene, EP = early pachytene, P = pachytene, P+OA = pachytene treated with okadaic acid, XII = stage XII sections, RS = round spermatids, RB = residual bodies, Adult = adult germ cells.

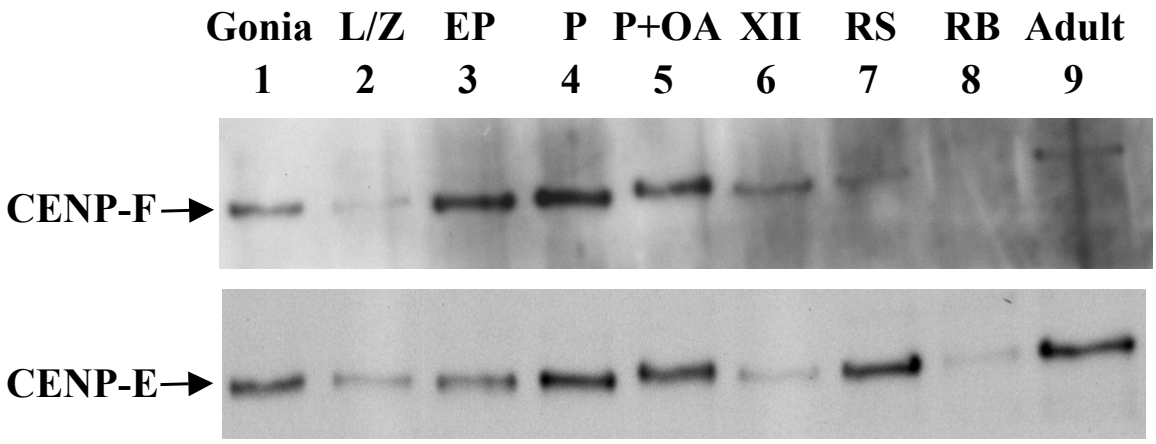
Gonia L/Z EP P P+OA XII RS RB Adult
1 2 3 4 5 6 7 8 9
CENP-F
CENP-E

properly aligned onto the metaphase plate. First identified in the budding yeast, MAD2 (Mitotic-Arrest Deficient) relays spindle damage and chromosome alignment signals to the anaphase promoting complex (APC). This complex, when active, causes the ubiquitination of proteins, initiating anaphase. MAD2 has previously been localized to the kinetochores of mouse meiotic metaphase spermatocytes (Kallio et al., 2000). Using an antibody against the *Xenopus* Mad2 protein (XMAD2), localization onto kinetochores was visualized throughout meiotic prophase and into metaphase (Figure 10). Western blot analysis showed that XMAD2 was ubiquitously expressed in spermatogonia, throughout meiotic prophase, and in round spermatids (Figure 11). Although XMAD2 is located on the kinetochore, a function for MAD2 during mammalian meiosis has not been determined.

Although some information is known about recombination and synapsis during meiotic prophase, little is known of the players involved in the G2/M transition. Here we have shown the localization of the checkpoint proteins MAD2, CENP-E and PLK1. What remains to be determined is how these proteins are involved in ensuring proper meiotic development. Does MAD2 play a role in detecting spindle damage and unaligned chromosomes? PLK1 may also regulate chromosomal dynamics, possibly through a checkpoint mechanism, in addition to playing a role in spindle duplication and formation. It was recently shown that the *Drosophila* POLO protein is required for the formation of MPM-2 phosphoepitopes (Logarinho and Sunkel, 1998). In addition, PLK1 may be responsible for phosphorylating the cyclin B1 subunit of the universal G2/M cell cycle transition protein maturation promoting factor (MPF), directing its localization to the nucleus

Figure 10. Developmental immunofluorescent localization of XMAD2 in cytological preparations. The images in each column represents antibody localization during specific meiotic developmental stages; MI=metaphase I. The images in rows represent specific antibody localization throughout meiotic prophase and division. The first and second rows display XMAD2 (red), and XMAD2 (red) and SYCP3 (green) co-localization, respectively.

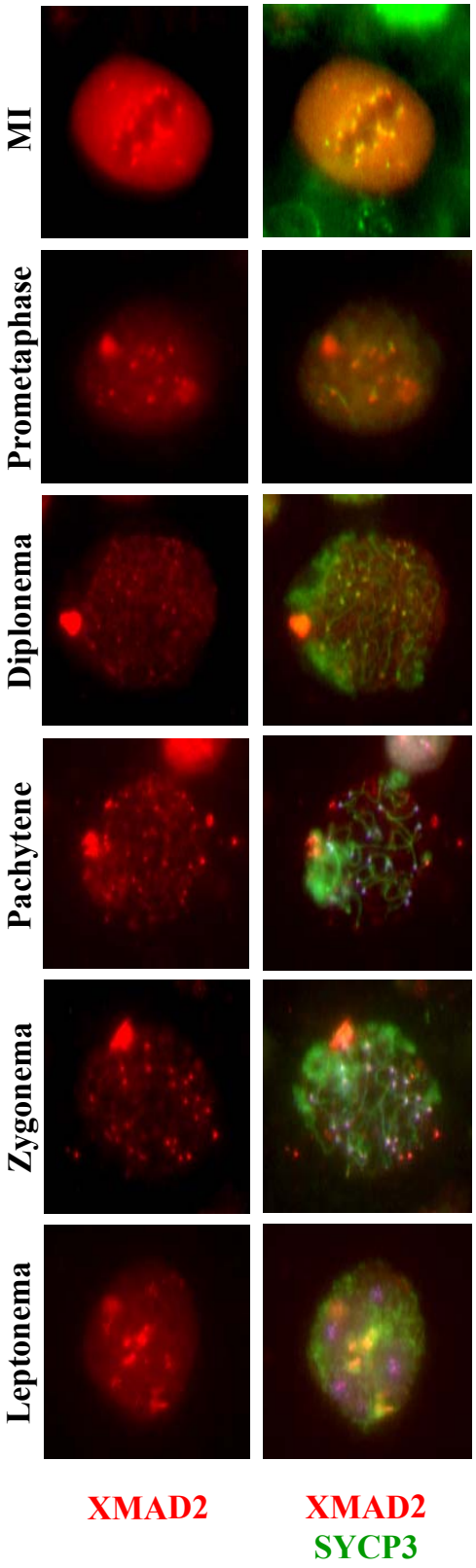
MI
Prometaphase
Diplonema
Pachytene
Zygonema
Leptonema
XMAD2
XMAD2
SYCP3

Figure 11. Western blot analysis of mouse MAD2 using antibodies against *Xenopus* MAD2 (XMAD2). Columns represent stages; G = spermatogonia, L/Z = leptotene/zygotene, EP = early pachytene, P = pachytene, P+OA = pachytene treated with okadaic acid, XII = stage XII sections, RS = round spermatids, Adult = adult germ cells, J = Jurkat control. Arrow = expected molecular weight of mouse MAD2.

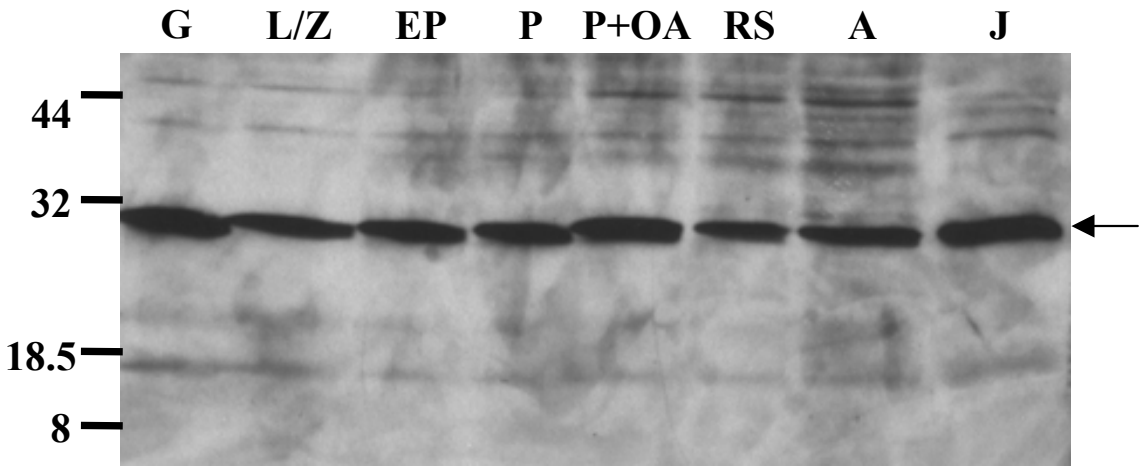
G
L/Z
EP
P
P+OA
RS
A
J
44
32
18.5
8

where it is needed for the meiotic division phase (Toyoshima-Morimoto et al., 2001). An accumulation of MPF, composed of the p34 kinase and the regulatory subunit cyclin B1, is seen during this transition. What is not clear is how this kinase might regulate downstream activities. How does MPF activity lead to nuclear envelope breakdown and spindle formation? How is MPF's activity regulated by the presence of spindle damage or unaligned chromosomes? The localization of these transitional proteins may lead to a better understanding of their role in meiotic events.

Conclusion

This work has established a meiotic "timeline" of events occurring in the male mouse. While determining the temporal order of events, mutations in functionally known as well as unknown genes can be studied in the context of normal meiotic development. For example, using the Cre/loxP recombination system, the cre recombinase linked to a meiotically-driven promoter (such as *Sycp1* or *Pgk-2*) can be used to remove any previously floxed meiotic gene (Ando et al., 2000; Vidal et al., 1998). This will allow testis-specific removal of the gene of interest in order to study its function during meiosis. This timeline will aid in determining the exact stage in which the removed or mutated gene may be required. It is certain that the future holds many undiscovered meiotic genes, and establishing a temporal framework will aid in determining the role of these genes in meiosis.

LIST OF REFERENCES

Amon A. 1999. The spindle checkpoint. Curr Opin Genet Dev 9:69-75.

Ando H, Haruna Y, Miyazaki J, Okabe M, Nakanishi Y. 2000. Spermatocyte-specific gene excision by targeted expression of cre recombinase. Biochem Biophys Res Commun 272:125-128.

Arnaud L, Pines J, Nigg EA. 1998. GFP tagging reveals human Polo-like kinase 1 at the kinetochore/centromere region of mitotic chromosomes. Chromosoma 107:424-429.

Ashley T, Plug AW, Xu JH, Solari AJ, Reddy G, Golub EI, Ward DC. 1995. Dynamic changes in Rad51 distribution on chromatin during meiosis in male and female vertebrates. Chromosoma 104:19-28.

Baudat F, Manova K, Yuen JP, Jasin M, Keeney S. 2000. Chromosome synapsis defects and sexually dimorphic meiotic progression in mice lacking *Spo11*. Mol Cell 6:989-998.

Bishop DK, Park D, Xu L, Kleckner N. 1992. *DMC1* : a meiosis-specific yeast homolog of E. coli *recA* required for recombination, synaptonemal complex formation, and cell cycle progression. Cell 69:439-456.

Chen RH, Waters JC, Salmon ED, A.W. M. 1996. Association of spindle assembly checkpoint component XMAD2 with unattached kinetochores. Science 274:242-246.

Cheung WL, Briggs SD, Allis CD. 2000. Acetylation and chromosomal functions. Curr Opin Cell Biol 12:326-333.

Cobb J, Cargile B, Handel MA. 1999a. Acquisition of competence to condense metaphase I chromosomes during spermatogenesis. Dev Biol 205:49-64.

Cobb J, Miyaike M, Kikuchi A, Handel MA. 1999b. Meiotic events at the centromeric heterochromatin: histone H3 phosphorylation, topoisomerase II alpha localization and chromosome condensation. Chromosoma 108:412-425.

Dernburg AF, McDonald K, Moulder G, Barstead R, Dresser M, Villeneuve AM. 1998. Meiotic recombination in *C. elegans* initiates by a conserved mechanism and is dispensable for homologous chromosome synapsis. Cell 94:387-398.

Dobson MJ, Pearlman RE, Karaiskakis A, Spyropoulos B, Moens PB. 1994. Synaptonemal complex proteins: occurrence, epitope mapping and chromosome disjunction. J Cell Sci 107:2749-2760.

Drabent B, Bode C, Bramlage B, Doenecke D. 1996. Expression of the mouse testicular histone gene H1t during spermatogenesis. Histochem Cell Biol 106:247-251.

Drabent B, Saftig P, Bode C, Doenecke D. 2000. Spermatogenesis proceeds normally in mice without linker histone H1t. Histochem Cell Biol 113:433-442.

Eaker SS, Pyle AD, Cobb JA, Handel MA. 2001. Evidence for meiotic spindle checkpoint from analysis of spermatocytes from Robertsonian-chromosome-heterozygous mice. J Cell Sci, In Press

Haaf T, Golub EI, Reddy G, Radding CM, Ward DC. 1995. Nuclear foci of mammalian Rad51 recombination protein in somatic cells after DNA damage and its localization in synaptonemal complexes. Proc Natl Acad Sci USA 92:2298-2302.

Handel MA, Cobb J, Eaker S. 1999. What are the spermatocyte's requirements for successful meiotic division? J Exp Zool 285:243-250.

Hassold T, Sherman S, Hunt P. 2000. Counting cross-overs: characterizing meiotic recombination in mammals. Hum Mol Genet 9:2409-2419.

Hsu JY, Sun ZW, Li XM, Reuben M, Tatchell K, Bishop DK, Grushcow JM, Brame CJ, Caldwell JA, Hunt DF, Lin RL, Smith MM, Allis CD. 2000. Mitotic phosphorylation of histone H3 is governed by IpI1/aurora kinase and Glc7/PP1 phosphatase in budding yeast and nematodes. Cell 102:279-291.

Ikeya T, Shinohara A, Sato S, Tabata S, Ogawa T. 1996. Localization of mouse Rad51 and Lim15 proteins on meiotic chromosomes at late stages of prophase 1. Genes Cells 1:379-389.

Kallio M, Eriksson JE, Gorbsky GJ. 2000. Differences in spindle association of the mitotic checkpoint protein Mad2 in mammalian spermatogenesis and oogenesis. Dev Biol 225:112-123.

Kallio M, Mustalahti T, Yen TJ, Lahdetie J. 1998. Immunolocalization of alpha-tubulin, gamma-tubulin, and CENP-E in male rat and male mouse meiotic divisions: Pathway of meiosis I spindle formation in mammalian spermatocytes. Dev Biol 195:29-37.

Lee J, Miyano T, Dai YF, Wooding P, Yen TJ, Moor RM. 2000. Specific regulation of CENP-E and kinetochores during meiosis I/meiosis II transition in pig oocytes. Mol Reprod Dev 56:51-62.

Liao H, Winkfein RJ, Mack G, Rattner JB, Yen TJ. 1995. CENP-F is a protein of the nuclear matrix that assembles onto kinetochores at late G2 and is rapidly degraded after mitosis. J Cell Biol 130:507-518.

Logarinho E, Sunkel CE. 1998. The *Drosophila* POLO kinase localises to multiple compartments of the mitotic apparatus and is required for the phosphorylation of MPM2 reactive epitopes. J Cell Sci 111:2897-2909.

Mahadevaiah SK, Turner JMA, Baudat F, Rogakou EP, de Boer P, Blanco-Rodriguez J, Jasin M, Keeney S, Bonner WM, Burgoyne PS. 2001. Recombinational DNA double-strand breaks in mice precede synapsis. Nat Genet 27:271-276.

Matsubara N, Yanagisawa M, Nishimune Y, Obinata M, Matsui Y. 1995. Murine polo-like kinase 1 gene is expressed in meiotic testicular germ cells and oocytes. Mol Reprod Dev 41:407-415.

McKim KS, Green-Marroquin BL, Sekelsky JJ, Chin G, Steinberg C, Khodosh R, Hawley RS. 1998. Meiotic synapsis in the absence of recombination. Science 279:876-878.

Meistrich ML, Bucci LR, Trostle-Weige PK, Brock WA. 1985. Histone variants in rat spermatogonia and primary spermatocytes. Dev Biol 112:230-240.

Moens PB. 1995. Histones H1 and H4 of surface-spread meiotic chromosomes. Chromosoma 104:169-174.

Moens PB, Chen DJ, Shen ZY, Kolas N, Tarsounas M, Heng HHQ, Spyropoulos B. 1997. Rad51 immunocytology in rat and mouse spermatocytes and oocytes. Chromosoma 106:207-215.

Moens PB, Spyropoulos B. 1995. Immunocytology of chiasmata and chromosomal disjunction at mouse meiosis. Chromosoma 104:175-182.

Nigg EA. 1998. Polo-like kinases: positive regulators of cell division from start to finish. Curr Opin Cell Biol 10:776-783.

Oko RJ, Jando V, Wagner CL, Kistler WS, Hermo LS. 1996. Chromatin reorganization in rat spermatids during the disappearance of testis-specific histone, H1t, and the appearance of transition proteins TP1 and TP2. Biol Reprod 54:1141-1157.

Padmore R, Cao L, Kleckner N. 1991. Temporal comparison of recombination and synaptonemal complex formation during meiosis in *S. cerevisiae*. Cell 66:1239-1256.

Parvinen M, Toppari J, Lahdetie J. 1993. Transillumination phase contrast microscope techniques for evaluation of male germ cell toxicity and mutagenicity. In RE Chapin and JJ Heindel (ed): "Methods in Toxicology," 3, part A. San Diego: Academic Press, pp 142-165.

Roeder GS, Bailis JM. 2000. The pachytene checkpoint. Trends Genet 16:395-403.

Romanienko PJ, Camerini-Otero RD. 2000. The mouse *Spo11* gene is required for meiotic chromosome synapsis. Mol Cell 6:975-987.

Santos JL. 1999. The relationship between synapsis and recombination: two different views. Heredity 82:1-6.

Schaar BT, Chan GKT, Maddox P, Salmon ED, Yen TJ. 1997. CENP-E function at kinetochores is essential for chromosome alignment. J Cell Biol 139:1373-1382.

Scherthan H, Eils R, Trelles-Sticken E, Dietzel S, Cremer T, Walt H, Jauch A. 1998. Aspects of three-dimensional chromosome reorganization during the onset of human male meiotic prophase. J Cell Sci 111:2337-2351.

Shinohara A, Ogawa H, Ogawa T. 1992. Rad51 protein involved in repair and recombination in *S. cerevisiae* is a RecA-like protein. Cell 69:457-470.

Smits VAJ, Klompmaker R, Arnaud L, Rijksen G, Nigg EA, Medema RH. 2000. Polo-like kinase-1 is a target of the DNA damage checkpoint. Nat Cell Biol 2:672-676.

Tarsounas M, Moens PB. 2001. Checkpoint and DNA-repair proteins are associated with the cores of mammalian meiotic chromosomes. Curr Top Dev Biol 51: 109-134.

Toyoshima-Morimoto F, Taniguchi E, Shinya N, Iwamatsu A, Nishida E. 2001. Polo-like kinase 1 phosphorylates cyclin B1 and targets it to the nucleus during prophase. Nature 410:215-220.

Van Hooser A, Goodrich DW, Allis CD, Brinkley BR, Mancini MA. 1998. Histone H3 phosphorylation is required for the initiation, but not maintenance, of mammalian chromosome condensation. J Cell Sci 111:3497-3506.

Vidal F, Sage J, Cuzin F, Rassoulzadegan M. 1998. Cre expression in primary spermatocytes: A tool for genetic engineering of the germ line. Mol Reprod Dev 51:274-280.

Wianny F, Tavares A, Evans MJ, Glover DM, Zernicka-Goetz M. 1998. Mouse polo-like kinase 1 associates with the acentriolar spindle poles, meiotic chromosomes and spindle midzone during oocyte maturation. Chromosoma 107:430-439.

Wiltshire T, Park C, Caldwell KA, Handel MA. 1995. Induced premature G2/M transition in pachytene spermatocytes includes events unique to meiosis. Dev Biol 169:557-567.

Yuan L, Liu JG, Zhao J, Brundell E, Daneholt B, Hoog C. 2000. The murine *SCP3* gene is required for synaptonemal complex assembly, chromosome synapsis, and male fertility. Mol Cell 5:73-83.

PART III

MEIOTIC ABNORMALITIES AND APOPTOSIS DURING METAPHASE IN MLH1-DEFICIENT MOUSE SPERMATOCYTES*

*The work for this part was accomplished by efforts of Shannon Eaker, April Pyle and John Cobb.

ABSTRACT

The MLH1 protein is known to be required for meiotic development, and when absent in the male mouse, sterility occurs, characterized by a lack of bivalent chromosomes at the first meiotic metaphase. Although germ cells from *Mlh1*$^{-/-}$ mice do not enter spermiogenesis, knowledge is lacking about the precise fate of the spermatocytes. It is known that *Mlh1*$^{-/-}$ spermatocytes do not maintain pairing of homologous chromosomes, since they are univalent at metaphase. The hypothesis of this work was that univalent chromosomes of spermatocytes lacking the MLH1 protein fail to align on the metaphase spindle, and apoptosis occurs after or at metaphase. To address these issues, we evaluated the meiotic competence, chromosomal behavior and apoptotic response of *Mlh1*$^{-/-}$ spermatocytes using immunofluorescence, in vitro culture of pachytene spermatocytes, and the TUNEL apoptosis assay. Pachytene spermatocytes from *Mlh1*$^{-/-}$ mice were competent to condense chromosomes when prompted into MI by okadaic acid (OA). Most of the prematurely condensed chromosomes were univalents with spatially distinct FISH signals, also seen in testicular MI spermatocytes. Although most *Mlh1*$^{-/-}$ spermatocytes do not develop beyond MI, most cells reached a metaphase I-like configuration. Typical metaphase events, such as synaptonemal complex breakdown and the phosphorylation of Ser10 on histone H3, occurred in *Mlh1*$^{-/-}$ spermatocytes. However condensed chromosomes did not align correctly onto the spindle apparatus of *Mlh1*$^{-/-}$ metaphases. Instead, most cells contained bipolar spindles, with chromosomes radiating away from the microtubule-organizing centers in a

prometaphase-like pattern. The TUNEL assay was used to determine if meiotic abnormalities might lead to apoptosis. A developmental analysis of testes revealed an increased level of apoptotic cells by day 22 in both knockout and normal mice. However, a higher percentage of tubules containing >3 apoptotic cells/tubule was seen in testes of *Mlh1*$^{-/-}$ mice compared to controls. Apoptosis was detected in the metaphase-like spermatocytes containing unaligned chromosomes, but not in diplotene spermatocytes. Taken together, these observations show that *Mlh1*$^{-/-}$ spermatocytes can reach a metaphase-like state, but fail to align chromosomes on to the spindle. It also suggests that a spindle assembly checkpoint, rather than a chiasmata checkpoint, may be activated to prevent meiotic errors. If apoptosis is downstream of a possible checkpoint activation, it might function after chromosome condensation is initiated.

CHAPTER I

INTRODUCTION

Mammalian gametogenesis has three important phases: mitotic proliferation of spermatogonia in the male and oogonia in the female, a meiotic phase characterized by an extended prophase and two subsequent divisions, and maturation of gametes. These phases occur continuously in the male, in contrast to the female, in which there are arrests in prophase of the first meiotic division and at metaphase of the second (reviewed in Handel and Eppig, 1998). During the extended prophase of meiosis in both sexes, recombination occurs via DNA double strand breaks followed by ligation through a DNA repair mechanism resulting in the formation of physical links, the chiasmata, between homologous chromosomes (reviewed in Smith and Nicolas, 1998). In addition to generating genotypic variability in offspring, recombination produces the chiasmata that are required for proper chromosome alignment during the first metaphase (Carpenter, 1994; Koehler et al., 1996).

In bacteria and yeast, the *mutL* gene is involved in mismatch repair during DNA replication and recombination (Grilley et al., 1989; Levinson and Gutman, 1987; Strand et al., 1993). Mutations in the human mutL homolog (hMLH1) have been linked to hereditary colon cancer, stemming from an elevation of spontaneous mutation rates by dinucleotide repeat instability (Bronner et al., 1994; Papadopoulos et al., 1994)]. The MLH1 protein is believed to be present at meiotic cross-over sites, and has been found to co-localize with specific regions of the synaptonemal complex in mouse spermatocytes (Baker et al. 1996; Anderson et al., 1999). The number and

position of MLH1 foci closely corresponded to the number and position of chiasmata in metaphase spreads (Anderson et al., 1999). Both sexes of mice homozygous for a targeted disruption of the *Mlh1* gene are sterile, with a failure to maintain pairing of homologous chromosomes, suggesting an important role for the MLH1 protein in holding homologous chromosomes together just prior to and during the first metaphase (Baker et al., 1996; Woods et al., 1999). Since the MLH1 protein localizes to presumed sites of recombination (Anderson et al., 1999), and has been shown to promote crossing-over during meiosis in the budding yeast (Hunter and Borts, 1997), it is thought to be essential for formation of chiasmata. Meiotic division-phase chromosomes of MLH1-deficient germ cells are univalent, though synapsis of the homologous chromosomes takes place in meiotic prophase (Baker et al., 1996). This suggests a defect in crossing-over, not chromosome pairing. Chromosome univalence in *Mlh1*$^{-/-}$ mouse oocytes is correlated with failure in bipolar attachment of chromosomes on the spindle, leading to failure of the chromosomes to congress to the spindle equator (Woods et al., 1999).

In this study, the consequences of chiasma failure in mouse spermatocytes were investigated. The *Mlh1*$^{-/-}$ mouse was used to detect the downstream effects of incomplete recombination on chromosome behavior, as well as cell cycle progression. Analysis of chromosome pairing by fluorescence *in-situ* hybridization (FISH) with chromosome-specific paint probes confirmed chiasma failure. We analyzed properties of cell-cycle progression, spindle formation, chromosome/spindle attachment, and apoptosis in order to seek evidence for checkpoint-mediated arrest during spermatogenesis. Many *Mlh1*$^{-/-}$ spermatocytes progressed into prometaphase

and exhibited many normal features of the meiotic G2/M transition in spite of the fact that the chromosomes were mostly univalent. However, the majority of *Mlh1*$^{-/-}$ spermatocytes became apoptotic at the beginning of meiotic metaphase. This suggests that some testicular process, perhaps a checkpoint, monitors the progress of meiosis and/or chiasmata formation during the meiotic division.

CHAPTER II

MATERIALS AND METHODS

Mice

Mice carrying the *Mlh1* targeted mutation were generously provided by Sean Baker (Baker et al., 1996). Mice were housed under 14 hour light /10 hour dark photo-periods at constant temperature (21° C), with free access to standard laboratory chow and water. Mice were genotyped by PCR reactions for the normal and targeted alleles of the *Mlh1* gene from DNA obtained from tail tips.

Cell and Tissue Preparation

Male mice were killed by cervical dislocation. Whole testes were removed and fixed by overnight immersion in cold 4% paraformaldehyde (Sigma) at 4° C. After fixation and dehydration washes in a series of increasing ethanol concentrations, the testes were embedded in paraffin and sectioned at 3μm. The deparaffinized sections were microwaved (10 min at power 3) to unmask antigens before reaction with antibody.

To obtain isolated germ cells, testes were detunicated, digested in 0.5mg/ml collagenase (Sigma) in KRB at 32° C for 20min, then digested in 0.5mg/ml trypsin (Sigma) in Krebs-Ringer bicarbonate (KRB) at 32° C for 13min. After being filtered through 80μM mesh and washed three times in KRB, spermatocytes were either fixed in a fibrin clot (see below) or enriched for isolation of pachytene spermatocytes by sedimentation on a bovine serum albumin gradient at unit gravity (Bellvé, 1993).

After isolation of pachytene spermatocytes, the cells were cultured in MEM medium/5% FBS (GibcoBRL). After overnight culture at 32° C with 5% CO_2, cells were treated for six hours with or without 5μM OA (Cobb et al., 1999). Chromatin configurations were visualized by Giemsa-staining of air-dried preparations of the treated cells (Evans et al., 1964; Wiltshire et al., 1998). Surface-spread chromatin preparations for synaptonemal complex visualization were performed as previously described (Cobb et al., 1999). Briefly, germ cells were fixed in 2% paraformaldehyde, and allowed to dry onto slides. The slides were fixed in 2% paraformaldehyde, then in 2% paraformaldehyde/0.03% SDS, then blocked in 10% goat serum/3% BSA in PBS prior to processing for immunofluorescence.

To obtain a preparation enriched in meiotically dividing spermatocytes, a variation of the transillumination procedure (Parvinen et al., 1993) was used (Eaker et al., 2001). Testes from adult mice were detunicated, then digested with 0.5mg/ml collagenase for 8min at 33° C. Tubule segments were excised and transferred onto microscope slides in KRB. A coverslip was then placed on top of the segment, allowing the tubules to spread onto the slide. The entire slide was then frozen in liquid N_2 for 30 sec, the coverslip was removed, and the slide fixed in 3:1 ethanol/acetic acid. Prior to incubation with antibodies, the slide was blocked in PBS/10% goat serum for 30 min.

Spermatocytes from germ cell preparations were embedded in fibrin clots as previously described (Eaker et al., 2001). Germ cells were isolated as described above, and brought to a concentration of 25 X 10^6 cells/ml. A 3 μl aliquot of fibrinogen (Calbiochem, 10 mg/ml fresh) and 1.5 μl of the cell suspension was

pipetted onto a slide. Then 2.5 µl of thrombin (Sigma, 250 units) was added, and the slide was allowed to clot for 2 min. The slide was then fixed in 4% paraformaldehyde (Sigma) for 15 min, washed in 0.2% Triton X-100 (Sigma) for 5 min, then processed for immunofluorescence.

Chromosome painting was performed as previously described (Eaker et al., 2001). Briefly, spermatocytes isolated from either germ cell preperations or after pachytene isolation from the BSA gradient were fixed in 3:1 ethanol:acetic acid, then dropped onto slides and allowed to dry. After dehydration in an increasing ethanol series, cells were denatured by incubation in 70% formamide/2X SSC at 65° C for 2 min, followed by another dehydration series. Chromosome paint probes, for chromosome 2 and chromosome 8 (Cambio Inc, Cambridge, UK) were warmed to 37° C, denatured at 65° C, then cooled to 37° C for 1 hr. A 15 µl aliquot of each chromosome paint probe was added to the slides. The slides were coverslipped, sealed, and incubated overnight at 37° C in a humidified chamber. After two washes at 45° C for 5 min in 50% formamide/2X SSC, followed by two washes in 0.1X SSC, detection reagents from the manufacturer (Cambio, Inc.) were added to each slide. The slides were then processed for fluorescent visualization as described below.

Apoptosis Analysis

Apoptosis assays were performed using the In Situ Cell Death Detection Kit (Roche Pharmaceuticals), utilizing the TUNEL reaction. Briefly, testes were fixed in 4% paraformaldehyde, embedded in paraffin, sectioned at 3µm, and placed onto slides as previously described. The end-labeling TUNEL reaction was performed

according to the manufacturer's protocol, with the exception of a 15 min incubation with the enzyme on the slides. After deparaffinization in xylene and rehydration in a decreasing ethanol series, the slides were incubated in 80 µl of the reaction mix at 37° C in a humidified chamber. After two 5 min washes in PBS, the slides were processed for immunofluorescence.

Immunolocalization

Antisera used were 1) polyclonal anti-SYCP3 (Eaker et al., 2001), 2) anti-tubulin (Amersham), 3) anti-phosphorylated histone H3 (Upstate Biotech.) and 4) anti-MPM-2 (Upstate Biotech). Following overnight incubation in primary antibody, the slides were incubated with rhodamine- or fluorescein-conjugated secondary antibodies (Pierce), and mounted with Prolong Antifade (Molecular Probes) containing DAPI (Molecular Probes) to stain DNA. Antibody localization was observed using an Olympus epifluorescence microscope, and images were captured to Adobe PhotoShop with a Hamamatsu color CCD camera. Confocal images were collected using a Leica TC SP2 laser-scanning confocal microscope.

CHAPTER III

RESULTS

Chromosome Univalence and Spatial Distance in Spermatocytes from Mlh1$^{-/-}$ Mice

Defects in chiasmata formation and maintenance of chromosome pairing in *Mlh1*$^{-/-}$ spermatocytes have been previously shown to cause chromosome univalence (Baker et al., 1996). In this work, we investigated the spatial relationship of homologous chromosomes (chromosomes 2 and 8) in *Mlh1*$^{-/-}$ spermatocytes to determine whether or not they were close to each other during metaphase. This was determined by FISH with chromosome-specific 2 and 8 paint probes on surface-spread chromosome preparations (Figure 1). In order to increase the number of metaphase spermatocytes for statistical purposes, the phosphatase inhibitor OA was used to induce the metaphase transition in mid- to late-pachytene spermatocytes (Figures 1C and 1D) (Cobb et al., 1999). In control *Mlh1*$^{+/+}$ mice, proper homologous chromosome pairing can be seen for both chromosomes 2 and 8 , both with and without OA treatment (Figures 1A and 1C). However, in *Mlh1*$^{-/-}$ mice, homologs for chromosomes 2 and 8 are not paired (Figures 1B and 1D). When scoring for metaphase spermatocytes containing unpaired chromosomes using the chromosome paint probes, 90% of *Mlh1*$^{-/-}$ MI's were found to have homologous chromosomes separated by at least one signal domain (Table 1). Spermatocytes from the control *Mlh1*$^{+/+}$ mice showed 0% mispairing (data not shown). Our findings show that the

Figure 1. FISH analysis of MI chromosomes in *Mlh1*$^{-/-}$ and *Mlh1*$^{+/+}$ spermatocytes, either treated with okadaic acid (OA) or untreated. Chromosome-specific paint probes identify chromosome 2 (green) and 8 (red). A. An untreated *Mlh1*$^{+/+}$ MI spermatocyte. B. An untreated *Mlh1*$^{-/-}$ MI spermatocyte. C. A *Mlh1*$^{+/+}$ MI spermatocyte treated with OA. D. A *Mlh1*$^{-/-}$ MI spermatocyte treated with OA. A. and C. *Mlh1*$^{+/+}$ spermatocytes showing paired bivalents identified by the presence of only one signal per chromosome pair. B. and D. *Mlh1*$^{-/-}$ spermatocyte showing univalents identified by 2 separate signals per chromosome.

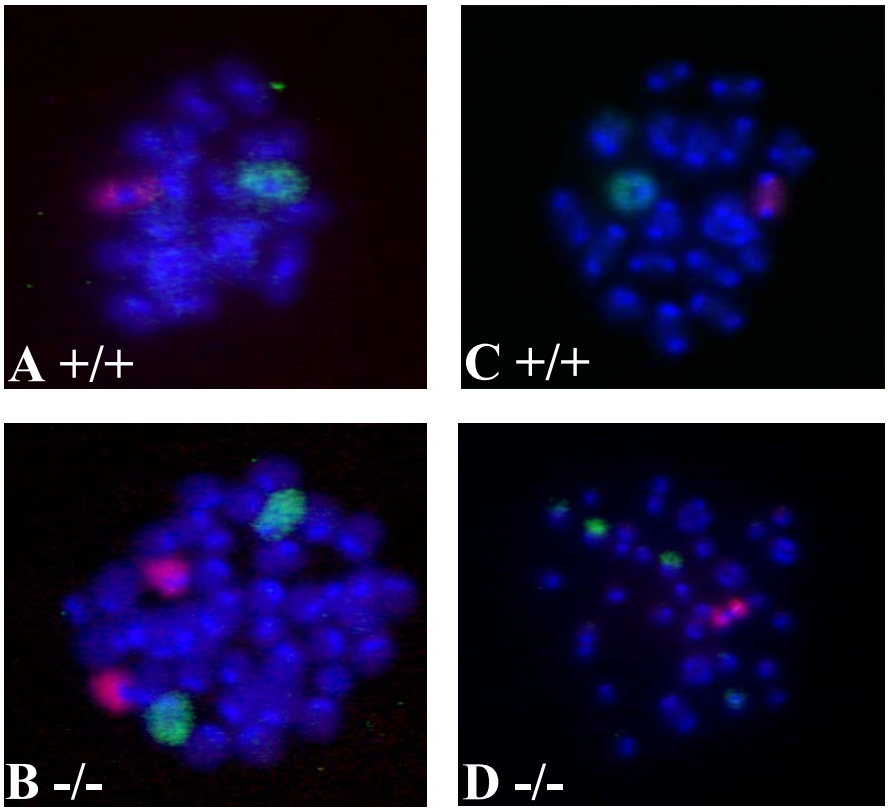
A +/+
C +/+
B -/-
D -/-

Table 1. Analysis of FISH signal domains in MI spermatocytes from 3 *Mlh1*$^{-/-}$ males. FISH analysis was conducted both for testicular spermatocytes in MI (-OA) and for pachytene spermatocytes cultured with okadaic acid (+OA) to increase the frequency of MIs. Chromosome-specific paint probes were used to identify chromosomes 8 and 2 (as in Figure 1). Cells were scored for the following categories: chromosomes 2 and 8 being in close proximity (1 signal for each pair), signals not close but separated by less than 1 signal domain, or signals separated by a distance greater than 1 signal domain. A domain is defined by the presence of one or more non-homologous chromosome(s) or a physical space equal in size to a chromosome signal between the homologous pair. 100 spermatocytes from 3 control mice were scored and showed 0% mispairing.

Chr. 8 and 2 Proximity	# cells -OA	# cells +OA	Total
Both 8 and 2 close	1	7	8
8 close, 2 distant	3	5	8
2 close, 8 distant	7	16	23
Both 8 and 2 distant	10	30	40
Percent mispaired	95.2	87.9	90

majority of homologous chromosomes are not spatially near each other in *Mlh1*$^{-/-}$ metaphase spermatocytes. Since surface-spread chromatin was scored, it is not known if homologous chromosomes are closer *in situ*. However, this analysis shows that there is not any structure or pairing mechanism serving to maintain the homologs in proximity to each other.

Mlh1$^{-/-}$ *Spermatocytes Exhibit Typical Features of the Meiotic G2/M Transition*

It has been previously shown that the phosphatase inhibitor OA can induce chromosome condensation in mid- to late-pachytene spermatocytes (Cobb et al., 1999). Thus, mid- to late-pachytene spermatocytes are competent to enter meiotic metaphase at the chromosomal level. The competence of *Mlh1*$^{-/-}$ pachytene spermatocyte to respond to OA treatment was tested. OA induced chromosome condensation in both the control *Mlh1*$^{+/+}$ (Fig 2A) and *Mlh1*$^{-/-}$ (Figure 2C) spermatocytes. The presence of metaphase I chromosomes was determined in air-dried chromosome preparations stained with Giemsa. Figure 2B depicts the chromosomal staining in two pachytene spermatocytes and a metaphase spermatocyte from *Mlh1*$^{-/-}$ mice prior to metaphase induction using OA. Note that all chromosomes are bivalent in all control *Mlh1*$^{+/+}$ spermatocytes (Figure 2A). Chromosomes are primarily univalent in *Mlh1*$^{-/-}$ metaphases (Figures 2B and 2C), but occasional bivalents were observed (arrowhead). These results demonstrate that *Mlh1*$^{-/-}$ pachytene spermatocytes are competent to condense their chromosomes when treated with OA, in spite of the absence of MLH1 protein.

Figure 2. Pachytene spermatocytes from *Mlh1*$^{-/-}$ mice are competent to condense chromosomes in response to OA treatment. A. Control *Mlh1*$^{+/+}$ spermatocytes treated with OA for 6 hrs. B. Untreated *Mlh1*$^{-/-}$ spermatocytes (Pach=Pachytene, MI = Metaphase I). C. *Mlh1*$^{-/-}$ spermatocytes treated with OA for 6 hrs. Notice in B and C that condensed chromosomes are usually univalents, although bivalents are occasionally seen (arrowhead in C).

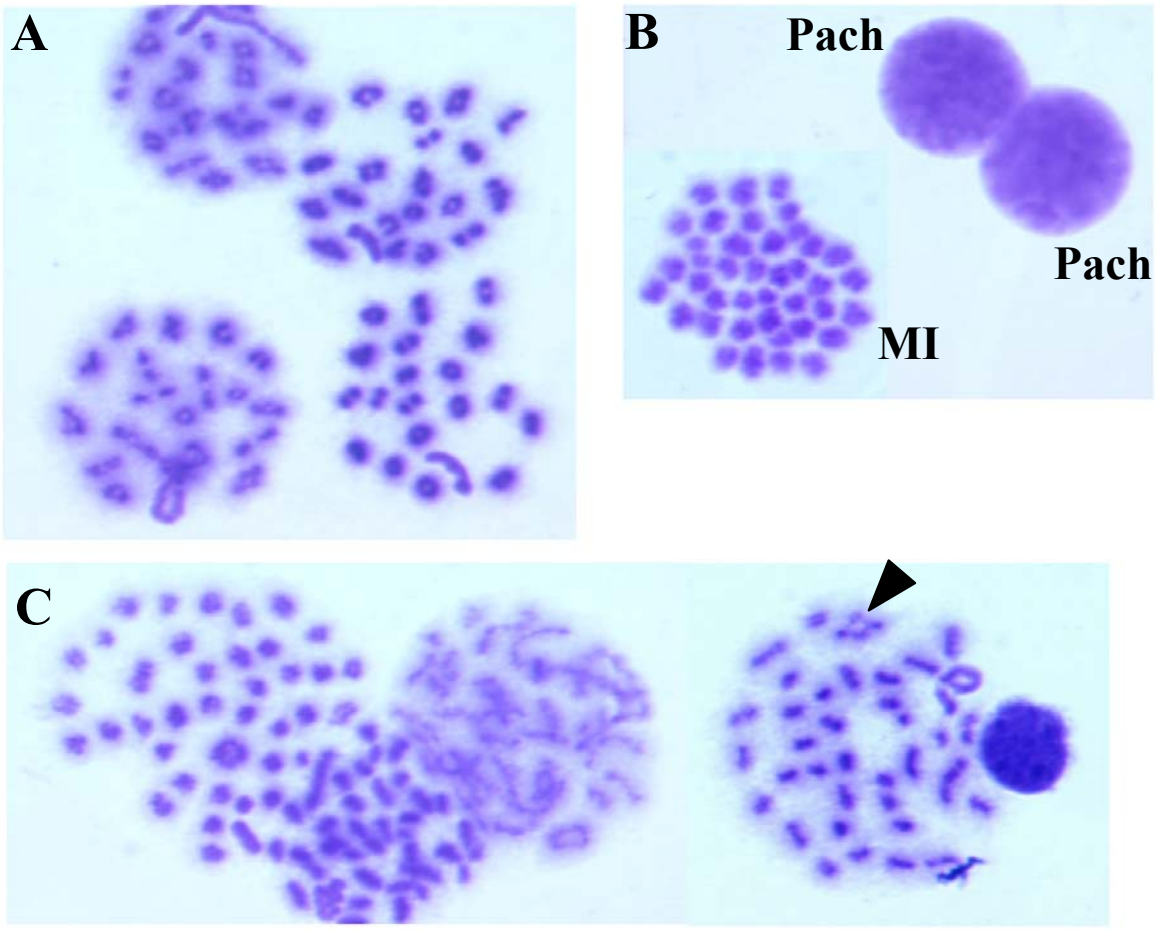
A
B
Pach
Pach
MI
C

Structural and phosphorylation changes consistent with metaphase entry were observed in *Mlh1*$^{-/-}$ spermatocytes. In order to detect these changes, immunofluorescent staining with antibodies against the synaptonemal complex protein SYCP3 and the phosphorylated form of histone H3 (a marker for chromosome condensation) were used. It had previously been shown that SC desynapsis occurs in *Mlh1*$^{-/-}$ spermatocytes (Baker et al., 1996). Complete synaptonemal complex breakdown occurs in both *Mlh1*$^{+/+}$ (Figures 3A to 3B) and *Mlh1*$^{-/-}$ (Figures 3C to 3D) meiotic metaphase spermatocytes. The SYCP3 protein was present along the paired region of homologous chromosomes during pachytene (Figures 3A and 3C), but was detected only near the centromeric region of each chromosome in metaphase (Figures 3B and 3D). A marker for chromosome condensation, phosphorylation of Ser10 on histone H3, was detected in both control *Mlh1*$^{+/+}$ and *Mlh1*$^{-/-}$ metaphases (Figures 3B and 3D). Note the presence of bivalent chromosomes in *Mlh1*$^{+/+}$ spermatocytes (Figure 3B) and univalent chromosomes in *Mlh1*$^{-/-}$ spermatocytes (Figure 3D). These data show that although univalent chromosomes are formed, the entry into metaphase in *Mlh1*$^{-/-}$ spermatocytes is similar to that of *Mlh1*$^{+/+}$ spermatocytes. These results imply that although the MLH1 protein may be required for chiasmata formation, chiasmata are not part of the signal machinery enabling either the normal or precocious, OA-induced, G2/M transition.

Figure 3. Immunofluorescence staining of pachytene (A and C) and metaphase (B and D) spermatocytes using antibodies against the synaptonemal complex protein SYCP3 (red) and the phosphorylated form of histone H3-Ser10 (green), associated with condensed chromosomes. A. and B. Spermatocytes from *Mlh1*$^{+/+}$. C. and D. Spermatocytes from *Mlh1*$^{-/-}$.

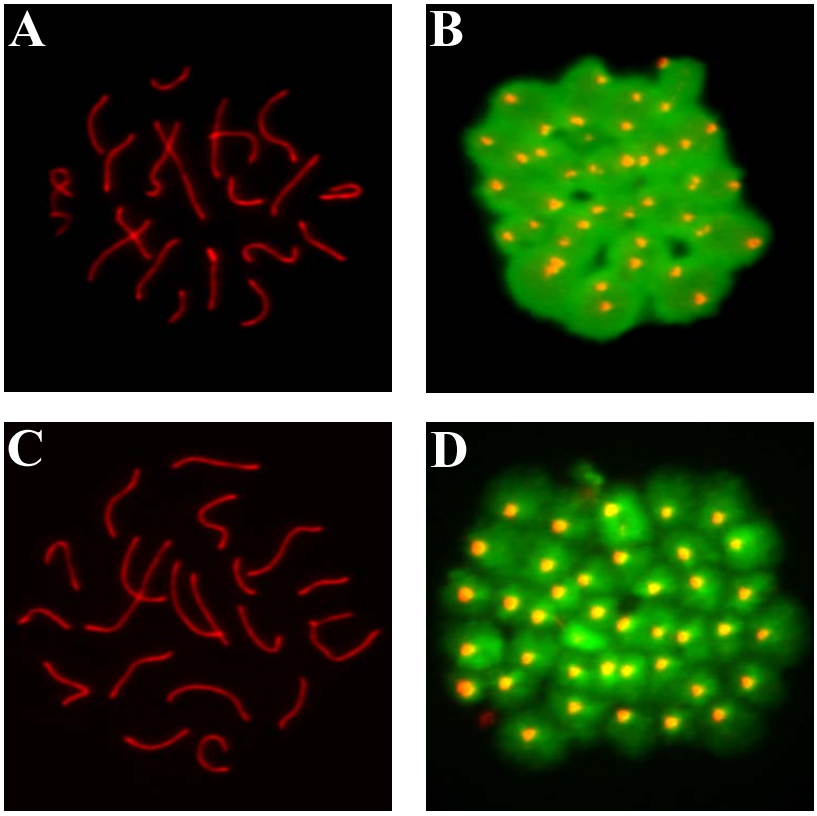
A
B
C
D

Spermatocytes of Mlh1$^{-/-}$ Mice Exhibit Abnormalities in Chromosome Alignment

Although *Mlh1*$^{-/-}$ spermatocytes show many characteristics of normal prophase to metaphase entry, their progress is halted soon after. In order to observe details of the metaphase transition in *Mlh1*$^{-/-}$ spermatocytes, we monitored spindle formation and chromosome behavior in spermatocytes using immunofluorescence with antibodies against β-tubulin and phospho-histone H3. Figure 4A shows a confocal image of *Mlh1*$^{-/-}$ spermatocytes in prometaphase and metaphase spermatocytes. In *Mlh1*$^{-/-}$ metaphase spermatocytes, chromosomes do not align at the spindle equator (Figure 4A). Bipolar spindle formation, however, does occur in the presence of univalent chromosomes. In the rare instance, anaphase occurs in *Mlh1*$^{-/-}$ spermatocytes (Figure 4B), characterized by lagging chromosomes in the spindle midzone, between other chromosomes which appear to be migrating towards the poles. It is important to note that although a few anaphases-like spermatocytes were detected, no metaphase II spermatocytes or round spermatids were seen in *Mlh1*$^{-/-}$ mice.

Mlh1$^{-/-}$ *Spermatocytes Undergo Apoptosis After Entry Into Metaphase*

We have previously shown in another mouse model that metaphase spermatocytes with unaligned chromosomes undergo apoptosis (Eaker et al., 2001; Part IV of this dissertation). In order to determine if apoptotic spermatocytes are present in testes of *Mlh1*$^{-/-}$ mice, the TUNEL assay was utilized. Apoptosis was

Figure 4. Abnormalities during chromosome alignment and segregation in *Mlh1*$^{-/-}$ spermatocytes seen by confocal microscopy. A. Two *Mlh1*$^{-/-}$ metaphase spermatocytes stained with anti-phospho-histone H3 (green) and anti-b-tubulin (red). The spermatocyte on the right is bipolar, with chromosomes in different positions within the same cell. Some chromosomes have migrated to the poles, some remain in the middle of the cell, while others seem to be behind the microtubule organizing center (MTOC). The cell on the left depicts a prometaphase-like configuration. B. A *Mlh1*$^{-/-}$ anaphase spermatocyte stained with MPM-2 (red) and phospho-histone H3-Ser10 (green) is shown. At anaphase (middle cell) most chromosomes have migrated to their respective poles, while some chromosomes are lagging in the middle of the spindle (arrow).

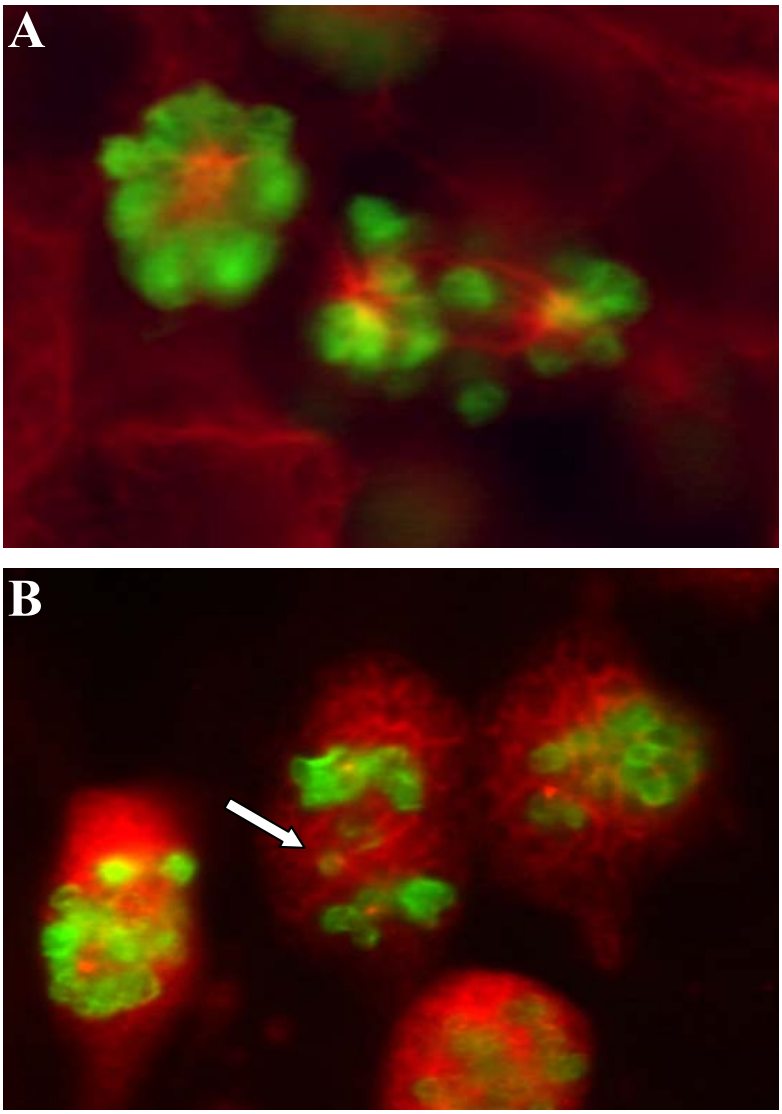
A
B

scored in cross-sectioned seminiferous tubules from mice 16, 18, 20, 22 and 24 days old, as well as from adults. Three mice from each age and from each strain were used. Tubules with more than three apoptotic cells were scored as being an apoptotic tubule, as the basal level of apoptosis in the background C57B/6J mouse was determined to be 1.9 +/-0.2 cells/tubule (Kon et al., 1999). An increased frequency of tubules with apoptosis was detected in *Mlh1*$^{-/-}$ mice, as compared to control *Mlh1*$^{+/+}$ mice (Figure 5A). Although most ages were statistically different (the exceptions being 16 and 20 days of age) the largest increase in the number of apoptotic tubules appeared at 22 days of age in tubules from *Mlh1*$^{-/-}$ mice (Figure 5A and 6A). Metaphase spermatocytes are known to appear at 22 days of age in both *Mlh1*$^{+/+}$ and *Mlh1*$^{-/-}$ mice. Additionally, the frequency of tubules with metaphase spermatocytes does not differ between *Mlh1*$^{+/+}$ and *Mlh1*$^{-/-}$ mice. This was determined by co-staining sectioned material with antibodies against phospho-histone H3 to label division-phase cells (Figure 6B).

In order to determine the timing of apoptosis relative to metaphase entry, spermatocytes were fixed in a fibrin clot, subjected to the TUNEL reaction, and processed for immunofluorescence using antibodies against SYCP3 and phospho-histone H3 (Figure 6B, 6C and 6D). The fibrin-clot preparation allows the native three-dimensional configuration the cell to be retained during fixation. Apoptosis was seen only in metaphase spermatocytes containing condensed chromosomes (Fig 6 - MI), occurring after synaptonemal complex disassembly and phosphorylation of histone H3. In 22 day old mice, apoptosis was not detected in diplotene

Figure 5. **A**. The frequency of tubules with apoptotic cells in *Mlh1*$^{-/-}$ mice increases dramatically at 22 days of age. At day 22, the percentage of apoptotic tubules containing >3 apoptotic cells/tubule from *Mlh1*$^{-/-}$ mice (black bars) is substantially greater than from wildtype mice (white bars). **B**. The frequency of tubules containing >3 phospho-histone H3 cells/tubule are shown. No statistical difference in frequency between *Mlh1*$^{+/+}$ (white bars) and *Mlh1*$^{-/-}$ (black bars) tubules is seen. Apoptotic spermatocytes appear at approximately the same time as spermatocytes containing phospho-histone H3. Asterisks represent paired values that differ significantly, which are seen only for apoptotic tubules (Student's t test; $p = 0.11$ for difference in frequency in 18 day old mice, $p = 0.230$ for differences in frequency in 22 day old mice, $p = 0.000$ for difference in frequency in 24 day old mice, and $p = 0.000$ for difference in frequency in adult mice).

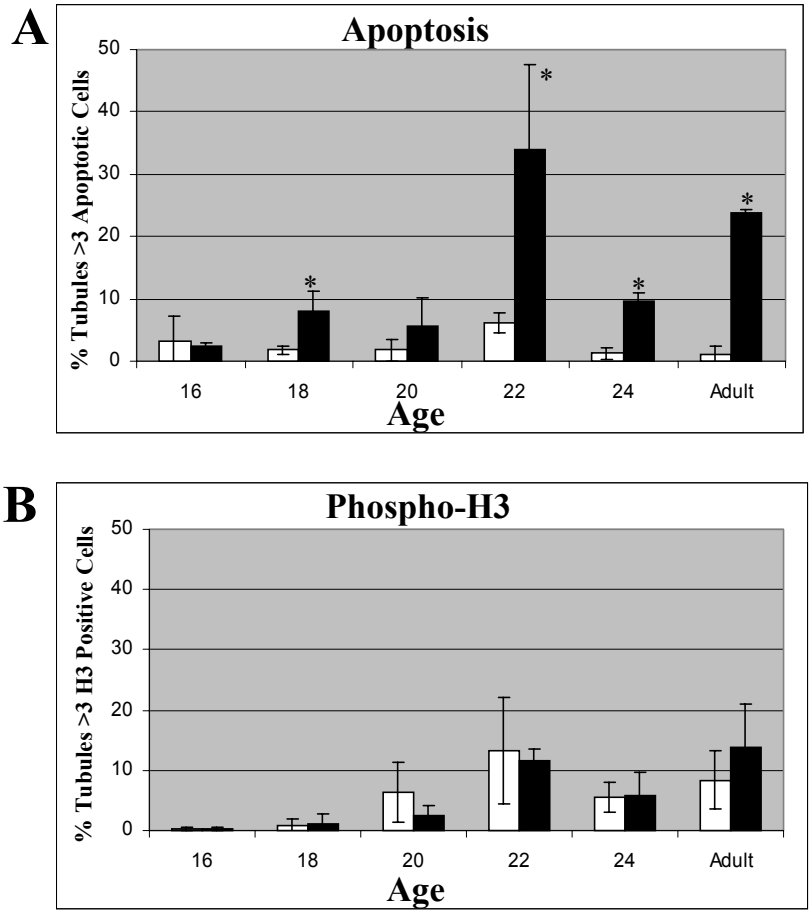
A
Apoptosis
% Tubules >3 Apoptotic Cells
50
40
30
20
10
0
*
*
*
*
16
18
20
22
24
Adult
Age
B
Phospho-H3
% Tubules >3 H3 Positive Cells
50
40
30
20
10
0
16
18
20
22
24
Adult
Age

Figure 6. Apoptosis in *Mlh1*$^{-/-}$ spermatocytes. Apoptotic cells, detected by the TUNEL reaction, are visualized as green. A. Paraffin-embedded sections stained for apoptotic cells (green) and phospho-histone H3 (red). B. *Mlh1*$^{-/-}$ spermatocytes (MI - metaphase I, Dipl - Diplotene) embedded in a fibrin clot. Apoptotic cells are visualized in green and the synaptonemal complex by the SYCP3 antibody (red). In B, a metaphase-like spermatocyte is shown to be apoptotic (left cell), while a diplotene spermatocyte is not apoptotic (right cell). A. is an overlay of SYCP3 staining (C-red) and apoptosis (D-green).

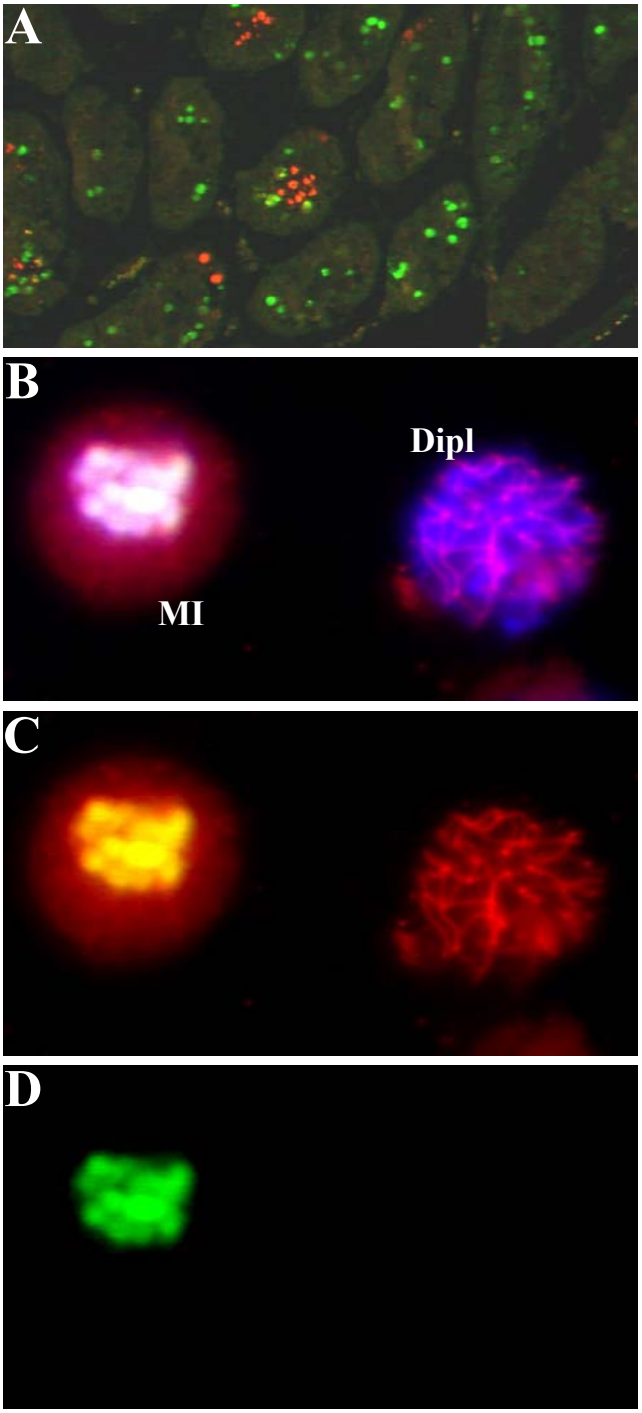
A
B
Dipl
MI
C
D

spermatocytes (Fig 6 - Dipl), or in any other pre-metaphase spermatocyte. These data show that apoptosis is first seen in the testes of 22 day old *Mlh1*$^{-/-}$ mice, coinciding with the first appearance of metaphase spermatocytes. We have also shown that apoptosis first appears after metaphase entry and chromosome condensation, and not in diplotene spermatocytes.

CHAPTER IV

DISCUSSION

Spermatocytes from Mlh1 $^{-/-}$ Mice are Characterized by Univalent and Spatially Distinct Chromosomes Present at the End of Meiotic Prophase

This study was performed to evaluate how spermatocytes cope with the removal of the MLH1 protein. The failure of *Mlh1*$^{-/-}$ spermatocytes to form chiasmata had been previously shown (Baker et al., 1996). Using chromosome paint probes on air-dried preparations, we determined the relative proximity of unpaired homologous chromosomes. It was shown that 90% of homologous chromosomes (for both chromosomes 2 and 8) were greater than one domain away from their homologous partner. Among these, only half have homologs of both chromosomes 8 and 2 distant. Within the other half of spermatocytes, a larger portion of chromosome 8 was distant relative to the portion in which chromosome 2 was distant, which possibly could be the result of chromosome size differences. Those chromosomes spatially near their homologous partner may not, however, be connected physically.

These findings provide evidence that the majority of homologous chromosome partners in *Mlh1*$^{-/-}$ spermatocytes are neither paired by physical links nor spatially close to each other during the metaphase transition. Since these preparations are of surface-spread chromatin, the preparation itself might alter the proximity calculation, although 100% of control homologous chromosomes were spatially near each other. Bivalents were detected in some *Mlh1*$^{-/-}$ metaphase spermatocytes (Figure 2C), although no more than two bivalents were detected in any

spermatocyte. These results imply that without any physical links connecting homologous chromosomes, the ability of chromosomes to congress on the spindle is lost in *Mlh1*$^{-/-}$ spermatocytes.

Chromosome Condensation and Hallmarks of the Meiotic G2/M Transition

We demonstrated that specific events, such as chromosome condensation, synaptonemal complex breakdown, and phosphorylation of Ser10 on histone H3, are observed in both the control *Mlh1*$^{+/+}$ and mutant *Mlh1*$^{-/-}$ spermatocytes. The ability of *Mlh1*$^{-/-}$ pachytene spermatocytes to enter metaphase I when treated with OA was also demonstrated, showing that *Mlh1*$^{-/-}$ pachytene spermatocytes are competent to make the G2/M transition when treated with OA. Bipolar spindle formation occurs in both *Mlh1*$^{-/-}$ spermatocytes (this study) and oocytes (Woods et al., 1999), although both show that the univalent *Mlh1*$^{-/-}$ chromosomes do not align on the metaphase plate. With the exceptions of a failure in homologous chromosome pairing and univalence, the transition from prophase into metaphase in the mutant and wild-type strains are comparable. This implies that if the MLH1 protein is required for chiasmata formation, chiasmata are not required for metaphase entry, at least not the entry that OA induces. If checkpoint mechanism(s) monitoring these events are present in mouse spermatocytes, the checkpoint may not be active until entry into metaphase. Otherwise, cell cycle delays and/or apoptosis would be seen in earlier stages.

Chromosomes of Mlh1$^{-/-}$ *Metaphase-like Spermatocytes Do Not Properly Align on the Metaphase Plate and the Spermatocytes Become Apoptotic*

In spite of a failure to form chiasmata, many cells progress to a metaphase-like configuration. Chromosomes are univalent and arrayed throughout the cell unpaired and unaligned (Figure 4A), similar to the phenotype seen in *Mlh1*$^{-/-}$ mouse oocytes (Woods et al., 1999). Woods et al. showed that although bipolar spindles were formed in *Mlh1*$^{-/-}$ oocytes and the spindle poles continued to elongate, the oocytes never entered anaphase. Meiotic progression in vitro is difficult to study in the male mouse, as mouse spermatocytes cannot be cultured through the first meiotic division. Thus, whether this "metaphase-blocked" phenotype of spermatocytes is checkpoint regulated or caused by structural abnormalities themselves remains to be determined. We would expect congression failure of chromosomes in MLH1-defecient spermatocytes, knowing that chiasmata play a role in development of tension and bipolar orientation by holding homologous chromosomes together physically.

We have shown that tubule sections from *Mlh1*$^{-/-}$ mice exhibited an increased level of apoptosis beginning at 22 days of age, which is the time point when a high frequency of MI spermatocytes are found in the testes. We have also shown that apoptosis, a mechanism which eliminates abnormal cells, is detected in metaphase-like *Mlh1*$^{-/-}$ spermatocytes. It is important to note that apoptosis was not detected in diplotene spermatocytes, the stage preceding metaphase. These results are also consistent with a spermatocyte mechanism for elimination of chromosomally abnormal spermatocytes, with the abnormality first detected during the transition into metaphase. Future studies will reveal whether the *Mlh1*$^{-/-}$ apoptotic events stem from

the supporting Sertoli cells (removing damaged meiotic germ cells) or the spermatocytes themselves through a checkpoint activation.

Chiasmata or Spindle Assembly Checkpoint?

We have shown that normal events leading up to the first meiotic division, such as synaptonemal complex disassembly and phosphorylation of histone H3, appear to occur normally in *Mlh1*$^{-/-}$ spermatocytes. We have also shown that a known mechanism of removing checkpoint-activated cells, apoptosis, is detected only in metaphase-like spermatocytes in *Mlh1*$^{-/-}$ mice. Apoptosis does not appear prior to this stage. Therefore, we can hypothesize the presence of two possible checkpoint mechanisms, both occurring after synaptonemal complex disassembly, chromosome condensation, nuclear envelope breakdown, and spindle formation: 1) Univalence causes unaligned chromosomes during metaphase which activates a spindle assembly checkpoint mechanism, or 2) the failure to form chiasmata itself is detected during entry into metaphase. We believe the latter to be unlikely, since the failure to form chiasmata appears prior to metaphase. Therefore, we would expect a more efficient means of repair/removal of the cells lacking chiasma formation prior to entry into metaphase in the presence of a chiasmata checkpoint. We also observed apoptosis only after chromosomal condensation, detected with the antibody against phosphorylated histone H3. If spermatocytes lacking chiasmata were allowed to condense chromosomes and enter metaphase, a spindle assembly checkpoint would be able to detect univalence by the presence of unaligned chromosomes. Because *Mlh1*$^{-/-}$ spermatocytes contain univalent chromosomes, this is why apoptosis was seen

in *Mlh1*$^{-/-}$ metaphase spermatocytes. Apoptosis may be a means to eliminate spermatocytes containing univalent/unaligned chromosomes. Future studies with similar recombination proteins, as well as possible gene and apoptosis rescue studies, will provide more information concerning the presence and role of meiotic checkpoints in mammals.

LIST OF REFERENCES

Anderson LK, Reeves A, Webb LM, Ashley T. 1999. Distribution of crossing over on mouse synaptonemal complexes using immunofluorescent localization of MLH1 protein. Genetics 151:1569-1579.

Baker SM, Plug AW, Prolla TA, Bronner CE, Harris AC, Yao X, Christie DM, Monell C, Arnheim N, Bradley A, Ashley T, Liskay RM. 1996. Involvement of mouse *Mlh1* in DNA mismatch repair and meiotic crossing over. Nat Genet 13:336-342.

Bellvé AR. 1993. Purification, culture and fractionation of spermatogenic cells. Methods in Enzymology 225:84-113.

Bronner CE, Baker SM, Morrison PT, Warren G, Smith LG, Lescoe MK, Kane M, Earabino C, Lipford J, Lindblom A, Tannergard P, Bollag RJ, Godwin AR, Ward DC, Nordenskjold M, Fishel R, Kolodner R, Liskay RM. 1994. Mutation in the DNA mismatch repair gene homologue hMLH1 is associated with hereditary non-polyposis colon cancer. Nature 368:258-261.

Carpenter ATC. 1994. Chiasma function. Cell 77:959-962.

Cobb J, Cargile B, Handel MA. 1999. Acquisition of competence to condense metaphase I chromosomes during spermatogenesis. Dev Biol 205:49-64.

Eaker SS, Pyle AD, Cobb JA, Handel MA. 2001. Evidence for meiotic spindle checkpoint from analysis of spermatocytes from Robertsonian-chromosome-heterozygous mice. J Cell Sci, In Press.

Evans EP, Breckon G, Ford CE. 1964. An air-drying method for meiotic preparations from mammalian testes. Cytogenetics 3:289-294.

Grilley M, Welsh KM, Su SS, Modrich P. 1989. Isolation and characterization of the *Escherichia coli mutL* gene product. J Biol Chem 264:1000-1004.

Handel MA, Eppig JJ. 1998. Sexual dimorphism in the regulation of mammalian meiosis. In MA Handel (ed): "Meiosis and Gametogenesis," 37. 525 B Street, Suite 1900, San Diego, CA 92101-4495: Academic Press Inc, pp 333-358.

Hunter N, Borts RH. 1997. Mlh1 is unique among mismatch repair proteins in its ability to promote crossing-over during meiosis. Gene Dev 11:1573-1582.

Koehler KE, Hawley RS, Sherman S, Hassold T. 1996. Recombination and nondisjunction in humans and flies. Hum Molec Genet 5:1495-1504.

Kon Y, Horikoshi H, Endoh D. 1999. Metaphase-specific cell death in meiotic spermatocytes in mice. Cell Tissue Res 296:359-369.

Levinson G, Gutman GA. 1987. High frequencies of short frameshifts in poly-CA/TG tandem repeats borne by bacteriophage M13 in *Escherichia coli* K-12. Nucleic Acids Res 15:5323-5338.

Odorisio T, Rodriguez TA, Evans EP, Clarke AR, Burgoyne PS. 1998. The meiotic checkpoint monitoring synapsis eliminates spermatocytes via p53-independent apoptosis. Nat Genet 18:257-261.

Papadopoulos N, Nicolaides NC, Wei Y-F, Ruben SM, Carter KC, Rosen CA, Haseltine WA, Fleischmann RD, Fraser CM, Adams MD, Venter JC, Hamilton SR, Petersen GM, Watson P, Lynch HT, Peltomaki P, Mecklin J-P, de la Chapelle A, Kinzler KW, Vogelstein B. 1994. Mutation of a *mutL* homolog in hereditary colon cancer. Science 263:1625-1629.

Parvinen M, Toppari J, Lahdetie J. 1993. Transillumination phase contrast microscope techniques for evaluation of male germ cell toxicity and mutagenicity. In RE Chapin and JJ Heindel (ed): "Methods in Toxicology," 3, part A. San Diego: Academic Press, pp 142-165.

Roeder GS, Bailis JM. 2000. The pachytene checkpoint. Trends Genet 16:395-403.

Smith KN, Nicolas A. 1998. Recombination at work for meiosis. Curr Opin Genet Dev 8:200-211.

Strand M, Prolla TA, Liskay RM, Petes TD. 1993. Destabilization of tracts of simple repetitive DNA in yeast by mutations affecting DNA mismatch repair. Nature 365:274-276.

Wiltshire T, Park C, Handel MA. 1998. Chromatin configuration during meiosis I prophase of spermatogenesis. Mol Reprod Dev 49:70-80.

Woods LM, Hodges CA, Baart E, Baker SM, Liskay M, Hunt PA. 1999. Chromosomal influence on meiotic spindle assembly: Abnormal meiosis I in female *Mlh1* mutant mice. J Cell Biol 145:1395-1406.

PART IV

EVIDENCE FOR MEIOTIC SPINDLE CHECKPOINT FROM ANALYSIS OF SPERMATOCYTES FROM ROBERTSONIAN-CHROMOSOME-HETEROZYGOUS MICE*

*This Part is being published in its entirety as Eaker SS, Pyle AD, Cobb JA, and Handel MA (2001): Evidence for meiotic spindle checkpoint from analysis of spermatocytes from Robertsonian-chromosome-heterozygous mice. J Cell Sci: In Press.

SUMMARY

Mice heterozygous for Robertsonian centric fusion chromosomal translocations frequently produce aneuploid sperm. In this study RBJ/Dn X C57BL/6J F1 males, heterozygous for four Robertsonian translocations (2N = 36), were analyzed to determine effects on germ cells of error during meiosis. Analysis of sperm by three color fluorescence *in situ* hybridization revealed significantly elevated aneuploidy, thus validating Robertsonian heterozygous mice as a model for production of chromosomally abnormal gametes. Primary spermatocytes from heterozygous males exhibited abnormalities of chromosome pairing in meiotic prophase and metaphase. In spite of prophase abnormalities, the prophase/metaphase transition occurred. However, an increased frequency of cells with misaligned condensed chromosomes was observed. Cytological analysis of both young and adult heterozygous mice revealed increased apoptosis in spermatocytes during meiotic metaphase I. Metaphase spermatocytes with misaligned chromosomes accounted for a significant proportion of the apoptotic spermatocytes, suggesting that a checkpoint process identifies aberrant meioses. Immunofluorescence staining revealed that kinetochores of chromosomes that failed to align on the spindle stained more intensely for kinetochore antigens CENP-E and CENP-F than did aligned chromosomes. Taken together, these observations are consistent with detection of malattached chromosomes by a meiotic spindle checkpoint mechanism that monitors attachment and/or congression of homologous chromosome pairs. However, the relatively high frequency of gametic aneuploidy suggests that the checkpoint

mechanism does not efficiently eliminate all germ cells with chromosomal abnormalities.

CHAPTER I

INTRODUCTION

Accurate meiotic segregation of chromosomes is essential for normal reproduction and a major determinant of gamete quality. Errors in chromosome segregation in either of the two meiotic divisions can lead to gametic loss, reduced fertility, or aneuploidy in offspring. Understanding the mechanisms that ensure normal chromosome segregation and of checkpoints that come into play in cases of chromosomal meiotic abnormalities could provide insights into the origin of aneuploidy, such as trisomy 21 (Down syndrome), in our own species. However, little is known of the mechanisms that determine gamete genetic quality.

Mitotic checkpoints govern functional assembly of the mitotic spindle apparatus and bipolar attachment of chromosomes (Burke, 2000; Gardner and Burke, 2000). These mechanisms respond to malattachment of chromosomes by delaying exit from mitosis. Tension developed as chromosomes achieve bipolar attachment appears to be critical to the mechanism (Li and Nicklas, 1995; Nicklas et al., 1995). Tension can be assessed by changes in phosphorylation of kinetochore proteins (Gorbsky et al., 1999; Li and Nicklas, 1997; Waters et al., 1999), and these proteins appear to monitor both spindle assembly and chromosome attachment, signaling the onset (or delay) of anaphase. For example, centromeric protein CENP-E is a kinesin-like motor protein whose activity at kinetochores is thought to be monitored by the spindle assembly checkpoint (Yen et al., 1992). CENP-E is essential for microtubule/kinetochore attachment, as chromosomes from HeLa cells lacking the

CENP-E gene or injected with antibodies against the CENP-E protein do not align properly on the metaphase plate, and subsequently do not proceed through division (Schaar et al., 1997). hCENP-E is thought to be involved in checkpoint signaling as it associates with the checkpoint protein hBUBR1 (Chan et al., 1999). The association of the checkpoint protein MAD2 with the kinetochore has recently been shown to be dependent on the presence of CENP-E, thus linking CENP-E to another component of the spindle assembly checkpoint mechanism (Abrieu et al., 2000).

Little is known about the checkpoints governing the meiotic divisions or their similarity to mechanisms that act in mitosis. The first meiotic division differs markedly from mitosis. In the first meiotic division, homologous chromosome pairs are separated from each other in a reductional division, while in the second mitotic-like equational division, sister chromatids are separated from each other. The information governing the mode of meiotic anaphase separation is apparently contained within the chromosome and is not a property of the spindle (Paliulis and Nicklas, 2000). Checkpoint mechanisms signaling error in the two distinct division processes might also be intrinsic to the meiotic chromosomes. Investigations using model organisms have confirmed localization of checkpoint protein BUB1 in *Drosophila* spermatocytes (Basu et al., 1998), and MAD2 in maize gametocytes (Yu et al., 1999) and mouse spermatocytes (Kallio et al., 2000). CENP-E is localized on the kinetochores in metaphase mouse spermatocytes (Kallio et al., 1998), in pig oocytes during both meiotic divisions (Lee et al., 2000), and has been implicated as essential for MII arrest of mouse oocytes (Duesbery et al., 1997). Whether these proteins act singly or in concert as a spindle checkpoint mechanism during meiotic

divisions is not known, nor is it known what the consequences of the checkpoint might be. One likely consequence of checkpoint-detected error might be apoptosis, which plays an important role in male germ cell development and regulation (Print and Loveland, 2000; Sinha Hikim and Swerdloff, 1999).

Interestingly, evidence suggests that mammalian female meiosis lacks stringent checkpoint control, which could explain high rates of aneuploidy, particularly in humans (Hunt and LeMaire-Adkins, 1998; LeMaire-Adkins et al., 1997). It has generally been assumed that there is more effective quality control during male meiosis, but this assumption has not been experimentally tested. Identifying division-phase mechanisms that might detect chromosomal abnormalities and eliminate defective gametes is not easy in normal males, where the number of abnormal cells is small by comparison to the vast numbers of normal gametes.

Checkpoint mechanisms might more readily be revealed in males where the potential for chromosomal error in alignment and segregation is elevated. The model used here is male mice heterozygous for Robertsonian (Rb) translocations. Rb chromosomes are metacentric, or sub-metacentric, chromosomes formed by the centric fusion of two acrocentric chromosomes (Robertson, 1916). During the first meiotic prophase in individuals heterozygous for Rb chromosomes, the Rb participates in a trivalent with the two homologous acrocentric chromosomes (Fig. 1). Pairing defects in this unusual configuration could give rise to the potential for error in either chromosome alignment at metaphase I (MI) or unbalanced segregation at anaphase I (Figure 1). We used mice simultaneously heterozygous (Rb/+) for four different Rb chromosomes, Rb(5.15)3Bnr, Rb(11.13)4Bnr, Rb(16.17)7Bnr,

Figure 1: Diagrammatic representation of a Rb chromosome meiotic pairing configuration involving chromosomes 2 (green) and 8 (yellow). The synaptonemal complex is diagrammed in red, centromeres in blue. Pairing errors could give rise to aberrant alignment at MI and/or unbalanced anaphase segregation, indicated by the arrows.

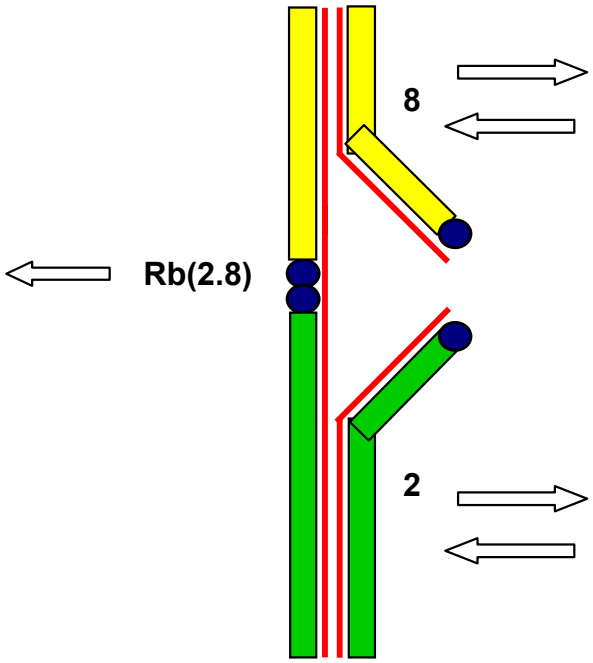
8
Rb(2.8)
2

Rb(2,8)2Lub, produced by mating individuals quadruply homozygous (RBJ/Dn) to chromosomally normal individuals. Two lines of previous evidence had suggested that these heterozygous mice could provide a model to test for meiotic checkpoints responding to chromosomal misalignment and malsegregation. First, heterozygotes for the single translocations Rb(5.15)3Bnr, Rb(11.13)4Bnr, and Rb(16.17)7Bnr have each been shown to be prone to nondisjunction of the involved chromosomes, both by assessment of metaphase II (MII) spermatocytes and by zygotic loss (Cattanach and Moseley, 1973; Nijhoff and de Boer, 1979). Elevation of sperm aneuploidy has been documented by fluorescence in situ hybridization (FISH) analysis of sperm from male mice carrying Rb(8.14), a Rb chromosome not present in the RBJ/Dn stock used in this study (Lowe et al., 1996). Second, heterozygosity for some of these Rb translocations is associated with abnormalities in pairing and recombination suppression (Cattanach and Moseley, 1973; Davisson and Akeson, 1993), both of which could lead to delays in synapsis and abnormalities during segregation (Koehler et al., 1996). However, extent of error appears to be chromosome-specific (Davisson and Akeson, 1993; Winking et al., 2000). Spindle abnormalities and lagging chromosomes have also been observed in oocytes of Rb-heterozygous mice (Eichenlaub-Ritter and Winking, 1990).

We provide new data on meiotic pairing abnormalities and nondisjunction leading to apoptosis and gametic aneuploidy in male Rb heterozygotes. Our observations indicate that the unusual chromosome constitution in Rb-heterozygous males leads to abnormalities during meiotic division, with concomitant cell death consistent with checkpoint surveillance of chromosome alignment on the spindle.

Nonetheless, aneuploid gametes are produced, suggesting that checkpoint mechanisms do not reliably eliminate all aneuploid germ cells.

CHAPTER II

MATERIALS AND METHODS

Animals

RBJ/Dn mice (The Jackson Laboratory, Bar Harbor, ME) were crossed with C57BL/6J (B6) mice (The Jackson Laboratory, Bar Harbor, ME) to produce F1 individuals heterozygous (Rb/+) for each of the four Rb chromosomes present in the Rb-homozygous parent (Rb(5.15)3Bnr, Rb(11.13)4Bnr, Rb(16.17)7Bnr, Rb(2,8)2Lub).

Three-color Fluorescence in Situ Hybridization (FISH)

For sperm FISH analysis, four Rb/+ and six B6 mice were killed by cervical dislocation and sperm from epididymides were collected in 2.2% citrate. Sperm were spread onto a slide and dried. The slides were soaked in DTT on ice for 30 min and placed immediately into LIS (diiodosalicyclic acid) for 1 hr. The slides were air dried and dehydrated in ethanol. Slides and probes were denatured at 78° C in formamide, then dehydrated and air-dried. The probes were specific for chromosomes 8, X and Y (gifts from Terry Hassold, Case Western University, Cleveland, Ohio). Biotin was used to label 1 µg of the Y probe pERS-532 (Eicher et al., 1991); the chr. 8 probe, which was a mixture (2 µg total) of four subclones (Boyle and Ward, 1992), was labeled with digoxygenin; and 1 µg of the X chromosome-specific probe DXWas (Disteche et al., 1987) was labeled with both biotin and digoxygenin separately. Probes were labeled with digoxygenin and biotin using a nick translation kit (Roche

Pharmaceutical) and purified over a Sephadex- G50 column. The probe mix was added to each slide and allowed to incubate at 37° C overnight. The next day, the slides were washed in 50% formamide/2X SSC, in 2X SSC, and then in PN Buffer (0.1M NaH_2PO_4, 0.1M Na_2HPO_4, 0.05% NP-40, pH 8). Slides were incubated in a BSA-blocking buffer and the appropriate fluorochrome-conjugated detector, also in BSA, at 37° C for 30 min, then washed in PN buffer twice. After adding DAPI/Antifade (Molecular Probes), slides were viewed with an epifluorescent microscope at 100X. Estimates of sperm aneuploidy were deliberately conservative. Only hyperhaploidy, and not hypohaploidy, was scored; the aneuploidy frequency represents twice the hyperhaploidy frequency. Additionally, sperm were deemed suitable for scoring only when the following criteria were met: fluorescent signals were clearly within and not on the edge of the sperm nucleus, fluorescent signals were all in the same plane of focus, and any two signals scored as separate were separated by a distance equal or greater than one signal domain.

Chromosome painting was performed on testicular cells fixed in 3:1 ethanol:acetic acid and then air-dried onto slides (Evans et al., 1964). The slides were air-dried overnight and dehydrated in a 70%, 90%, 90% and 100% ethanol series, then air-dried again. The DNA of the cells was denatured by incubation in 70% formamide/2X SSC at 65° C for 2 min. The slides were then quenched in the ethanol series above and air-dried again. Chromosome paint probes, for chr. 2 and chr. 8 (Cambio Inc, Cambridge, UK), were warmed to 37° C, and denatured at 65° C for 10 min, then at 37° C for 60-90 min. Subsequently, 15µl of each chromosome paint probe was added to each slide and the cells were coverslipped, sealed and incubated

overnight at 37° C in a humidified chamber. The slides were washed twice for 5 min at 45° C in 50% formamide/2X SSC and then twice in 0.1X SSC. Detection reagents 1 and 2, provided by the manufacturer (Cambio, Inc.) for the chr. 2 probe, which required amplification, were made in a 3% BSA/4X SSC blocking solution and slides were incubated with the appropriate detection reagent for 40 min in a humidified chamber at 37° C. The slides were then processed for visualization as above.

Testis Fixation and In Situ Apoptosis Detection

Mice were killed by cervical dislocation, testes removed, and fixed either in 4% paraformaldehyde overnight at 4° C or in Bouin's solution overnight at room temperature. Testes from 3 Rb/+ mice and 3 B6 mice at ages 14, 18 and 23 days old, as well as adult, were fixed in this manner. The testes were dehydrated through an ethanol series and toluene, then embedded in paraffin. The tissue was sectioned at 3-6 μM, and the sections placed on slides to dry. After deparaffination in xylene and rehydration in a decreasing ethanol series, the slides were subjected to the TUNEL reaction for assessment of apoptosis (see below). For staging of tubule sections, periodic acid-Schiff (PAS) staining was performed following the manufacturer's (Sigma) protocol with some modifications. After the TUNEL reaction, slides were rinsed in phosphate-buffered saline (PBS), then placed in 0.5% periodic acid for 10 min. After a 10 min wash in dH_2O, followed by incubation for 1 hr in Schiff reagent in the dark, the slides were placed in 1% potassium metabisulfite for 2 min. The slides were then washed in dH_2O, stained with hematoxylin for 2 min, rinsed with tap water, and placed in lithium carbonate (1.38g/100ml dH_2O saturated) for 3 sec.

Following washes in an increasing ethanol series and xylene, the slides were mounted with Permount (Fisher).

Apoptosis assays were performed using the In Situ Cell Death Detection Kit (Roche/Boehringer Mannheim), employing the TUNEL reaction following the manufacturer's protocol, with the exception that the enzyme incubation was for 15 min. Scoring of apoptosis frequency was performed by counting alkaline phosphatase-positive (brown) cells in tubule sections. Tubule cross-sections were scored as apoptotic when three or more apoptotic meiotic cells were observed per tubule cross-section.

Fixation and Immunofluorescent Labeling of Tubule Segments and Isolated Germ Cells

To obtain cytological preparations enriched in meiotically dividing spermatocytes (stage XII of the mouse seminiferous epithelium) a variation of the transillumination procedure (Parvinen et al., 1993) was used. Testes from adult mice (3 B6 males and 3 Rb/+ males) were detunicated, then digested with collagenase for 8 min at 33°C in Krebs-Ringer bicarbonate (KRB) buffered media. Transillumination patterns were observed using a dissecting microscope and the desired stage XII segments (visualized as 3 mm beyond the site of transition from optically dense to light) were excised and transferred onto a microscope slide in KRB. For fixation, a coverslip was placed on top of the segment, then the entire slide was frozen in liquid N_2 for 30 sec. The coverslip was removed, and the slide was fixed in 3:1 ethanol/acetic acid. Prior to incubation with antibody, the slide was placed in

PBS/0.2% Triton X-100 (Sigma) for 5 min, then placed in blocking solution (PBS/10% goat serum) for 30 min.

Cell preparations enriched in germ cells were prepared as previously described (Cobb et al., 1999a). Briefly, testes were detunicated and digested in 0.5 mg/ml collagenase (Sigma) in Krebs-Ringer buffer for 20 min at 32°C and then in 0.5 mg/ml trypsin (Sigma) for 13 min, followed by filtering through 80 μm mesh and washing in buffer. To make surface-spread preparations for visualization of nuclei, cells were fixed in 2% paraformaldehyde with 0.03% SDS (Cobb et al., 1999a). Spermatocytes from germ cell preparations were also embedded in a fibrin clot using modifications to a previously published protocol (LeMaire-Adkins et al., 1997). Germ cells were isolated as mentioned above, and brought to a concentration of 25 X 10^6 cells/ml. Onto a slide, 3 μl of fibrinogen (Calbiochem, 10mg/ml fresh) and 1.5 μl of the cell suspension were mixed. Then 2.5 μl of thrombin (Sigma, 250 units) was added, and allowed to clot for 5 min. The slide was fixed in 4% paraformaldehyde, washed in 0.2% Triton X-100, then processed for immunofluorescence.

The antisera used were 1) polyclonal anti-SYCP3, 2) anti-β-tubulin (Amersham), 3) anti-phosphorylated histone H3-Ser10 (Upstate Biotech), 4) anti-CENP-E (Schaar et al., 1997) and anti-CENP-F (Liao et al., 1995), generously provided by T. Yen, and 5) anti-MPM-2 (Upstate Biotech). The polyclonal antibody recognizing SYCP3 was prepared by Covance Research Products (Richmond, CA) against recombinant his-tagged protein expressed in *E. coli*. The *Sycp3* cDNA was synthesized by RT-PCR from testicular RNA, cloned into the pPROExHta expression vector (GibcoBRL) and the sequence verified by direct sequencing. Rats were

injected intramuscularly with 0.5 mg of purified SYCP3 protein in 6M urea followed by booster injections of 0.25 mg protein at three-week intervals. Serum was collected at three-week intervals beginning one month after the initial injection. All sera collected after the injections contained specific antibodies that recognized the SYCP3 protein. The specificity of the antiserum was determined by immunoblotting using extracts from pachytene spermatocytes, known to contain SYCP3 protein. Preimmune serum did not recognize any proteins in extracts from pachytene spermatocytes and did not stain cells. Serum collected after antigen injection recognized only protein of the appropriate molecular weight and stained axial elements and synaptonemal complexes in spermatocytes.

Following overnight incubation in primary antibody, slides were incubated with rhodamine- or fluorescein-conjugated secondary antibodies (Pierce), followed by mounting with Prolong Antifade (Molecular Probes) containing DAPI (Molecular Probes) to stain DNA. Control slides were stained with either secondary antibodies only, or pre-immune sera as a primary antibody. Staining was observed with an Olympus epifluorescence microscope and images were captured and transferred to Adobe PhotoShop with a Hamamatsu color 3CCD camera. Confocal imaging was performed using a Leica TC SP2 laser-scanning confocal microscope.

CHAPTER III

RESULTS

Rb-Heterozygous Mice Exhibit Elevated Levels of Sperm Aneuploidy

Analysis of sperm by three-color fluorescence *in situ* hybridization (FISH) was used to seek evidence that Rb/+ mice are models for error-prone meiosis. This analysis revealed elevated levels of sperm aneuploidy in Rb/+ males by comparison to age-matched control males (Table 1). Disomy for chromosomes 8, X and Y was determined using probes specific for each chromosome, and sperm from 6 Rb/+ males were scored. The combined hyperhaploidy frequency for chromosomes 8, X and Y was 4.57% in sperm from Rb/+ males compared to 0.25% in sperm from B6 males (Figure 2 and Table 1). The hyperhaploidy frequency for chromosome 8 was 4.38% among sperm from Rb/+ males compared to 0.075% among sperm from B6 males. Since nullisomic sperm (those lacking signals) were not scored, the estimated overall aneuploidy frequency for chromosome 8 is twice the disomy frequency, or approximately 9%. Moreover, sperm from Rb/+ males were characterized by a significantly elevated level of chr. 8 aneuploidy, compared to sex-chromosome aneuploidy. This is an important point, as chr. 8 is involved in Rb(2.8)Lub in the Rb/+ males, while chromosomes X and Y are not a member of any of the translocation chromosomes. Since strict criteria were used for scoring sperm aneuploidy (see Materials and Methods), this estimate is a conservative one. Although probes were not used to detect aneuploidy of the chromosomes involved in the other Rb translocations in this RBJ/Dn stock, it can be assumed that a frequency

Figure 2: Illustrations of sperm stained by the three-color FISH method. **A)** A chromosomally normal sperm from a B6 mouse containing a single Y chromosome (green) and a single 8 chromosome (red). **B)** An aneuploid sperm from a Rb/+ mouse containing a single Y chromosome (green) and two 8 chromosomes (red). Scale bar = 5 μm.

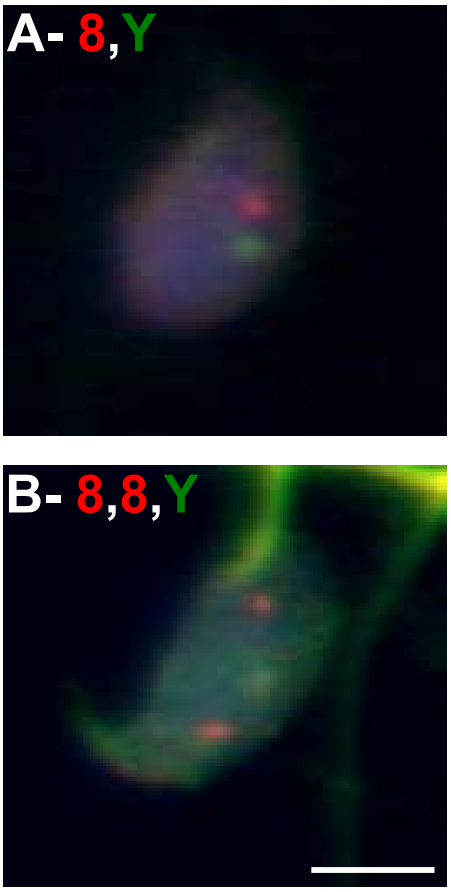
A- 8,Y
B- 8,8,Y

Table 1. Sperm FISH analysis of frequencies of aneuploid sperm from B6 and Rb-heterozygous mice. *****Dis = disomy, values are percent of total sperm counted.

Mouse #	Dis8*	DisX*	DisY*	XY	Total	Total Sperm Counted
B6 201	0	0	0	0	0	1000
B6 202	0	0.1	0.2	0.1	0.4	1000
B6 203	0.1	0.1	0.1	0	0.3	1000
B6 204	0.2	0	0	0.1	0.3	1000
Avg%	0.075+/-0.1	0.05+/-0.06	0.075+/-0.1	0.05+/-0.06	**0.25+/-0.18**	
Rb/+ 197	4.3	0.1	0	0.2	4.5	1013
Rb/+ 198	3.9	0.1	0.1	0.1	4.1	1000
Rb/+ 199	5.5	0	0	0.09	5.6	1001
Rb/+ 200	4.5	0.09	0.09	0	4.7	1001
Rb/+ 204	3.8	0	0.2	0	4	1000
Rb/+ 205	4.3	0	0	0.2	4.5	1025
Avg%	**4.38+/-0.61**	0.048+/-0.05	0.065+/-0.08	0.098+/-0.09	**4.57+/-0.57**	

of 9% sperm aneuploidy is a minimal estimate of the overall frequency and that Rb/+ mice are a model for meiosis with errors in chromosome segregation.

Spermatocytes from Rb-Heterozygous Mice Exhibit Meiotic Pairing Abnormalities and Chromosome Misalignment

Since failure to maintain normal bivalent chromosomes could cause the observed gamete aneuploidy, metaphase chromosome pairing was examined from air-dried chromosome preparations. FISH with chromosome-specific paint probes was used to examine MI pairing configurations of the Rb(2.8)Lub and its homologs, the acrocentric chromosomes 2 and 8. Fig. 3A shows among spermatocytes from B6 control males, the signals for chromosomes 2 and 8 are combined, suggesting maintenance of homologous pairing at MI. In contrast, typical images of spermatocyte nuclei from the Rb/+ males revealed two types of signal configurations: those suggesting apparent homologous pairing (Fig. 3B) and those with apparent pairing disruption, where signals for homologous chromosomes are separated and sometimes one of the painted chromosomes (either chr. 2 or chr. 8) is juxtaposed with an unpainted DAPI-stained chromosome (Fig. 3C). Among the 5 individual males scored, the overall frequency of spermatocytes with apparently unpaired chromosomes 2 and/or 8 was 28.18% compared to 0% for B6 control spermatocytes (Table 2).

In addition to the univalence and pairing abnormalities illustrated in Fig. 3, earlier prophase pairing abnormalities were seen in surface-spread spermatocyte nuclei stained with antiserum against mouse SYCP3 for visualization of the

Figure 3: Air-dried meiotic metaphase I (MI) chromosome spreads labeled with chromosome paint probes (2: green, 8: red). **A)** MI from a B6 mouse displaying proper pairing of homologs. **B)** Homologous pairing in an MI spermatocyte from a Rb/+ male. **C)** Failure in homologous chromosome pairing in an MI spermatocyte from a Rb/+ mouse. Scale bar = 5 μm.

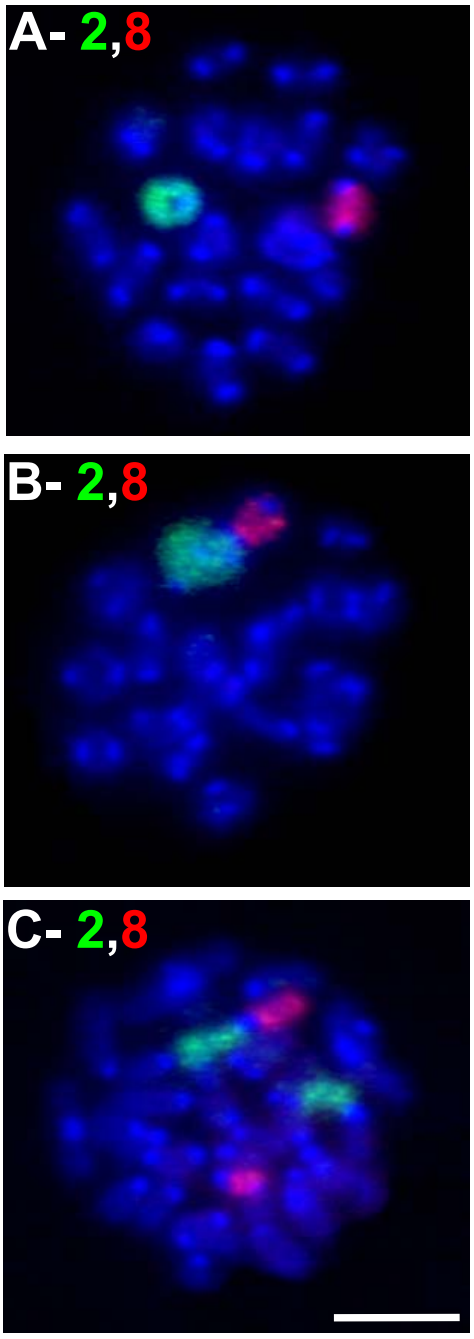
A- 2,8
B- 2,8
C- 2,8

Table 2. Frequencies of unpaired chromosomes (chromosomes 2 and 8) in MI spermatocytes of Rb-heterozygous mice.

Mouse	Unpaired/Total	% Unpaired
Rb/+ 201	35/102	34.3
Rb/+ 202	16/64	25
Rb/+ 203	14/48	29.2
Rb/+ 204	14/54	25.9
Rb/+ 205	9/34	26.5
	Avg.	**28.18**
	STDEV	**3.76**

synaptonemal complex. These pairing abnormalities consisted primarily of incompletely paired regions, sometimes seen as pairing "protrusions" at the centromeric regions (Fig. 4).

Additionally, unaligned chromosomes were seen on meiotic MI spindles, which could be a consequence of the observed pairing abnormalities. In order to retain the three-dimensional configuration of division-phase spermatocytes, germ cells were fixed and embedded in a fibrin clot and visualized by confocal microscopy. When scoring these cells, prometaphase cells were identified as having condensed chromosomes, loss of nuclear envelope and a unipolar spindle. Metaphase cells exhibit bipolar spindles and aligned chromosomes. Metaphase I cells retain SYCP3 epitopes, while metaphase II cells are spatially close to their sister cell and do not retain SYCP3 epitopes. These criteria allowed us to determine that cells with unaligned chromosomes were in metaphase (not prometaphase). Additionally, all frequencies of abnormalities were compared to control B6 spermatocytes. Spermatocytes from B6 mice consistently exhibited a "compact" MI configuration of chromosomes, with all chromosomes congressed to the meiotic spindle equator (Fig. 5A), revealed by immunofluorescence with antibodies against the phosphorylated form of histone H3-Ser10 and β-tubulin. Phosphorylation of histone H3 on Ser10 is correlated with chromosome condensation at G2/M in spermatocytes (Cobb et al., 1999b) and thus antibody staining provides a marker for cells in the division phase. In contrast to chromosomally normal spermatocytes, MI spermatocytes from Rb/+ mice frequently exhibited chromosomes that were unaligned or malattached at a distance from the metaphase equator (Fig. 5B). This pattern of misalignment was

Figure 4: Pairing abnormalities in surface-spread spermatocytes from Rb/+ mice. **A)** A nucleus showing the pairing abnormalities (arrowheads) in an Rb/+ spermatocyte stained with antserum against the synaptonemal complex protein SYCP3 (red). **B)** A protrusion in the pairing regions (arrowhead). Scale bars = 10 μm (A) and 1 μm (B).

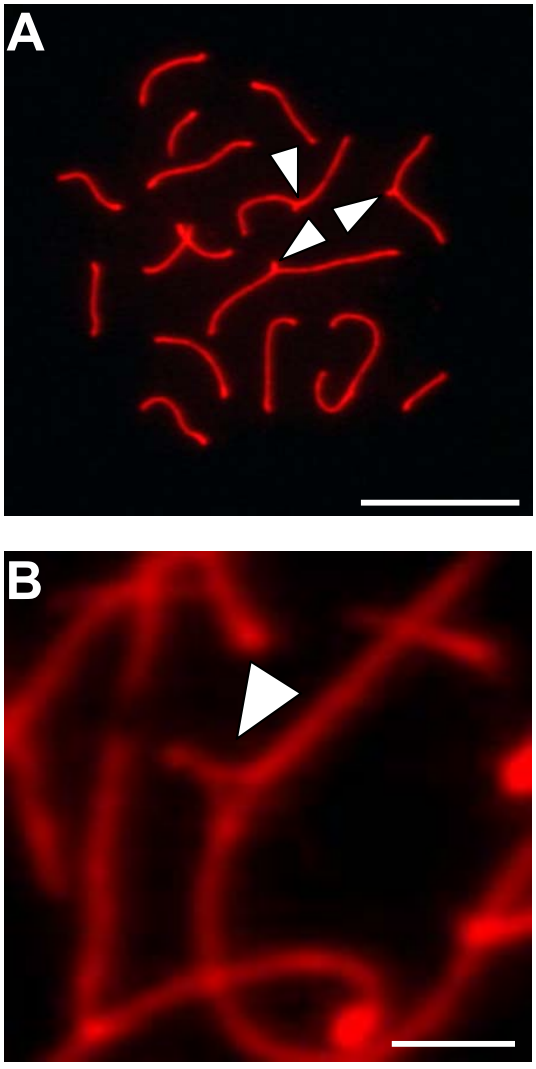
A
B

Figure 5: Confocal imaging of MI chromosomes and spindles from B6 and Rb/+ spermatocytes (β-tubulin in red, phospho-histone H3 in green). **A)** A MI spermatocyte from a control B6 mouse in which all chromosomes are found to be properly aligned on the metaphase plate. **B)** A MI spermatocyte from a Rb/+ mouse, illustrating unaligned chromosomes (arrowheads). **C**) A MI spermatocyte from a Rb/+ mouse displaying a misaligned chromosome (arrowhead) and an abnormal spindle, in which one pole is undeveloped (arrow). **D)** Rb/+ MII spermatocytes depicting chromosomes lagging behind the spindle poles (arrowheads). Scale bar = 10 μm.

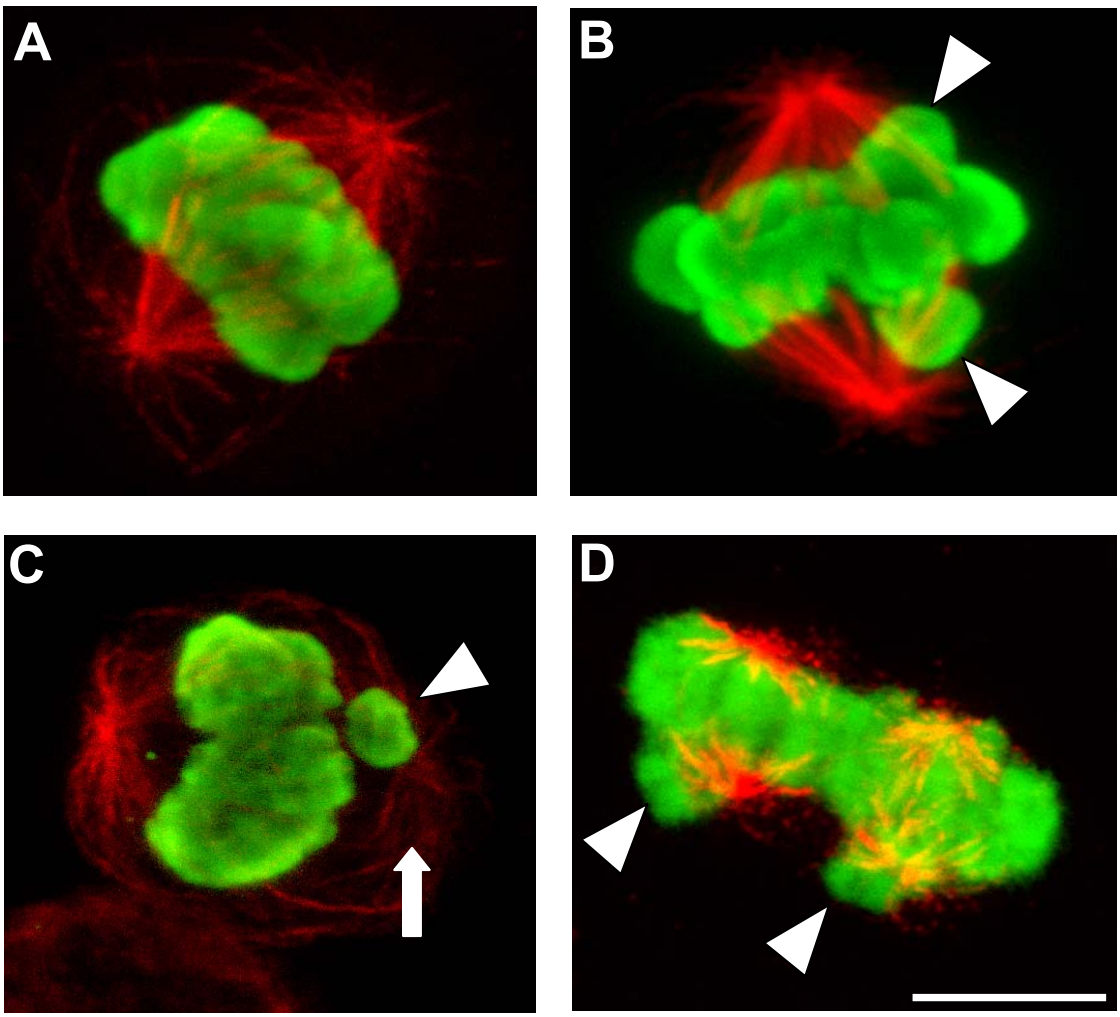
A
B
C
D

seen after establishment of the bipolar and elongated spindle, which in rodents occurs during prometaphase (Kallio et al., 1998). This configuration was sometimes accompanied by abnormalities in spindle structure; for example, in Fig. 5C, note that one spindle pole is not developed, while the microtubule arrays radiate away from the metaphase plate. Such spindle abnormalities may be an early step in apoptosis (see below). Although spindle abnormalities were less frequent, nonaligned chromosomes were found in 23% of the 500 phospho-histone H3-positive MI spermatocytes scored in each of 3 Rb/+ mice, whereas unaligned chromosomes were seen in only 4.8% of 500 MI spermatocytes from each of 3 B6 males. In addition to the MI abnormalities, some MII spermatocytes from Rb/+ mice also exhibited aberrant chromosome configurations, for example, chromosomes that are positioned behind rather than between the spindle poles (Fig. 5D).

The frequency of spermatogenic cell stages was determined to test the hypothesis that these pairing and metaphase alignment abnormalities could cause a loss of cells and/or delay in the normal progression of spermatogenesis. Germ cells were isolated and the frequency of cell types was obtained from nuclei spreads (Fig. 6). The frequency of post-meiotic round spermatids, relative to the frequency of leptotene/zygotene spermatocytes, was decreased in the germ cell population from Rb/+ compared to that from B6 mice, and a concomitant increased frequency of pachytene spermatocytes, but not of leptotene/zygotene spermatocytes, was found among germ cells from Rb/+ mice compared to germ cells from the control B6 mice (Fig. 6). Additionally, when sectioned material was analyzed, the frequencies of stage XII, and VII-IX, tubule sections in Rb/+ testes were found to be greater than

Figure 6: The frequencies of spermatogenic cell stages from B6 (white bars) and Rb/+ (black bars) adult mice. Germ cells were isolated as an enriched population from testes of 3 adult mice, and the number of leptotene/zygotene spermatocytes (L/Z), pachytene spermatocytes (Pach), and round spermatids (RS) were determined in a total of 250 cells per mouse. These cells represented most but not all of the cell types in the population, which also included somatic cells and elongated spermatids. Asterisks represent paired values that differ significantly (Student's t test; $p = 0.001$ for difference in frequency of pachytene spermatocytes and $p = 0.008$ for difference in frequency of round spermatids).

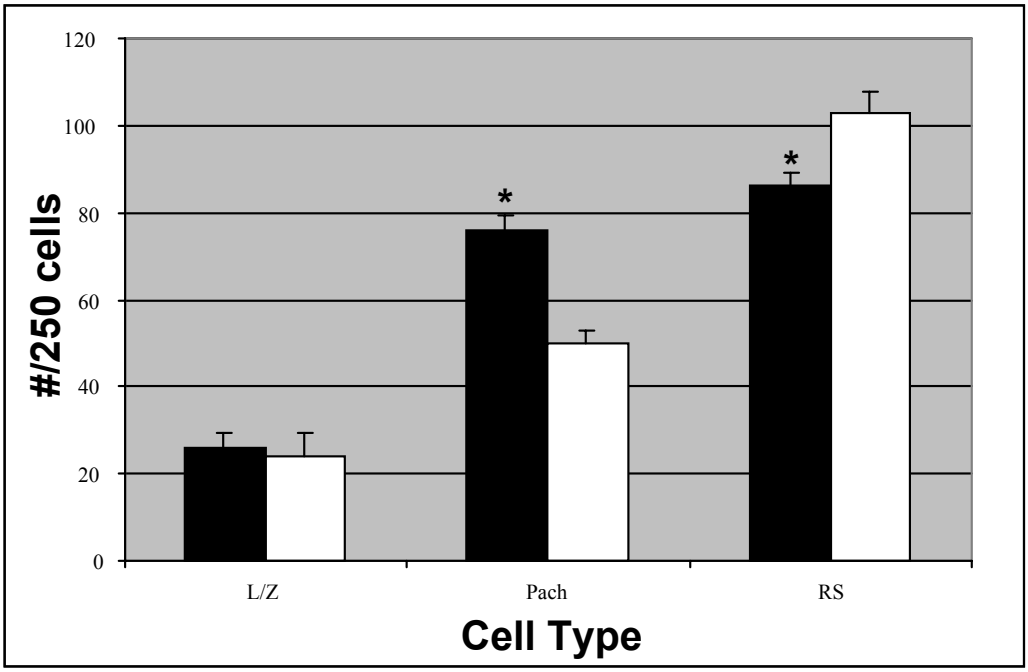
120
100
80
60
40
20
0
#/250 cells
*
*
L/Z
Pach
RS
Cell Type

those in control B6 testes, while the frequency of the other stages did not differ statistically between the two (Fig. 7). Taken together, these data suggest loss of cells and possible delay in progress of spermatogenesis in Rb/+ mice.

Spermatocytes from Rb-Heterozygous Males with Misaligned Chromosomes Exhibit Elevated Frequency of Apoptosis in Meiotic Division Phase

To test the hypothesis that chromosome abnormalities might activate a meiotic checkpoint leading to apoptosis, apoptotic cells in tissue sections were identified and enumerated using the TUNEL reaction and periodic acid-Schiff reagent to stage tubule sections. The criterion for identifying individual cross-sections as apoptotic was the presence of three or more apoptotic cells per tubule section. Relatively few cells were found to be apoptotic in testes of control B6 males (Figs. 7 and 8). However, in testes of Rb/+ males, apoptosis was found to be elevated among MI spermatocytes in seminiferous epithelium stage XII. In a developmental analysis of the onset of apoptosis, testes from 3 Rb/+ and 3 control B6 mice were examined on days 14, 18 and 23 after birth. These time points were chosen to precede (days 14 and 18) and coincide with (day 23) appearance of significant numbers of MI cells. An elevated number of apoptotic meiotic germ cells were found in testes from Rb/+ mice only after 23 days of age (Fig. 8), with a frequency of 15.8 +/-2.8 apoptotic cells/stage XII tubule cross-section (data not shown).

In order to determine if the apoptotic cells seen in stage XII cross sections were due to MI spermatocytes with unaligned chromosomes, microdissected stage XII segments were analyzed for both apoptosis by the TUNEL reaction, for DNA by

Figure 7: Frequencies of seminiferous tubules at indicated stages and of apoptotic tubules (hatched bar) in B6 (white bars) and Rb/+ (black bars) adult mice. Sectioned material was staged with periodic acid-Schiff reagent and hematoxylin, and processed using the TUNEL method for detecting apoptotic cells. All stage XII tubules in Rb/+ mice were apoptotic (red). Asterisks represent paired values that differ significantly (Student's t test; $p = 0.035$ for difference in frequency of stage VII-IX tubules and $p = 0.033$ for difference in frequency of stage XII tubules).

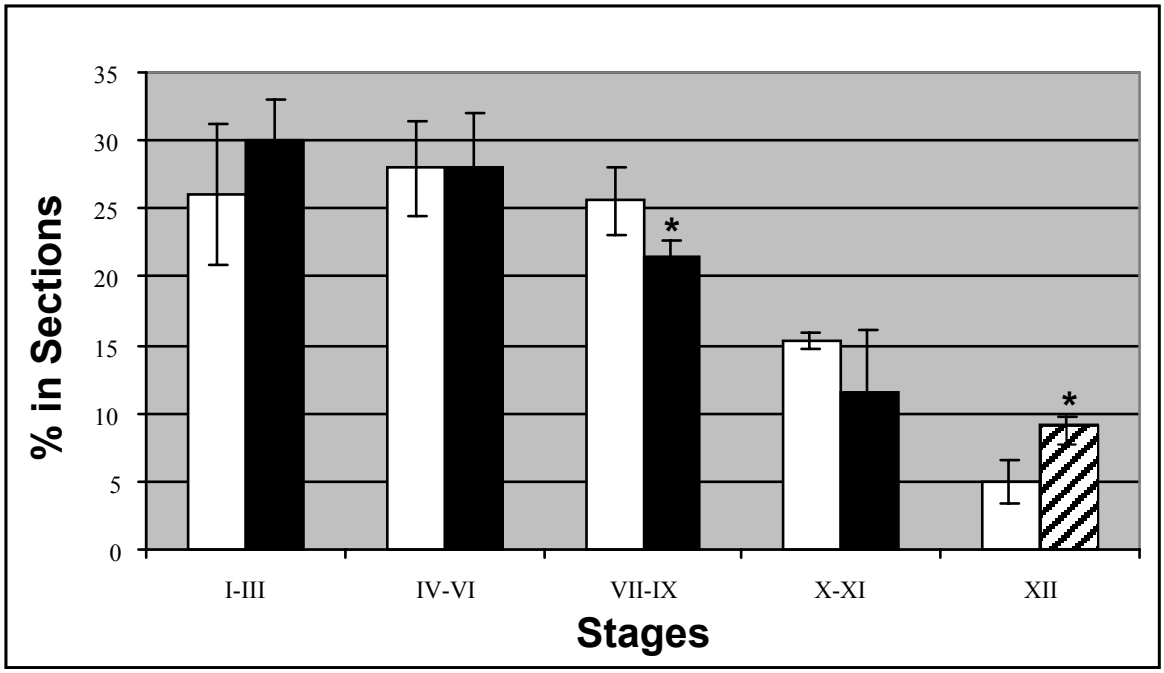
35
30
25
20
15
10
5
0
% in Sections
*
*
I-III
IV-VI
VII-IX
X-XI
XII
Stages

Figure 8: Apoptotic cells in stage-XII tubule sections of B6 **(A)** and Rb/+ **(B)** 23 day-old mice. Sections were stained with hematoxylin, periodic acid-Schiff reagent, and processed to observe apoptotic cells (brown cells) by the TUNEL reaction. **C)** Germ cells from a preparation of micro-dissected stage XII tubule from a Rb/+ mouse. The red staining represents antibody against phosphorylated histone H3 to visualize meiotic division-stage cells and the green staining denotes apoptosis (detected by the TUNEL method). Scale bars = 100 μm (A and B) or 10 μm (C).

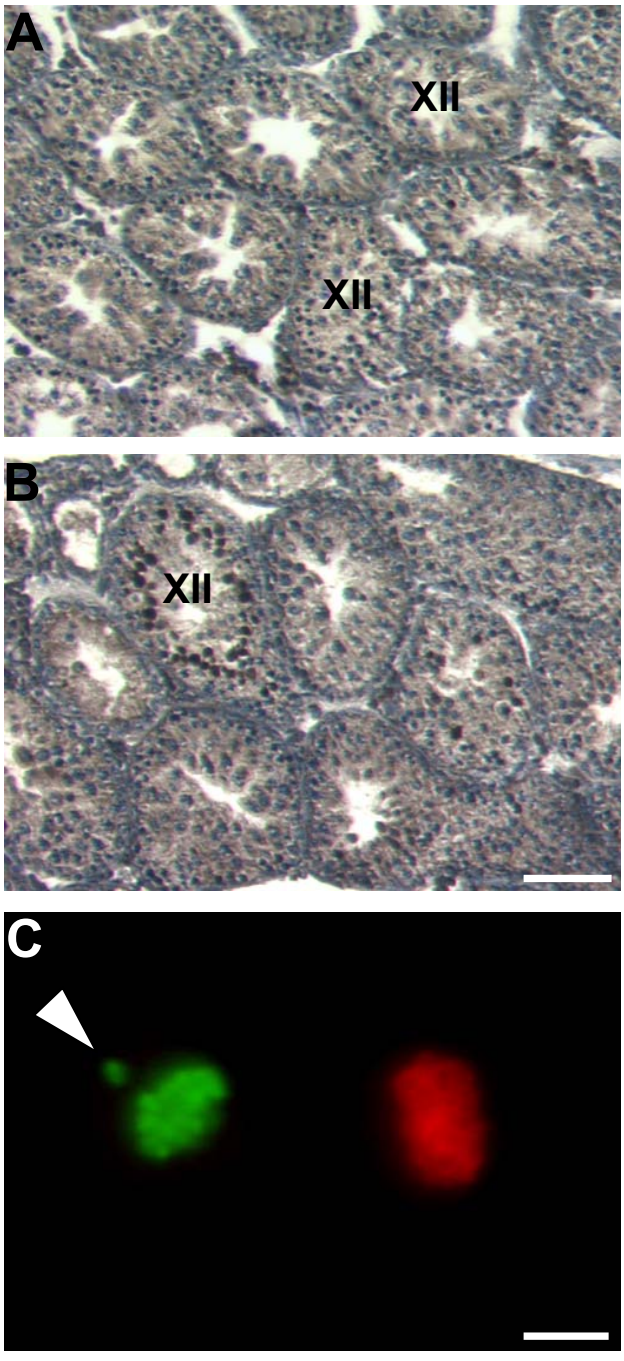
A
XII
XII
B
XII
C

DAPI stain and by immunofluorescence with antibody against phosphorylated histone H3 to visualize chromosome alignment at MI. This analysis revealed that a significant proportion of the apoptotic MI spermatocytes exhibited a misaligned chromosome (Fig. 8C). A total of 1000 apoptotic MI spermatocytes were scored in tubules from 3 Rb/+ males and 79.8% contained chromosomes not properly aligned on the metaphase plate (Table 3). This observation directly links apoptosis to spermatocytes with unaligned chromosomes. Interestingly, it was observed that many of the apoptotic MI spermatocytes did not stain with the antibody against phospho-histone H3, suggesting loss of phosphorylation on Ser10 as part of the apoptotic process. This observation suggests that the previous estimate that 23% of MI spermatocytes in Rb/+ testes have misaligned chromosomes (above and Fig. 5) is low since this was derived only from MI spermatocytes that stained positively for phospho-histone H3.

Taken together, these analyses show increased germ-cell apoptosis in testes of Rb/+ mice, provide evidence that the susceptible meiotic stage encompasses the division phases, and suggest that it is cells with chromosomal abnormalities that are undergoing apoptosis.

Meiotic Spermatocytes from Rb-Heterozygous Mice Exhibit Features of Normal G2/M but Also Abnormalities in Behavior of Putative Checkpoint Proteins

In spite of chromosome pairing abnormalities and apparent meiotic delay, many features of the meiotic prophase-metaphase (G2/M) transition were normal in spermatocytes from Rb/+ mice compared to those from B6 controls. In surface-

Table 3. Frequencies of apoptosis and chromosome misalignment in metaphase spermatocytes.

* UC= with unaligned chromosomes

** Data compiled across 3 B6 and 3 Rb/+ mice (250-500 cells scored per mouse)

*** Data compiled across 3 B6 mice (20-40 apoptotic MI's scored per mouse)

Strain	# MIs	# MIs Apop (%)	# Apop MIs	# Apop MIs-UC* (%)
B6	1000**	89 (8.9)	100***	28 (28)
Rb/+	1000**	603 (60.3)	1000**	798 (79.8)

spread spermatocytes from both control and Rb/+ spermatocytes, we observed orderly disassembly of the synaptonemal complex, chromatin condensation and individualization, and appearance at MI of newly phosphorylated epitopes, detected by phospho-histone H3-Ser10 antibody (a marker for chromosome condensation) and MPM antibody (a marker for epitopes phosphorylated at division phase) (data not shown).

Because of evidence for spindle abnormalities in Rb/+ spermatocytes and for elimination of spermatocytes by apoptosis, attention was given to localization of proteins that might act directly or indirectly in checkpoint mechanisms. In mitotic HeLa cells, kinetochores on lagging chromosomes stain more intensely with antibodies against hBUBR1 and CENP-E, known spindle assembly checkpoint proteins, than do kinetochores on chromosomes that are properly aligned (Chan et al., 1999). Consequently, the pattern of localization and intensity of signal of CENP-E was monitored at kinetochores of chromosomes associated with spindles in Rb/+ spermatocytes, especially at the kinetochores of improperly attached or lagging chromosomes (such as in Figs. 5 and 8). In Fig. 9, the normal prometaphase (A and B) and metaphase (C and D) patterns of CENP-E staining of B6 spermatocytes from microdissected stage XII tubule sections is shown. This pattern of staining was also the predominant one in Rb/+ spermatocytes, with the important exception of kinetochores of chromosomes not aligned at the metaphase spindle equator (arrows in Fig. 9 E, F and G), where staining was more intense. Kinetochores on all of the malattached chromosomes stained more intensely with antibodies against CENP-E. A similar staining pattern was seen with antibodies against CENP-F (Fig. 10). The

Figure 9: CENP-E staining in prometaphase and metaphase spermatocytes from B6 and Rb/+ mice. CENP-E staining in B6 early prometaphase **(A and B)** and late prometaphase spermatocytes **(C and D)** (β-tubulin staining in red, CENP-E staining in green). **A** and **C** are overlays of CENP-E and β-tubulin staining, while **B** and **D** show CENP-E staining only. **E-G)** CENP-E (green) staining in a Rb/+ MI spermatocyte, containing misaligned chromosomes (arrows). **E)** CENP-E staining in green, **F)** DAPI (for DNA) in blue, and **G)** overlay of E and F with MPM-2 staining in orange. Scale bar = 10 μm.

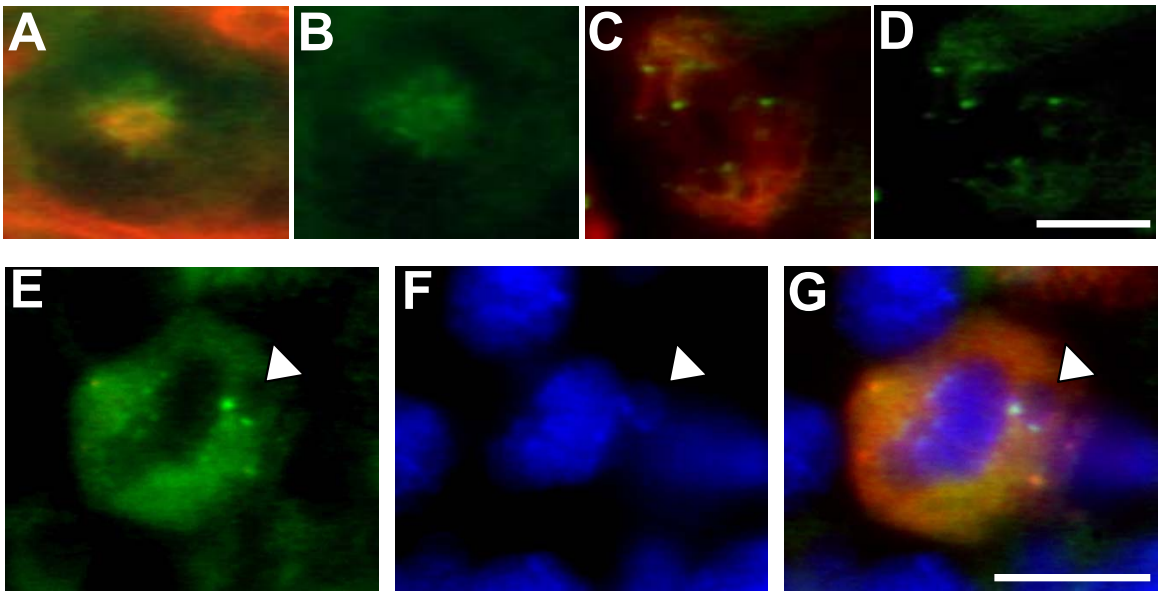
A
B
C
D
E
F
G

Figure 10: CENP-F staining in prometaphase and metaphase spermatocytes from B6 and Rb/+ mice. CENP-F staining in B6 prometaphase **(A and B)** and metaphase spermatocytes **(C and D)** (β-tubulin staining in red, CENP-F staining in green). **A** and **C** are overlays of CENP-F and β-tubulin staining, while **B** and **D** show CENP-F staining only. **E-G)** CENP-F (green) staining in a Rb/+ MI spermatocyte, containing misaligned chromosomes (arrows). **E)** CENP-F staining in green, **F)** DAPI (for DNA) in blue, and **G)** overlay of E and F with MPM-2 staining in orange. Scale bar = 10 μm.

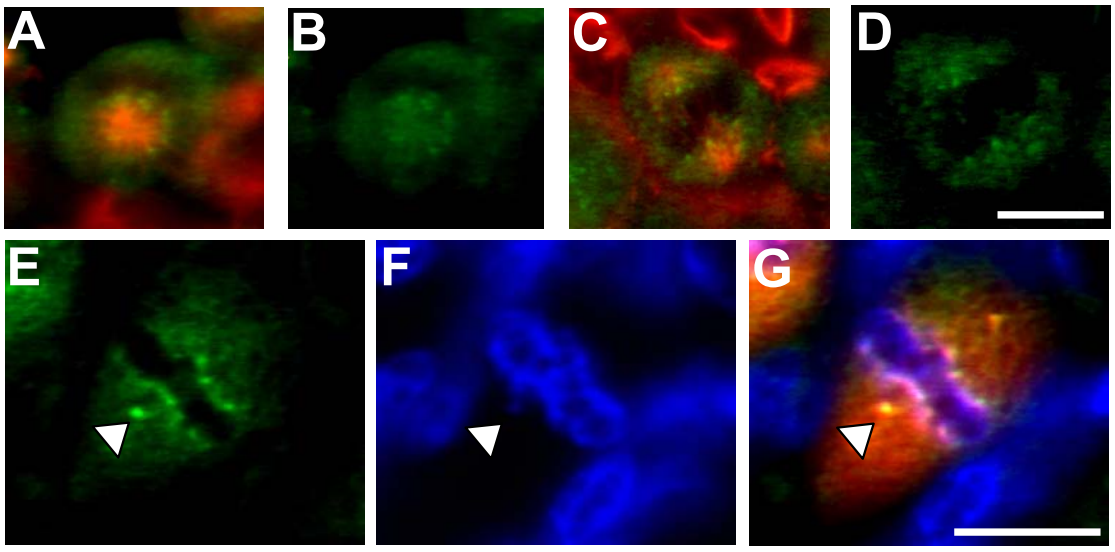
A
B
C
D
E
F
G

increase in fluorescence intensity in detection of these proteins may be due to either an increase in the amount of protein at the kinetochore on unaligned chromosomes, or an increased accessibility of the epitope to the antibody, possibly due to a conformational alteration.

Antibodies against the polo-like kinase PLK1 protein, MAD2 and SYCP3, as well as CREST antisera, were used to assess the possibility of an elevation in staining intensity of other proteins in centromeric regions, as well as to detect multiple kinetochores (data not shown). Staining with these antibodies revealed similar intensity on kinetochores of both properly aligned chromosomes and those that were not in Rb/+ spermatocytes. Although a role for PLK1 protein in both DNA repair and centrosome maturation has been suggested, it is not thought to be involved in a spindle checkpoint mechanism. While MAD2 is thought to play a role in the spindle assembly checkpoint, its function during mammalian meiosis has not been established. It was previously shown that MAD2 is present at most, but not all, kinetochores of mouse spermatocytes during the first metaphase of meiosis (Kallio et al., 2000). When we stained mouse metaphase I spermatocytes using antibodies against MAD2, we also observed variability in kinetochore staining within and amongst spermatocytes. This suggests that MAD2 may not be required for the first meiotic division during mammalian meiosis. The exact role of MAD2 during a possible spindle assembly checkpoint mechanism during meiosis awaits further experimental evidence.

CHAPTER IV

DISCUSSION

This study was conducted to seek evidence for how male germ cells cope with error in meiotic division. Mice heterozygous for Rb chromosome translocations have previously been shown to produce aneuploid gametes, and it is not clear if there are any correction mechanisms that might diminish the overall level of gamete aneuploidy. The results show that mice heterozygous for four different Rb chromosomes derived from RBJ/Dn are a good model in that they produce sperm characterized by a higher than normal frequency of aneuploidy. Abnormalities of chromosome pairing at metaphase of the first meiotic division were demonstrated by use of whole-chromosome FISH paint probes. Additionally, MI spermatocytes from Rb heterozygotes were characterized by an elevated frequency of chromosomes misaligned and failing to congress on the spindle. Evidence that there is ensuing cell death, delay and arrest, which could be mediated by a checkpoint mechanism, includes detection of increased apoptosis of meiotic division-phase spermatocytes, predominantly those with misaligned chromosomes, as well as changes in the kinetics of spermatogenesis and presence of putative checkpoint signals on misaligned chromosomes at metaphase. Nonetheless, the relatively high frequency of gametic aneuploidy suggests that the checkpoint mechanism might not be an efficient block to meiotic progress in cells faced with multiple chromosomal abnormalities.

Meiotic Division of Spermatocytes from Rb-Heterozygous Mice Is Error-Prone

There are three lines of evidence from this work suggesting that gametic aneuploidy is a characteristic of Rb/+ mice. The first, and most direct, derives from assessment of sperm aneuploidy by FISH. Sperm aneuploidy for chromosome 8, participating in a Rb chromosome, was 8.8%, compared to 0.15% for control sperm. Similarly increased aneuploidy has been observed previously. Specifically, a ten-fold increase in the sperm aneuploidy frequency was found for males heterozygous for the Rb(8.14)16Rma translocation, although hyperhaploidy in the sex chromosomes did not differ from control values (Lowe et al., 1996). It is highly likely that most of the sperm aneuploidy we have observed derives from unbalanced segregation of metacentric Rb chromosomes and their acrocentric homologs at anaphase I. Since chromosome 8 is involved in only one of the four Rb chromosomes (Rb(2,8)2Lub), 9% is likely to be a minimum estimate of the total sperm aneuploidy. The overall aneuploidy frequency could be as high as 72% if sperm FISH probes for all the other seven chromosomes involved in Rb translocations (chromosomes 2, 5, 11, 13, 15, 16 and 17) had been used. However, most probably aneuploidy frequencies are chromosome-specific (Winking et al., 2000) and thus the multiplicative estimate of 72% could be inaccurate. Previous observations also suggest that heterozygotes for the single translocations Rb(5.15)3Bnr, Rb(11.13)4Bnr, and Rb(16.17)7Bnr are prone to nondisjunction, as assessed both by metaphase II (MII) chromosome analysis and by zygotic loss (Cattanach and Moseley, 1973). Additionally, other data derived from scoring chromosome arms in MII spermatocytes suggests malsegregation of chromosomes in heterozygotes for Rb(11.13)4Bnr (Everett et al., 1996). Thus, Rb/+

mice are a model for production of aneuploid sperm, and, furthermore, the aneuploidy appears to be restricted to the chromosomes involved in the Rb translocations.

The second line of evidence provides clues to what could be an origin of meiotic error in spermatocytes of Rb/+ mice. Spermatocytes scored at MI with whole-chromosome paint probes for chromosomes 2 and 8 (forming Rb(2,8)2Lub) displayed an abnormally high level (28%) of apparent univalence or nonhomologous pairings for these two chromosomes. This observation suggests that homolog pairing is diminished or that chiasmata are lacking or are prematurely resolved. Reduced chiasmata formation is also suggested by observations of pachytene spermatocytes showing abnormalities of chromosome pairing. Other studies have also shown that mispairing and recombination suppression occurs in Rb/+ spermatocytes, (Davisson and Akeson, 1993; Everett et al., 1996). However, this is the first study where mispaired chromosomes have been positively identified at MI by the use of chromosome-specific paint probes.

The third line of evidence also provides insight to a possible mechanism of aneuploidy. Spermatocytes scored at MI for misaligned or malattached chromosomes or for failure in congression showed an abnormally high frequency (23%) of these errors. The lagging chromosomes were seen after establishment and elongation of the bipolar spindle in prometaphase (Kallio et al., 1998). Careful comparison was made to the frequency of lagging chromosomes in control (B6) spermatocytes with elongated spindles to ensure that we were observing metaphase and not a stage in prometaphase congression. Although scoring was based on a sensitive immunofluorescence detection of MI chromosomes with phosphorylated histone H3,

specific chromosomes could not be identified since the preparative techniques for visualization of spindles were not compatible with chromosome FISH. Furthermore, the estimate of mislaigned chromosomes derived by using antibody to phosphorylated histone H3 may be low, because further analysis showed that many MI spermatocytes with misaligned chromosomes were apoptotic and did not stain with antibody against phospho-histone H3 (Fig. 8C and Table 3). These observations are consistent with a previous finding of lagging chromosomes in anaphase mouse oocytes containing Rb translocations (Eichenlaub-Ritter and Winking, 1990). We assume, but do not know, that univalent or mispaired Rb trivalents contributed to the majority of misaligned chromosomes detected at MI. Taken together, these observations imply that there was premature separation of chromosome homologs and that univalent or non-homologously-paired chromosomes were delayed in spindle attachment and/or congression.

These three lines of evidence lend support to the hypothesis that meiosis in Rb/+ mice is fraught with an increased level of error. The common effect is malsegregation leading to gametic aneuploidy, but the causes can lie in diminished chromosome pairing leading to univalence or misaligned chromosomes as well as unbalanced segregation of paired trivalents involving Rb chromosomes. These errors undoubtedly contribute to germ cell aneuploidy and embryo death. Since roughly 9% of sperm from these quadruple Rb/+ mice were aneuploid for chromosome 8, we estimated (above) that the total of the four translocations involving eight chromosomes events could produce an aneuploidy frequency as high as 72%. Nonetheless, somewhat amazingly, male mice heterozygous for 4 different Rb

chromosomes are fertile in spite of seemingly great potential for chromosomal disaster.

Apoptosis May Serve as an Elimination Mechanism for Abnormal Germ Cells

Evidence for a testicular mechanism for elimination of chromosomally aberrant germ cells was found in the elevated frequency of stage-specific apoptosis observed in testes of Rb/+ mice compared to both chromosomally normal B6 mice and Rb homozygotes. Apoptosis is a known mechanism for control of germ-cell number and elimination of abnormal and/or damaged germ cells in the testis (Print and Loveland, 2000); however, normally background levels of apoptosis are low. For example, previous observations documented a mean value of 1.9+/-0.2 apoptotic cells per tubule in testes of B6 mice (Kon et al., 1999) and this is consistent with our values for apoptosis frequency in control B6 mice (Figs. 7 and 8). In contrast, germ cell apoptosis was elevated in Rb/+ mice. Most apoptosis was seen in spermatocytes of stage XII tubules where spermatocytes undergo meiotic divisions. Moreover, apoptosis was not detected in Rb/+ mice until 23 days after birth, a time point coinciding with an increase in MI spermatocytes. Most significantly, apoptosis was found predominantly among MI spermatocytes that exhibited misaligned chromosomes (Fig. 8 and Table 3). Previously, correlations have been made between induced chromosome damage or genetic abnormalities and increased apoptosis. Now, these data directly link apoptosis to the presence of misaligned chromosomes at MI, thereby suggesting that the presence of a misaligned chromosome triggers a spindle checkpoint mechanism leading to cell death. Analysis of apoptosis in testes

of mice homozygous for the Rb chromosomes revealed more frequent cell death in stage XII tubules than detected in B6 mice, but the frequency was not as high as found in the testes of Rb/+ mice (data not shown). Importantly, apoptosis was not detected during pachynema, even though Rb/+ mice exhibited an elevated frequency of pachytene spermatocytes compared to B6 mice (Fig. 6). Thus there was no evidence for a "pachytene checkpoint," one that might monitor success in pairing of homologous chromosomes. Such a checkpoint might be expected to lead to apoptotic cells at a stage earlier than stage XII, although the more convoluted scenario of detection of error in pachytene leading to elimination at MI cannot be excluded.

The fact that Rb/+ testes contain an increased frequency of stage XII sections compared to B6 testes (Figure 8), in spite of the fact that there was no significant variation in frequency for any other stage between the two strains, is also suggestive of an arrest, or delay, in meiosis. This was also observed in various other Rb/+ strains (Hansmann et al., 1988) and suggests that some consequence of heterozygosity for Rb chromosomes, most likely a checkpoint-mediated mechanism detecting misaligned chromosomes, activates developmental arrest and elimination by apoptosis. Elimination of division-phase spermatocytes was also reflected in a reduced number of round spermatids among germ cells from testes of Rb/+ mice compared to B6 controls (Fig. 6), in spite of the fact that no differences were ascertained in frequencies of early prophase, leptotene and zygotene, spermatocytes. The elevated frequency of pachytene spermatocytes and reduced frequency of round spermatids in Rb heterozygotes compared to controls (Fig. 6) suggests that there was a delay in entry into division phase. Similar conclusions were reached from different

kinds of analyses of mice carrying fewer and different Rb translocations (Nijhoff and de Boer, 1979; Speed and de Boer, 1983).

Surprisingly, the concurrent analysis of TUNEL reaction and phosphorylated histone H3 (Fig. 8C) revealed that most apoptotic MI spermatocytes do not react with the antibody to phosphorylated histone H3, suggesting that the epitope may be dephosphorylated or no longer accessible. Antibody to another protein, SYCP3, also did not react with many apoptotic cells, suggesting changes in either antibody penetration or accessibility of epitopes in apoptotic cells. Although it has previously been determined that phosphorylation of histone H3 is not involved in apoptosis-induced condensation of interphase chromatin (Hendzel et al., 1998), this is, to our knowledge, the first suggestion that phosphorylated histone H3 could be dephosphorylated as part of apoptosis.

Taken together, these data suggest a delay in completion of MI and elimination of spermatocytes by apoptosis in Rb/+ mice. If this is checkpoint mediated, the important biological problem is to determine the checkpoint signal. The main events culminating in the first metaphase are chromosome condensation, spindle morphogenesis and alignment of chromosomes onto the spindle at the equator. In our observations, no differences were detected between Rb/+ and B6 mice with respect to timing of chromosome condensation and spindle formation. Thus, if a checkpoint is present, we hypothesized that the signal is improper alignment of chromosomes at metaphase.

Altered Staining Intensity of CENP-E and CENP-F Proteins on Improperly Aligned Kinetochores May Reveal an Element of a Meiotic Spindle Checkpoint Mechanism

Evidence for a spindle checkpoint mechanism responding to improperly attached chromosomes in Rb/+ spermatocytes stems from differences between properly attached and malaligned chromosomes in the staining intensity of proteins known to localize to kinetochores and to be components of a spindle assembly checkpoint mechanism. Among metaphase spermatocytes identified by anti-phospho-histone H3 staining from Rb/+ mice, 23% contain unaligned chromosomes (Figure 5B). All of the unaligned kinetochores assessed stained more intensely with antibodies against CENP-E and CENP-F than did kinetochores of chromosomes that were properly positioned on the spindle. However, antibodies against proteins that are unrelated to the spindle assembly checkpoint (PLK1, CREST and SYCP3) yielded equal staining signal on aligned compared to unaligned chromosomes in Rb/+ metaphase spermatocytes. This observation suggests that the increased signal of CENP-E and CENP-F on unaligned chromosomes is specific and signals the state of chromosome alignment or attachment on the spindle.

Similar observations have been made of mitotic cells, where it was shown that kinetochores on lagging chromosomes stained more intensely with antibodies against CENP-E than did chromosomes aligned on the metaphase plate (Chan et al., 1999). Dynein has been shown to relocate onto kinetochores of chromosomes mechanically detached from spindle microtubules in grasshopper spermatocytes (King et al., 2000), where the relocation of dynein is a transient interaction, and not caused by structural

alterations of the dynein protein itself, affecting antibody binding. Comparable results have been obtained for *Drosophila* mitotic and meiotic cells (Basu et al., 1998) using antibodies recognizing the BUB1 spindle checkpoint protein. CENP-E is a kinesin-like motor protein whose function in kinetochore-microtubule attachments has been proposed to be monitored by the hBUBR1 checkpoint kinase (Chan et al., 1999). During mitosis, this mechano-sensor complex relays signals from the kinetochore to inhibit the anaphase-promoting complex (APC) from ubiquitinating proteins whose destruction is required for entry into anaphase. We hypothesize that the increase in staining intensity for CENP-E and CENP-F on malattached meiotic chromosomes in Rb/+ spermatocytes may initiate a signal either to correct the attachment problem, or, if the error cannot be corrected, to initiate apoptotic elimination of a spermatocyte likely to give rise to aneuploid gametes.

Abnormalities of Meiotic Chromosome Behavior May Activate a Checkpoint Leading to Elimination of Aberrant Germ Cells

Good gamete quality in males with increased potential for gametic aneuploidy could be maintained by the operation of checkpoint mechanisms. Indeed, this study provided data consistent with the hypothesis that chromosomal abnormalities, specifically misalignment, are detected in the meiotic division phase and lead to elimination of aberrant germ cells by apoptosis. These data suggest that mechanisms ensure the elimination of germ cells with abnormal chromosomal configurations or behavior. Similar mechanisms have been implicated by the MI arrest of male mice with a single sex chromosome, the XO*Sxr* male (Kot and Handel, 1990; Sutcliffe et

al., 1991) and the improvement of gametogenic progress resulting from providing a partner for the X*Sxr* chromosome (Burgoyne et al., 1992). These examples are in contrast to the situation of mammalian female meiosis, where data suggest that checkpoint mechanisms may be inefficient or absent. For example, a single unpaired sex chromosome (in the XO female) does not trigger a meiotic arrest (LeMaire-Adkins et al., 1997), suggesting lack of apparent checkpoint control. Arrest in the female does occur when the oocyte is faced with massive chromosome univalency, as in the *Mlh1*-null female. Here spindle assembly fails, suggesting a role for the chromosomes in the morphogenesis of the oocyte's MI spindle.

Surprisingly however, it is not clear how much improvement in gamete quality is brought about by elimination of aberrant MI germ cells. From FISH analysis of MI spermatocytes it can be extrapolated that the frequency in the sperm population of sperm disomic or nullisomic for chromosome 8 would be 10-11% if there were no elimination of chromosomally aberrant germ cells. This frequency is not greatly different from the observed frequency of 9%. However, the potential frequency of aneuploidy deriving from adjacent segregation of the trivalent is not known, and it might increase the predicted aneuploidy for chromosome 8. Thus, at this point, it is not known if the frequency of 9% sperm scored as aneuploid for chromosome 8 represents a reduction from the expected frequency.

Taken together, the results from this study provide evidence for a meiotic spindle checkpoint mechanism in male gametogenic cells, but one that may not be totally efficient in eliminating germ cells destined to form aneuploid gametes. First, data on meiotic pairing abnormalities and nondisjunction leading to gametic

aneuploidy in Rb/+ spermatocytes validate Rb/+ mice as a model for error-prone meiotic chromosome segregation. Second, abnormalities of chromosome attachment to and alignment on the meiotic spindle were prevalent in Rb/+ spermatocytes. Third, staining patterns for candidate checkpoint proteins differed between properly attached and malaligned chromosomes in meiotic metaphase spermatocytes. Fourth, an increased frequency of post-prophase meiotic germ cell death was seen in testes of Rb/+ mice, as well as developmental delays consistent with checkpoint surveillance. Most significantly, the data show that cells with misaligned chromosomes account for the apoptotic cells, providing a direct link between chromosome error and elimination by apoptosis. However, when aneuploidy for chromosome 8 was considered, the frequency of chromosomally unbalanced sperm was not substantially less than the frequency estimated from observed meiotic abnormalities. Thus, considered in toto, these observations provide indirect but compelling evidence, for detection of meiotic chromosome error leading to subsequent elimination of spermatocytes. What is not yet known is how effective the checkpoint is. Clearly, aneuploid sperm are produced and this undoubtedly can lead to reduction of reproductive efficiency. Further insight into the role and efficacy of the spindle checkpoint mechanism in male gametes is sorely needed, and will derive, in part, from mutation of putative checkpoint genes and analysis of the phenotypic effects in models for meiotic error, such as Rb/+ mice.

Acknowledgements

This work was supported by a grant from the NIH, HD33816 to MAH. We are grateful to Debby Andreadis, Sally Fridge and Trisha Smith for maintenance of mice, to Dr. John Dunlap for his generosity in assistance with confocal imaging, to Dr. Terry Hassold for initial instruction in procedures for FISH as well as for providing FISH probes, to Dr. Tim Yen for generously providing antibodies recognizing CENP-E and CENP-F, and to Dr. Marko Kallio for instruction in procedures for microdissection by transillumination. We are indebted to Drs. John Eppig and Bruce McKee, Tim Yen, members of the Handel laboratory, and two anonymous reviewers for critical comments on the manuscript and discussions.

LIST OF REFERENCES

Abrieu, A., J.A. Kahana, K.W. Wood, and D.W. Cleveland. (2000). CENP-E as an essential component of the mitotic checkpoint in vitro. *Cell*. 102:817-826.

Basu, J., E. Logarinho, S. Herrmann, H. Bousbaa, Z.X. Li, G.K.T. Chan, T.J. Yen, C.E. Sunkel, and M.L. Goldberg. (1998). Localization of the *Drosophila* checkpoint control protein Bub3 to the kinetochore requires Bub1 but not Zw10 or Rod. *Chromosoma*. 107:376-385.

Boyle, A.L., and D.C. Ward. (1992). Isolation and initial characterization of a large repeat sequence element specific to mouse chromosome 8. *Genomics*. 12:517-525.

Burgoyne, P.S., S.K. Mahadevaiah, M.J. Sutcliffe, and S.J. Palmer. (1992). Fertility in mice requires X-Y pairing and a Y-chromosomal "spermiogenesis" gene mapping to the long arm. *Cell*. 71:391-398.

Burke, D.J. (2000). Complexity in the spindle checkpoint. *Curr Opin Genet Develop*. 10:26-31.

Cattanach, B.M., and H. Moseley. (1973). Nondisjunction and reduced fertility caused by the tobacco mouse metacentric chromosomes. *Cytogenet. Cell Genet.* 12:264-287.

Chan, G.K.T., S.A. Jablonski, V. Sudakin, J.C. Hittle, and T.J. Yen. (1999). Human BUBR1 is a mitotic checkpoint kinase that monitors CENP-E functions at kinetochores and binds the cyclosome/APC. *J Cell Biol*. 146:941-954.

Cobb, J., B. Cargile, and M.A. Handel. (1999a). Acquisition of competence to condense metaphase I chromosomes during spermatogenesis. *Develop Biol*. 205:49-64.

Cobb, J., M. Miyaike, A. Kikuchi, and M.A. Handel. (1999b). Meiotic events at the centromeric heterochromatin: histone H3 phosphorylation, topoisomerase II alpha localization and chromosome condensation. *Chromosoma*. 108:412-425.

Davisson, M.T., and E.C. Akeson. (1993). Recombination suppression by heterozygous Robertsonian chromosomes in the mouse. *Genetics*. 133:649-667.

Disteche, C.M., S.L. Gandy, and D.A. Adler. (1987). Translocation and amplification of an X-chromosome DNA repeat in inbred strains of mice. *Nucl. Acids Res.* 15:4393-4401.

Duesbery, N.S., T.S. Choi, K.D. Brown, K.W. Wood, J. Resau, K. Fukasawa, D.W. Cleveland, and G.F. Vande Woude. (1997). CENP-E is an essential kinetochore motor in maturing oocytes and is masked during Mos-dependent, cell cycle arrest at metaphase II. *Proc Natl Acad Sci USA*. 94:9165-9170.

Eichenlaub-Ritter, U., and H. Winking. (1990). Nondisjunction, disturbances in spindle structure, and characteristics of chromosome alignment in maturing oocytes of mice heterozygous for Robertsonian translocations. *Cytogenet. Cell Genet.* 54:47-54.

Eicher, E.M., D.W. Hale, P.A. Hunt, B.K. Lee, P.K. Tucker, T.R. King, J.T. Eppig, and L.L. Washburn. (1991). The mouse Y* chromosome involves a complex rearrangement, including interstitial positioning of the pseudoautosomal region. *Cytogenet. Cell Genet.* 57:221-230.

Evans, E.P., G. Breckon, and C.E. Ford. (1964). An air-drying method for meiotic preparations from mammalian testes. *Cytogenetics*. 3:289-294.

Everett, C.A., J.B. Searle, and B.M.N. Wallace. (1996). A study of meiotic pairing, nondisjunction and germ cell death in laboratory mice carrying Robertsonian translocations. *Genet Res*. 67:239-247.

Gardner, R.D., and D.J. Burke. (2000). The spindle checkpoint: two transitions, two pathways. *Trends Cell Biol*. 10:154-158.

Gorbsky, G.J., M. Kallio, J.R. Daum, and L.M. Topper. (1999). Protein dynamics at the kinetochore: cell cycle regulation of the metaphase to anaphase transition. *FASEB J*. 13:S231-S234.

Hansmann, I., P. de Boer, and R.M. Speed. (1988). Aneuploidy-related delay of meiotic development in the mouse and the Djungarian hamster. *In* The Cytogenetics of Mammalian Autosomal Rearrangements. A. Daniel, editor. Alan R. Liss, Inc., New York. 295-314.

Hendzel, M.J., W.K. Nishiokas, Y. Raymond, C.D. Allis, D.P. Bazett-Jones, and J.P. Th'ng. (1998). Chromatin condensation is not associated with apoptosis. *J. Biol. Chem.* 273:24470-24478.

Hunt, P.A., and R. LeMaire-Adkins. (1998). Genetic control of mammalian female meiosis. *In* Meiosis and Gametogenesis. Vol. 37. M.A. Handel, editor. Academic Press Inc, 525 B Street, Suite 1900, San Diego, CA 92101-4495. 359-381.

Kallio, M., J.E. Eriksson, and G.J. Gorbsky. (2000). Differences in spindle association of the mitotic checkpoint protein Mad2 in mammalian spermatogenesis and oogenesis. *Develop Biol*. 225:112-123.

Kallio, M., T. Mustalahti, T.J. Yen, and J. Lahdetie. (1998). Immunolocalization of alpha-tubulin, gamma-tubulin, and CENP-E in male rat and male mouse meiotic divisions: Pathway of meiosis I spindle formation in mammalian spermatocytes. *Dev Biol*. 195:29-37.

King, J.M., T.S. Hays, and R.B. Nicklas. (2000). Dynein is a transient kinetochore component whose binding is regulated by microtubule attachment, not tension. *J Cell Biol*. 151:739-748.

Koehler, K.E., R.S. Hawley, S. Sherman, and T. Hassold. (1996). Recombination and nondisjunction in humans and flies. *Hum. Molec. Genet.* 5:1495-1504.

Kon, Y., H. Horikoshi, and D. Endoh. (1999). Metaphase-specific cell death in meiotic spermatocytes in mice. *Cell Tissue Res*. 296:359-369.

Kot, M.C., and M.A. Handel. (1990). Spermatogenesis in XO*Sxr* mice: Role of the Y chromosome. *J. Exp. Zool.* 256:92-105.

Lee, J., T. Miyano, Y.F. Dai, P. Wooding, T.J. Yen, and R.M. Moor. (2000). Specific regulation of CENP-E and kinetochores during meiosis I/meiosis II transition in pig oocytes. *Mol Reprod Dev*. 56:51-62.

LeMaire-Adkins, R., K. Radke, and P.A. Hunt. (1997). Lack of checkpoint control at the metaphase/anaphase transition: A mechanism of meiotic nondisjunction in mammalian females. *J Cell Biol*. 139:1611-1619.

Li, X., and R.B. Nicklas. (1995). Mitotic forces control a cell-cycle checkpoint. *Nature*. 373:630-632.

Li, X.T., and R.B. Nicklas. (1997). Tension-sensitive kinetochore phosphorylation and the chromosome distribution checkpoint in praying mantid spermatocytes. *J Cell Sci*. 110:537-545.

Liao, H., R.J. Winkfein, G. Mack, J.B. Rattner, and T.J. Yen. (1995). CENP-F is a protein of the nuclear matrix that assembles onto kinetochores at late G2 and is rapidly degraded after mitosis. *J Cell Biol*. 130:507-518.

Lowe, X., S. O'Hogan, D. Moore, J. Bishop, and A. Wyrobek. (1996). Aneuploid epididymal sperm detected in chromosomally normal and Robertsonian translocation-bearing mice using a new three-chromosome FISH method. *Chromosoma*. 105:204-210.

Nicklas, R.B., S.C. Ward, and G.J. Gorbsky. (1995). Kinetochore chemistry is sensitive to tension and may link mitotic forces to a cell cycle checkpoint. *J Cell Biol*. 130:929-939.

Nijhoff, J.H., and P. de Boer. (1979). A first exploration of a Robertsonian translocation heterozygote in the mouse for its usefulness in cytological evaluation of radiation-induced meiotic autosomal non-disjunction. *Muta. Res.* 61:77-86.

Paliulis, L.V., and R.B. Nicklas. (2000). The reduction of chromosome number in meiosis is determined by properties built into the chromosomes. *J Cell Biol*. 150:1223-1231.

Parvinen, M., J. Toppari, and J. Lahdetie. (1993). Transillumination phase contrast microscope techniques for evaluation of male germ cell toxicity and mutagenicity. *In* Methods in Toxicology. Vol. 3, part A. R.E. Chapin and J.J. Heindel, editors. Academic Press, San Diego. 142-165.

Print, C.G., and K.L. Loveland. (2000). Germ cell suicide: new insights into apoptosis during spermatogenesis. *BioEssays*. 22:423-430.

Robertson, W.R.B. (1916). Chromosome studies I. Taxonomic relationships shown in the chromosomes of *Tettigidae* and *Acrididae*: V-shaped chromosomes and their significance in *Acrididae*, *Locustidae*, and *Gryllidae*: Chromosomes and variation. *J. Morphol.* 27:179-331.

Schaar, B.T., G.K.T. Chan, P. Maddox, E.D. Salmon, and T.J. Yen. (1997). CENP-E function at kinetochores is essential for chromosome alignment. *J Cell Biol*. 139:1373-1382.

Sinha Hikim, A.P., and R.S. Swerdloff. (1999). Hormonal and genetic control of germ cell apoptosis in the testis. *Rev Reprod*. 4:38-47.

Speed, R.M., and P. de Boer. (1983). Delayed meiotic development and correlated death of spermatocyes in male mice with chromosome abnormalities. *Cytogenet. Cell Genet.* 35:257-262.

Sutcliffe, M.J., S.M. Darling, and P.S. Burgoyne. (1991). Spermatogenesis in XY, XY*Sxr*^{b} and XO*Sxr*^{a} mice: A quantitative analysis of spermatogenesis throughout puberty. *Mol. Reprod. Dev.* 30:81-89.

Waters, J.C., R.H. Chen, A.W. Murray, G.J. Gorbsky, E.D. Salmon, and R.B. Nicklas. (1999). Mad2 binding by phosphorylated kinetochores links error detection and checkpoint action in mitosis. *Curr Biol*. 9:649-652.

Winking, H., C. Reuter, and H. Bostelmann. 2000. Unequal nondisjunction frequencies of trivalent chromosomes in male mice heterozygous for two Robertsonian translocations. *Cytogenet. Cell Genet.* 91:303-306.

Yen, T.J., G. Li, B.T. Schaar, I. Szilak, and D.W. Cleveland. (1992). CENP-E is a putative kinetochore motor that accumulates just before mitosis. *Nature*. 359:536-539.

Yu, H.G., M.G. Muszynski, and R.K. Dawe. (1999). The maize homologue of the cell cycle checkpoint protein MAD2 reveals kinetochore substructure and contrasting mitotic and meiotic localization patterns. *J Cell Biol*. 145:425-435.

PART V

CONCLUSION

CHAPTER 1

SUMMARY

The goal of the work presented in this Dissertation was to provide insight into mechanisms governing the meiotic division in mouse spermatocytes. The establishment of a meiotic timeline of events occurring during male meiosis will allow future investigators to study meiosis in both normal and abnormal environments, as has been done in Parts III and IV of this Dissertation. Using the mouse as a model organism, these studies will hopefully provide information as to why meiotic errors occur in our own species. This Part serves to summarize how these pieces fit together, and what is left to accomplish on the road to finishing the puzzle.

Establishment of Meiotic Timeline

In order to study how an event goes awry, it is important to understand how the event unfolds normally. In Part II of this Dissertation, we have localized meiotic proteins as an approach to establishing temporal order. These data aid in the study of mammalian meiosis in that abnormalities caused by environmental stimuli, mutations or gene knock-outs can be studied with respect to normal meiotic development. For example, the mouse meiotic gene *mei1* was discovered through a mutagenesis screen (Munroe et al., 2000). To determine the exact stage of arrest of *mei1*$^{-/-}$ spermatocytes, our developmental timeline and repertoire of marker proteins was useful. We demonstrated that the *mei1*$^{-/-}$ spermatocytes arrest in zygotene, and RAD51 foci are

not present (Figure 1, Part V). This was determined by using immunofluorescence with antibodies against the synaptonemal complex protein SYCP3 and the recombinase protein RAD51, whose localization was previously determined and is provided in the meiotic timeline. This timeline serves as a baseline for which future proteins and genes can be compared to known proteins and genes, which will aid in determining the overall function of the unknowns. Although extensive documentation has been provided, this project is ongoing, as new genes will be added to the timeline as they are discovered.

Models to Study Meiotic G2/M Transition in Mouse Spermatocytes

The mouse has been used as a genetic model to understand how meiotic errors occur. The knock-out strategy for removal of specific genes in the mouse genome has provided researchers with the ability to study gene function in a variety of systems. In meiosis, the removal of the *Mlh1* gene causes univalence and sterility in both males and females (Baker et al., 1996; Woods et al., 1999). The univalence is due to the loss of chiasmata during pachytene, a structural product required for homologous chromosome pairing during the first metaphase. We have shown that although homologous chromosomes are not spatially near one another during the metaphase transition, spermatocytes proceed to condense chromosomes, form bipolar spindles and undergo synaptonemal complex breakdown, all events indicative of metaphase entry (Part III). However, these spermatocytes to do not proceed through metaphase into anaphase as do normal spermatocytes. Instead of aligning chromosomes on the metaphase plate, the chromosomes from *Mlh1*$^{-/-}$ metaphase

Figure 1. Immunofluorescent staining of *Mei1*$^{+/+}$ and *Mei1*$^{-/-}$ mouse spermatocytes. SYCP3-red and RAD51-green in all images. A) Pachytene *Mei1*$^{+/+}$ spermatocyte. B) Zygotene-arrested *Mei1*$^{-/-}$ spermatocyte. C) RAD51 foci in *Mei1*$^{+/+}$ spermatocyte. D) Lack of RAD51 foci in *Mei1*$^{-/-}$ spermatocyte.

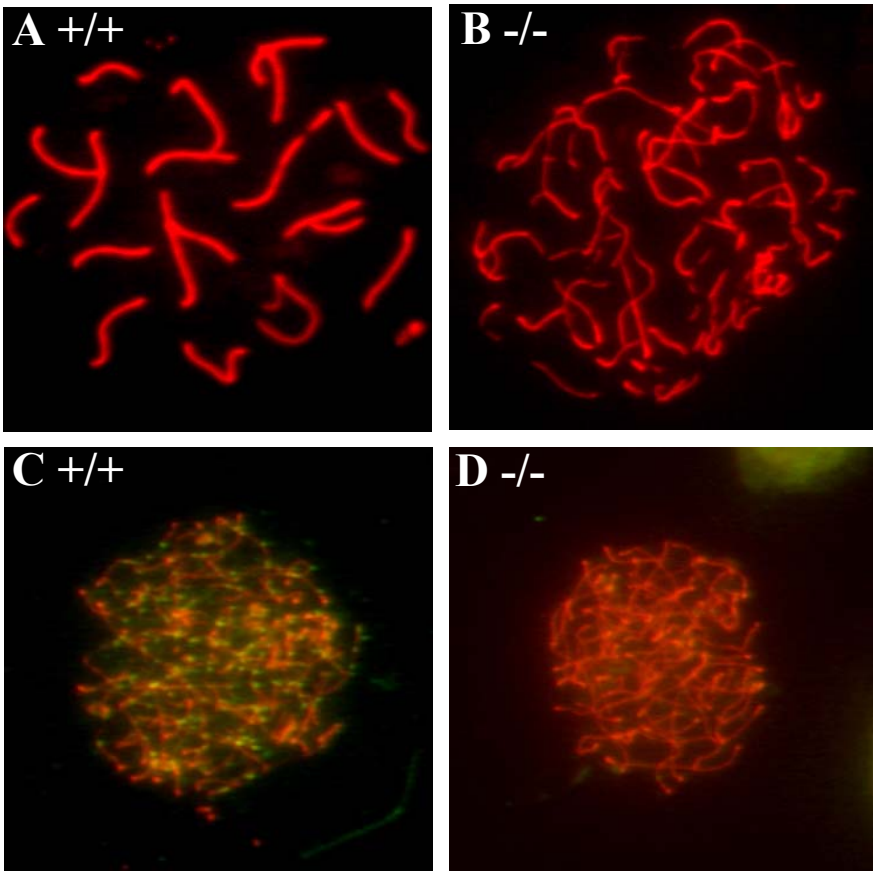
A +/+
B -/-
C +/+
D -/-

spermatocytes are arrayed throughout the cell. A similar phenotype was seen in *Mlh1*$^{-/-}$ oocytes (Woods et al., 1999). Critical questions remain. What stops these cells from progressing into anaphase? It is thought that the lack of chiasmata produces the univalence and spatial separation of homologous chromosomes during metaphase, but at what point is error detected? How is error detected? How is this signal transduced to induce an apoptotic response?

Another model used to study an abnormal metaphase entry in mouse spermatocytes is the Robertsonian-heterozygous (Rb/+) mouse, known to have pairing abnormalities and reduced recombination near the centromeric ends of homologous chromosomes (Davisson and Akeson, 1993). Pairing abnormalities can be visualized with antibodies against the synaptonemal complex protein SYPC3 (Figure 4, Part IV). The reduced recombination near the centromere can also be seen using an antibody that recognizes double strand breaks, γ-H2AX (Figure 2, Part V). During pachytene, the γ-H2AX antibody localizes only to the sex chromosomes, but in an Rb/+ spermatocyte, it is sometimes detected in areas of abnormal pairing, implying a failure in DNA repair and the completion of meiotic recombination in these regions. Homologous chromosome pairing failure, much like the failure seen in *Mlh1*$^{-/-}$ spermatocytes, is seen in chromosomes involved in the Robertsonian translocation. This event is thought to cause chromosomes to fail to align or congress onto the metaphase plate (Figure 5, Part IV). Similar to *Mlh1*$^{-/-}$ spermatocytes, Rb/+ spermatocytes are normal up to diplotene, with the exception of reduced recombination in areas of their chromosomes, causing univalence during metaphase. Although Rb/+ mice produce sperm, many metaphase spermatocytes containing

Figure 2. Localization of PLK1 in C57 and Rb/+ metaphase spermatocytes. PLK1-red and DNA/DAPI-blue in a images. A) and B) PLK1 localization in control C57BL6/J spermatocytes (A and B are images of the same cell). C) and D) PLK localization in Rb/+ spermatocytes containing unaligned chromosomes (C and D are images of the same cell). Note that PLK1 intensity on aligned versus unaligned chromosomes are similar.

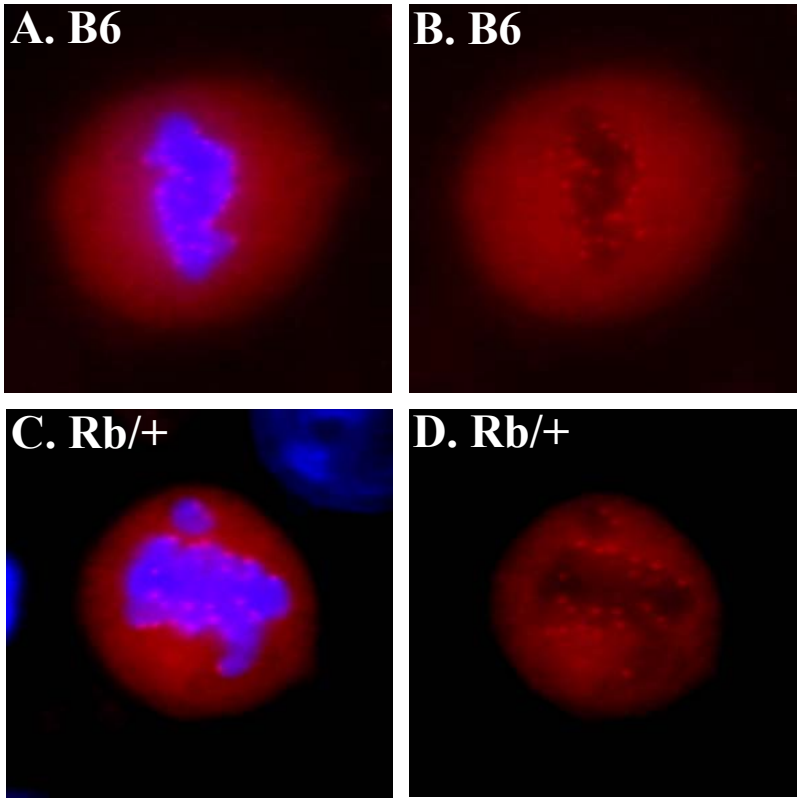
A. B6
B. B6
C. Rb/+
D. Rb/+

unaligned chromosomes were shown to be apoptotic (Figure 8 and Table 3, Part IV). What triggers the spermatocyte to undergo apoptosis? Meiotic apoptosis during the metaphase transition is seen in Rb/+, *Mlh1*$^{-/-}$ and normal C57BL6/J mice (albeit at a much lower level). Is there a mechanism monitoring proper chromosome alignment in mouse spermatocytes? Much work should be done to elucidate the players involved in such mechanisms.

Role of Apoptosis in Chromosomally Abnormal Spermatocytes

Apoptosis is a known mechanism for removal of damaged cells. In mammalian meiosis, little is known as to how this mechanism functions. Evidence for an apoptotic mechanism during the metaphase I transition in mouse spermatocytes is provided in Parts III and IV. Although mouse models and environmental treatments have been shown to induce apoptosis in the mouse testis (Sinha Hikim and Swerdloff, 1999), the mechanism itself remains to be elucidated.

What regulates apoptosis in the mouse testis? Do spermatocytes themselves detect abnormalities, or do the supporting Sertoli cells? Does the universal "molecular policeman", p53, play a role? It has been shown that unpaired chromosomes in mouse spermatocytes cause apoptosis, first arising at metaphase I (Odorisio et al., 1998). This is similar to the timing of apoptosis seen in *Mlh1*$^{-/-}$ spermatocytes, also containing unpaired chromosomes at MI (Part III of this Dissertation). Odorisio et al. also showed that apoptosis in spermatocytes with unpaired chromosomes is p53-independent. However, *Atm*$^{-/-}$ spermatocytes (lacking the ATM protein involved in DNA damage recognition) also undergo apoptosis, but

the defects are partially rescued in a p53 background (Barlow et al., 1997). This was determined by producing a double knock-out mouse, removing both the *Atm* and *p53* genes. This suggests that if p53 is not involved in the meiotic spindle assembly checkpoint, ATM is also not part of the relevant checkpoint. If there are different mechanisms of cell recognition of abnormal germ cells, future double knock-out studies will identify the players involved.

Meiotic Spindle Assembly Checkpoint During Metaphase I

Whether a meiotic spindle assembly checkpoint mechanism is present in mouse spermatocytes is unknown. Downstream events of spindle checkpoint activation in mammalian cells are cell-cycle arrest and elimination of aberrant cells by apoptosis. The abnormalities inducing arrest and/or apoptosis range from environmental stress to abnormal chromosome configurations or behavior, and may be sex specific. Male mice with a single sex chromosome (XO*Sxr*) arrest at the first metaphase (Kot and Handel, 1990; Sutcliffe et al., 1991). However a single unpaired sex chromosome in female mice (XO) does not trigger a meiotic arrest (LeMaire-Adkins et al., 1997). These data suggest that a checkpoint mechanism monitoring meiotic chromosome alignment and congression onto the metaphase plate is present in the male mouse, but may be inefficient or absent in the female.

The Robertsonian-heterozygous (Rb/+) mouse model was used to observe protein/kinetochore function in abnormal situations, and possible relationship to a checkpoint mechanism. Antibodies against the motor proteins CENP-E and CENP-F were shown to localize more intensely onto kinetochores of unaligned versus aligned

chromosomes (Figures 9 and 10, Part IV). This increase in intensity could suggest a mechanism for recognition of an abnormality, a cellular attempt to fix the problem by placing more of the motor protein at the site of the abnormality. Immunofluorescence is a useful method to observe the localization of other putative checkpoint proteins. For example, it was recently shown that the PLK1 protein (named polo-like kinase 1 after the *Drosophila melanogaster* protein POLO) is involved in both spindle development (Nigg, 1998) and possibly DNA damage repair (Smits et al., 2000), but not recognition of unaligned chromosomes. The Rb/+ model was used to study the action of the PLK1 protein on unaligned kinetochores (Figure 3, Part V). PLK1 intensity on unaligned versus aligned chromosomes did not differ, as did the intensity of CENP-E and CENP-F staining. This might imply that PLK1 does not play a role in the meiotic spindle checkpoint mechanism, but it may have another function during meiosis. Mice with knock-outs of specific genes such, as PLK1, will ultimately provide further information about protein function during meiosis. The elucidation of meiotic checkpoint mechanisms will be important in developing an understanding of meiotic error in our own species, as the majority of aneuploidy in humans is thought to arise from an abnormal MI meiotic division (Hassold and Hunt, 2001).

However, players involved in the meiotic spindle checkpoint mechanism must first be discovered and studied. Thus far, most information about putative meiotic checkpoint proteins stems from sequence homology with proteins involved in the budding yeast spindle checkpoint mechanism. Through the discovery of the yeast proteins, much has been learned about mammalian mitotic checkpoints, but the meiotic system has not profited nearly as much. The localization of these putative

Figure 3. γ-H2AX (green) and SYCP3 (red) staining in a Rb/+ spermatocyte. A) A Rb/+ pachytene spermatocyte, showing normal γ-H2AX staining of the sex chromosomes (largest green area). The white box in A represents an unpaired region of a Robertsonian-heterozygous fused chromosome (magnified in B and C). Note that in B and C, γ-H2AX localizes to the unpaired region, but not paired regions. This is not seen in control C57BL6/J pachytene spermatocytes.

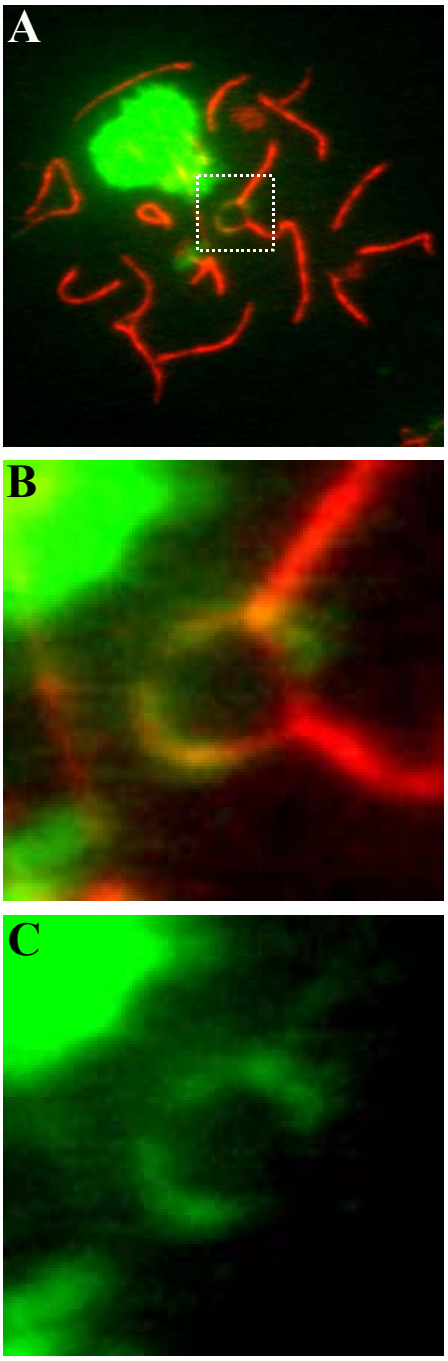
A
B
C

proteins from the yeast and mitosis systems in meiotic cells is proving to be a useful first step. A major hurdle to overcome is that most null mutations of these checkpoint genes are embryonic lethals, therefore the gene's role in specific tissues of the adult mouse cannot be studied. With the recent advent of the Cre/loxP system, this hurdle can be bypassed. By placing designed lox sites around the gene or region to be knocked out, the tissue-driven expression of cre recombinase will remove the lox-flanked (or floxed) region by recombination. Cre recombinase expression can be controlled by a tissue-specific promoter, such as the meiotic synaptonemal complex gene *Syn1* (Vidal et al., 1998). This system will aid in the production of tissue-specific gene knock-outs, from which systems such as the meiotic spindle assembly checkpoint mechanism can be further studied. The utility of mutagenesis protocols, using chemical mutagens such as ENU and EMS, will also aid in the discovery of novel genes involved in meiotic development.

Conclusion

The field of mammalian meiotic research is clearly in its infancy. With the expanding list of completed genomes, production of knock-out mice, and systems such as the Cre/loxP tissue-specific gene removal system and mutagenesis protocols, knowledge of meiosis will grow considerably in the near future. Information from the yeast and mammalian mitotic cell cycles has and will provide insight into mammalian meiotic development. But not all questions can be answered from these relationships. It is important that meiotic research takes advantage of the gene-discovery systems available in order to better understand meiotic development.

LIST OF REFERENCES

Baker SM, Plug AW, Prolla TA, Bronner CE, Harris AC, Yao X, Christie DM, Monell C, Arnheim N, Bradley A, Ashley T, Liskay RM. 1996. Involvement of mouse *Mlh1* in DNA mismatch repair and meiotic crossing over. Nat Genet 13:336-342.

Barlow C, Liyanage M, Moens PB, Deng CX, Ried T, Wynshaw-Boris A. 1997. Partial rescue of the prophase I defects of *Atm*-deficient mice by p53 and p21 null alleles. Nat Genet 17:462-466.

Davisson MT, Akeson EC. 1993. Recombination suppression by heterozygous Robertsonian chromosomes in the mouse. Genetics 133:649-667.

Hassold T, Hunt P. 2001. To ERR (meiotically) is human: the genesis of human aneuploidy. Nature Reviews Genetics 2:280-291.

Munroe RJ, Bergstrom RA, Zheng QY, Libby B, Smith R, John SWM, Schimenti KJ, Browning VL, Schimenti JC. 2000. Mouse mutants from chemically mutagenized embryonic stem cells. Nat Genet 24:318-321.

Nigg EA. 1998. Polo-like kinases: positive regulators of cell division from start to finish. Curr Opin Cell Biol 10:776-783.

Odorisio T, Rodriguez TA, Evans EP, Clarke AR, Burgoyne PS. 1998. The meiotic checkpoint monitoring synapsis eliminates spermatocytes via p53-independent apoptosis. Nat Genet 18:257-261.

Sinha Hikim AP, Swerdloff RS. 1999. Hormonal and genetic control of germ cell apoptosis in the testis. Rev Reprod 4:38-47.

Smits VAJ, Klompmaker R, Arnaud L, Rijksen G, Nigg EA, Medema RH. 2000. Polo-like kinase-1 is a target of the DNA damage checkpoint. Nat Cell Biol 2:672-676.

Vidal F, Sage J, Cuzin F, Rassoulzadegan M. 1998. Cre expression in primary spermatocytes: A tool for genetic engineering of the germ line. Mol Reprod Dev 51:274-280.

Woods LM, Hodges CA, Baart E, Baker SM, Liskay M, Hunt PA. 1999. Chromosomal influence on meiotic spindle assembly: Abnormal meiosis I in female *Mlh1* mutant mice. J Cell Biol 145:1395-1406.

VITA

Shannon Stewart Eaker was born on January 31st, 1975 in Knoxville, Tennessee. He attended and was class president of Farragut High School, graduating in 1993. He attended The University of Tennessee from 1993-1997 as an undergraduate, double majoring in Biology and Zoology. In 1996, he took an internship at the Los Alamos National Laboratory in New Mexico, where he was first introduced to the field of cell biology by Dr. Harry Crissman. After graduating in 1997, he became a graduate student at UT in the Department of Biochemistry and Cellular and Molecular Biology in the Division of Biology. He joined the laboratory of Dr. Mary Ann Handel and received the Ph.D. degree in Biochemistry and Cellular and Molecular Biology in 2001.